Towards Net Zero Energy Performance of the Montpetit Hall Building

Borzou Afraz

A thesis submitted to the University of Ottawa

In partial fulfillment of the requirements for the degree of

Master of Applied Science in Civil Engineering

Department of Civil Engineering

Faculty of Engineering

University of Ottawa

Ottawa, Canada

Abstract

This thesis develops a simulation-based optimization framework for the deep energy retrofit of Montpetit Hall, a multifunctional institutional facility at the University of Ottawa. Constructed in 1972, the building exhibits high energy intensity due to its mixed uses, aging envelops and systems, and complex thermal interactions. In Ottawa's cold climate, the study aims to reduce energy consumption and improve economic performance through integrated modeling, calibration, and multi-objective optimization.

A detailed building energy model was developed in Design Builder and Energy Plus and optimized in MATLAB using the Non-Dominated Sorting Genetic Algorithm II (NSGA-II). The model incorporated detailed 3D geometry, 128 thermal zones, envelope characteristics, and HVAC systems. Input data included Ottawa-specific weather records, institutional occupancy profiles, and NECB-based schedules. Baseline simulations were validated against 2022 utility data, meeting ASHRAE Guideline 14 with less than 5% Normalized Mean Bias Error (NMBE) and less than 15% Coefficient of Variation of Root Mean Square Error (CVRMSE).

The optimization process was carried out in two stages, addressing envelope retrofits and HVAC improvements. Stage 1 focused on envelope and window retrofits, identifying Pareto-optimal solutions to balance primary energy demand and NPV. Results indicated that upgrading semi-exposed floors, roofs, and south- and east-facing glazing reduced heating demand by up to 19.4%, leading to overall energy savings of nearly 13%. Double-glazed, argon-filled windows provided the most favorable trade-offs. Cost-oriented scenarios prioritized selective glazing upgrades, while maximum-savings cases involved full envelope replacements.

Stage 2 evaluated HVAC retrofits on the most energy-efficient envelope configuration, testing Variable Air Volume (VAV), Demand-Controlled Ventilation (DCV), Economizers, and Heat Recovery (HR) systems. Combination of these HVAC showed highest saving in energy and economical perspective by more than 50%. Moreover, renewable retrofit strategies , Photovoltaic Panels (PV), Solar Thermal Collector, Photovoltaic-Thermal panel (PVT) and Green Roof, were also analyzed, and a comprehensive feasibility assessment was undertaken to identify the scenarios that provide the most favorable economic returns.

This research contributes to the literature by assessing the effectiveness of a two-stage retrofit optimization framework applied to a complex institutional building in a heating-dominated climate. By integrating simulation, calibration, and optimization, the study establishes a replicable methodology with direct implications for institutional decarbonization and sustainable retrofit strategies in mid-century Canadian buildings.

Acknowledgment

I would like to express my deepest gratitude to my supervisor, Dr. Miroslava Kavgic, for her invaluable guidance, academic insight, and unwavering support throughout the course of this thesis. Her mentorship, patience, and dedication to excellence have played a crucial role in shaping this research and in my development as a scholar.

My sincere thanks also go to Yasaman Dadras for her generous assistance, technical advice, and thoughtful encouragement. Her contributions were instrumental during critical phases of this work, and I am truly grateful for her support.

I am profoundly thankful to my family for their unconditional love and continuous encouragement. To my father, Ahmad Afraz, and my mother, Shahin Ghobadi, your strength, sacrifices, and belief in me have been the foundation of all my achievements. To my sisters, Zhamak and Vanousheh, thank you for your constant support and for always being there when I needed it most.

Lastly, I would like to thank myself for never giving up even when things felt overwhelming; for showing up every day and believing in the journey; for the late nights, early mornings, and everything in between.

To all who have supported and inspired me on this academic journey, I extend my heartfelt appreciation.

Table of Contents

List of Figures

List of Tables

List of Symbols and Abbreviations

Acronym	Description
AC	Air Conditioning
AHU	Air Handling Unit
ANN	Artificial Neural Network
ASHRAE	American Society of Heating, Refrigerating and Air-Conditioning Engineers
AWD	Actual Weather Data
BAS	Building Automation System
BEM	Building Energy Modeling
BPIE	Buildings Performance Institute Europe
CAV	Constant Air Volume system
CO_2	Carbon Dioxide
CVRMSE	Coefficient of Variation of the Root Mean Square Error
DCV	Demand-Controlled Ventilation
DHW	Domestic Hot Water
DOE	U.S. Department of Energy
EEM	Energy Efficiency Measure
EUI	Energy Use Intensity
FCU	Fan Coil Unit
GA	Genetic Algorithm
GHGs	Greenhouse Gases
GJ	Gigajoule
HDD/CDD	Heating or Cooling Degree Days
HR	Heat Recovery
HRV	Heat Recovery Ventilator
HVAC	Heating, Ventilation, and Air Conditioning
IAQ	Indoor Air Quality
IEA	International Energy Agency
IEQ	Indoor Environmental Quality

IRR	Internal Rate of Return
LCA	Life Cycle Assessment
LCCA	Life Cycle Cost Analysis
LAI	Leaf Area Index
MNT	Montpetit Hall
MOO	Multi-Objective Optimization
MUA	Make-Up Air Unit
NECB	National Energy Code of Canada for Buildings
NMBE	Normalized Mean Bias Error
NPV	Net Present Value
NSGA-II	Non-Dominated Sorting Genetic Algorithm II
NSRDB	National Solar Radiation Database
O&M	Operations and Maintenance
PJ	Petajoule
PV	Photovoltaic
PVT	Photovoltaic-Thermal hybrid system
RH	Relative Humidity
SHGC	Solar Heat Gain Coefficient
VAV	Variable Air Volume
VRF	Variable Refrigerant Flow
kCAD	Thousands of Canadian Dollars
.csv	Comma-Separated Values File
.idf	Energy Plus Input Data File

1. Introduction

1.1. Problem Statement

Global energy demand continues to rise, driven by rapid urbanization, industrial growth, and population expansion. The International Energy Agency [1] projects that, under current policy frameworks, global primary energy consumption will increase by approximately 25% by 2050. Electricity demand is expected to nearly double, particularly in emerging economies where urban infrastructure development outpaces efficiency gains [2]. This accelerating trajectory places increasing strain on global energy systems while intensifying the challenges of climate change and resource depletion.

Despite significant progress in clean energy technologies and international commitments to carbon neutrality, the global energy mix remains dominated by fossil fuels [3]. This dependence continues to drive greenhouse gas (GHG) emissions, with the energy sector responsible for more than 73% of total global emissions [4]. If current consumption patterns persist, the opportunity to limit global warming to below 1.5°C will diminish rapidly [5]. These circumstances highlight the urgent need for scalable strategies that address both supply-side transitions and demand-side reductions, particularly through enhanced efficiency within the built environment. Moreover, long-term energy outlooks underscore the intricate relationship between economic growth, energy security, and sustainability. Rahman et al. note that, without targeted efficiency measures, rising demand may exceed the capacity of decarbonization technologies, creating a rebound effect that diminishes the benefits of renewable energy investments [6]. Meeting climate targets therefore requires a dual strategy: decarbonizing energy supply while systematically reducing demand, particularly in energy-intensive sectors.

Among these sectors, the building and construction industry stands out as both a major consumer and a significant emitter. Buildings account for approximately 34% of total final energy consumption and 28% of global carbon dioxide emissions [7]. This includes energy used for heating, ventilation, air conditioning (HVAC), lighting, and the operation of appliances. Residential and commercial buildings, in particular, contribute heavily to both peak energy loads and baseline consumption in developed and developing regions alike.

A substantial share of this energy consumption arises during the operational phase of buildings. In heating dominated climates, space heating remains the dominant end-use, while in cooling dominated regions, cooling demand is rising at unprecedented rates [8]. In both contexts, energy intensity is amplified by aging infrastructure, insufficient insulation, and outdated HVAC systems [9]. [10] report that more than 70% of existing buildings in Europe and North America were constructed prior to the adoption of modern energy codes, underscoring the Substantial opportunity for energy conservation via retrofitting.

Furthermore, the building sector's impact extends beyond environmental concerns to significant economic implications. Zhai and Helman [11] estimate that energy expenditures can represent up to 30% of a building's annual operating costs, depending on building type and regional climate. This substantial financial burden underscores the importance of improving building performance, not only as a means of reducing emissions but also as a strategy for long-term cost efficiency. Retrofitting existing buildings thus emerges as a critical pathway for achieving both environmental and economic sustainability.

The implications of excessive energy use in buildings extend far beyond consumption statistics. Environmentally, the sector is a major driver of global warming, given its continued reliance on fossil fuels for space conditioning and electricity. This dependence results in the release of vast quantities of GHGs, significantly contributing to climate change. Huang and Zhai [12] estimate that, to remain within the 1.5°C target outlined in the Paris Agreement, building-related emissions must decline by at least 50% by 2030. Without aggressive intervention, however, the sector is projected to fall well short of this goal. Energy-intensive buildings also exacerbate urban heat island effects and local air pollution, particularly in densely populated regions with aging building stock and underperforming envelopes. From a life-cycle perspective, The operational stage accounts for the majority of a building's overall environmental impact [13].

Economically, high energy consumption translates into substantial operating costs, which can constitute 25–35% of total annual expenditures in large institutional facilities [14]. This burden is especially acute for organizations managing multi-building portfolios, such as universities, hospitals, and municipalities. Energy price volatility adds further uncertainty, complicating long-term financial planning and undermining the stability of public budgets. At the policy level, inefficient building stock weakens the effectiveness of carbon pricing and emissions trading systems, reducing the overall efficiency of national decarbonization frameworks. The dual environmental and economic consequences of building energy use therefore highlight the urgent need for integrated strategies that improve efficiency without compromising occupant comfort or functionality. Retrofitting existing buildings has consequently emerged as a central pillar of global energy transition agendas.

Passive retrofit measures represent the first and most cost-effective step toward reducing a building's energy demand [15]. By enhancing the thermal performance of the building envelope, walls, roofs, and fenestration, passive strategies lower heat losses in winter and heat gains in summer, reducing reliance on mechanical systems [16] Improving insulation is particularly impactful; studies show that upgrading walls, roofs, and floors can cut heating and cooling demand by 30–50%, depending on baseline conditions and climate [17]. Ascione et al. [18], demonstrated that optimized insulation levels in educational buildings yielded energy savings of over 40% while maintaining comfort. Windows also play a critical role, especially in cold climates where poor glazing accounts for 15–30% of heating loads [19]. High-performance glazing solutions, such as triple-pane units with low-emissivity coatings and thermally broken frames, can reduce heating demand by up to 20% [20] Beyond energy savings, passive measures enhance comfort, reduce drafts and condensation, and improve acoustics, qualities particularly valuable in public and educational facilities. Importantly, passive strategies provide the foundation for further interventions by lowering baseline thermal loads, thereby increasing the effectiveness of active systems and renewable energy technologies [21], [22].

Active retrofit strategies target the performance of HVAC systems, which often account for 40–50% of total building energy use [23]. Optimization efforts include upgrading equipment efficiency, improving system design, and integrating advanced controls. [24] demonstrated that building automation and user-adaptive controls can reduce HVAC consumption by 20–35% in variable-occupancy environments. [25] reported that hybrid configurations, including variable refrigerant flow (VRF) systems with Heat Recovery (HR), achieved savings of up to 30% in hot climates. Retro-commissioning and right-sizing equipment further enhance efficiency, while also extending system lifespans [26]. Modern digital solutions, such as Demand-Controlled Ventilation (DCV), smart thermostats, and predictive analytics, enable real-time responsiveness to occupancy and climate conditions, ensuring energy is consumed only when necessary [27] [28].

Renewable energy integration provides an additional dimension to retrofit strategies, directly reducing operational carbon emissions and reliance on fossil fuels. Rooftop solar photovoltaics (PV) can offset grid electricity use significantly, with potential operating cost reductions of up to 50%, depending on irradiance and system scale [29]. Solar thermal systems can cover up to 70% of domestic hot water demand in sunny climates [30], while vegetative systems such as green roofs lower cooling loads by 20–30% [31] and deliver co-benefits including stormwater management and improved air quality. Together, these measures strengthen building resilience to climate variability and energy market volatility.

Beyond environmental performance, retrofits deliver measurable economic returns. A meta-analysis by Ma et al. [32] found that comprehensive interventions combining passive, active, and renewable measures reduced operating costs by 25–60%, depending on building type, scope, and climate. These savings stem from reduced energy bills, lower maintenance needs, and longer equipment lifespans. Zuo and Zhao [33] reported favorable payback periods, often under 10 years, for HVAC upgrades and solar PV integration, while the Buildings Performance Institute Europe documented average post-retrofit energy use intensity reductions of 35% across 200 EU projects, with lifecycle cost savings exceeding initial capital outlays. Public-sector buildings, such as schools and hospitals, are particularly well-positioned to benefit, with retrofit programs providing both fiscal relief and improved indoor environmental quality. As energy prices grow more volatile and carbon pricing expands, the financial case for retrofitting continues to strengthen, reinforcing its role as both a mitigation and adaptation strategy.

1.2. Objectives and Contributions

The main objective of this thesis is to develop and apply a comprehensive energy modeling and optimization framework for Montpetit Hall at the University of Ottawa, a large and multi-functional institutional building located in a heating dominated climate. Specifically, the study aims to: (i) construct a detailed building energy model that accurately represents the complex geometry, diverse zones, and detailed HVAC configurations of the facility; (ii) calibrate the model against available metered data using standards-aligned verification approaches; (iii) evaluate a series of retrofit scenarios, including envelope upgrades, individual HVAC improvements, and combined system strategies, to assess their impacts on heating, cooling, and electricity demand; (iv) integrate life-cycle cost analysis to account for capital, operational, and maintenance expenditures; and (v) employ a multi-objective optimization approach to identify envelop retrofit solutions that balance energy efficiency and financial feasibility. By achieving these objectives, this research provides a robust decision-support framework to guide cost-effective and sustainable retrofit planning for Montpetit Hall, while also offering a transferable methodology applicable to similar complex institutional buildings.

This thesis introduces several unique contributions that make it different from previous studies on building retrofits and optimization:

1) Complexity of the building geometry and functions

Montpetit Hall's design incorporates two expansive glazed façades positioned at non-orthogonal angles, creating challenging conditions for modeling solar gains and daylighting effects. In addition, it is a large, multi-functional facility that houses a diverse mix of spaces, including classrooms, offices, laboratories, a swimming pool, a gymnasium, locker rooms, and extensive circulation areas. Each of these zones operate under distinct schedules, internal load profiles, and ventilation requirements. Capturing this diversity demanded meticulous data collection and highly detailed zoning in the simulation model, making the analysis considerably more comprehensive than conventional single-use case studies.

2) Detailed HVAC system modeling with thirteen unique AHUs

The building is served by thirteen distinct air handling units (AHUs), each characterized by unique configurations, control strategies, and zone assignments. Rather than simplifying these systems into a single generic HVAC representation, this research modeled each AHU individually, incorporating its coils, fans, outdoor air strategy, and HR potential. This system-level detail enabled the analysis to capture the distribution of energy consumption across the building and to evaluate how retrofit measures influence the performance of each AHU differently.

3) Multi-objective optimization combining energy and economics

This research employs a multi-objective optimization approach that simultaneously evaluates energy savings and economic performance. By applying Pareto front analysis, the study identifies solutions that balance energy use and cost, providing clear insights into trade-offs, for example, how much additional investment is justified to achieve a given level of savings.

In summary, the contribution of this thesis lies in uniting building complexity, system-level detail, and rigorous multi-objective optimization within a single framework. This integration moves beyond the limitations of studies that examine these aspects individually and provides a more realistic and transferable basis for retrofit analysis. The resulting framework offers practical guidance for cost-effective and sustainable retrofit strategies in cold-climate institutional buildings.

1.3. Thesis Structure

Chapter 2 – Literature Review

This chapter situates the study within the broader academic and professional discourse on building energy retrofits in heating dominated climates. It synthesizes knowledge on energy use profiles, retrofit potential, and barriers in institutional buildings, classifies retrofit strategies into passive, active, and renewable categories, and reviews building energy modeling and optimization frameworks. It also highlights economic and environmental assessment methods, providing the theoretical foundation for the research.

Chapter 3 – Methodology

Chapter 3 presents the methodological framework adopted for the study. It introduces Montpetit Hall as the case study, details the creation of a detailed building energy model, and outlines inputs such as geometry, construction, occupancy, and HVAC system specifications. The chapter further describes the optimization process using NSGA-II, as well as the integration of life-cycle cost analysis, thereby establishing a robust framework for evaluating retrofit scenarios.

Chapter 4 – Discussion and Results

This chapter reports and analyzes the findings of the study. It begins with model calibration against measured data, followed by evaluation of envelope and window retrofit solutions, HVAC strategies, and renewable energy measures. Optimization outcomes are presented in terms of energy savings, cost, and trade-offs, complemented by an economic feasibility assessment. The results collectively demonstrate the performance and financial implications of different retrofit pathways for Montpetit Hall.

Chapter 5 – Summary and Conclusions

The final chapter synthesizes the main findings of the research. It summarizes the methodological approach, discusses the significance of the results, and draws conclusions on the feasibility and impact of deep energy retrofits in cold-climate institutional buildings. Limitations of the study are acknowledged, and directions for future research are proposed, emphasizing the potential for scaling the framework to similar building types.

2. Literature Review

2.1. Introduction and Context

The building sector is a major contributor to global energy use and climate change. In 2022, it accounted for approximately 30% of final global energy consumption and 28% of energy-related carbon dioxide (CO_2) emissions, including both operational and embodied sources [34]. These emissions stem largely from space heating, cooling, ventilation, lighting, and equipment loads. As a result, improving building energy efficiency has become a central priority in international sustainability agendas, including the United Nations Sustainable Development Goals (SDGs) and the Paris Agreement.

Within this context, retrofitting existing buildings is widely recognized as one of the most effective strategies for reducing energy consumption and associated emissions. Unlike new construction, retrofits involve upgrading systems and components within existing structures, simultaneously improving performance, extending lifespan, and reducing operating costs. However, large institutional buildings present unique challenges for retrofitting due to their size, diverse space functions, and operational constraints. These challenges are particularly pronounced in cold climates, where space heating can account for more than half of total building energy demand, and envelope as well as mechanical systems must perform reliably under prolonged and severe thermal conditions [35].

Montpetit Hall, a mixed-use institutional building at the University of Ottawa, provides a relevant case study for retrofit assessment. The building supports athletic, academic, and administrative functions and exhibits many typical features of older institutional buildings, including poor insulation, outdated HVAC systems, and high energy use intensity (EUI). This research explores a multi-stage energy retrofit framework to reduce Montpetit Hall's energy consumption and associated environmental impact. The framework includes optimization of envelope and window parameters using a multi-objective genetic algorithm (NSGA-II), followed by active system retrofitting (HVAC), integration of renewable energy systems, and economic feasibility assessment.

2.2. Building Energy Use and Retrofit Potential in Heating Dominated Climate

Heating-dominated climates pose unique challenges for building performance, with space heating often representing more than half of total energy demand. The severity and duration of winter conditions place considerable pressure on envelopes' integrity and mechanical systems, making efficiency improvements particularly impactful in these contexts. In Canada, where heating is required for much of the year, the commercial and institutional sector consumed over 937 PJ of energy in 2021, with space heating alone accounting for more than 50% of this total. Reliance on natural gas in provinces such as Alberta and Ontario further underscores the urgency of decarbonization, despite cleaner grids in provinces like Quebec and British Columbia [36].

Institutional buildings, and university campuses in particular, are among the most energy-intensive typologies. Their diverse mix of classrooms, laboratories, recreational spaces, and offices, combined with year-round operation, results in high energy use intensities (typically 1.5–2.0 GJ/m^2/year) and significant carbon footprints [37]. Many of these facilities are also characterized by aging envelopes and outdated HVAC systems, leading to thermal losses of up to 60% [38]. Addressing these inefficiencies demands retrofit interventions guided by multi-objective frameworks that balance energy savings, occupant comfort, and cost [39]. However, [40]. These climatic pressures necessitate high-performance envelope systems, triple-glazed fenestration, smart ventilation with HR, and airtight, insulated structures supported by advanced climate-responsive modeling tools like Energy Plus, and Design Builder [41].

Despite the availability of advanced solutions such as airtight envelopes, triple glazing, and HR ventilation, retrofit implementation in Canada remains limited. Current rates are below 1% of the building stock per year, well short of the 3–5% required to meet 2030 climate targets [42]. Accelerating this transition will require phased strategies, policy support, and innovative financing mechanisms. University campuses, with centralized governance and high public visibility, are well positioned to act as living laboratories for retrofit innovation and to demonstrate scalable pathways for the broader institutional sector.

2.3. Barriers to Retrofitting Institutional Buildings

Retrofitting institutional buildings is widely recognized as a critical strategy for reducing carbon emissions and improving energy performance, but implementation in cold-climate contexts is particularly challenging [43]. Large, continuously operated, and mixed-use university facilities must contend with intersecting technical, operational, and financial barriers, while also managing aging infrastructure, legacy systems, and governance structures that complicate decision-making [44]. These conditions make such campuses both prime candidates for deep retrofits and complex settings where successful implementation depends on integrated planning, long-term investment, and coordinated action across multiple stakeholders.

One of the most significant obstacles arises from architectural and structural constraints. One of the most significant barriers relates to architectural and structural constraints. Constructed prior to the adoption of Canada's first national energy code in 1997, many institutional buildings have envelopes that are poorly insulated and not airtight, leading to substantial heat losses, high heating demand, and compromised indoor comfort [32]. In some cases, heritage preservation requirements further restrict façade alterations or window replacements [45]. Structural limitations can also prevent the addition of rooftop solar panels, while incomplete or outdated documentation such as mechanical drawings or structural load data introduces additional uncertainty. Limited ceiling and shaft space make it even more difficult to integrate modern ductwork and ventilation systems. [46] emphasize that these architectural realities require case-specific engineering solutions that increase both design complexity and costs.

Occupancy and operational scheduling present another major challenge. University buildings rarely close, operating year-round to accommodate teaching, research, administration, athletics, and community functions. This continuous use narrows the construction windows available for retrofitting, often limiting work to short summer breaks or requiring phased implementation over several years. Different zones within the same building also have distinct thermal, lighting, and air quality requirements, complicating the application of uniform HVAC or control strategies [47], [48]. [49] emphasize that zoning-aware design and phased planning are essential to minimize disruption, particularly in critical spaces such as laboratories and computer facilities.

Financial and funding limitations remain among the most cited barriers. Although retrofits yield clear long-term benefits, universities often face difficulties in securing upfront capital as energy projects compete with academic expansions, technology upgrades, and deferred maintenance. Dedicated retrofit budgets are uncommon, while complex instruments such as performance contracts or public–private partnerships can be difficult to structure. Uncertainty in future energy prices further complicates investment appraisals based on NPV and internal rate of return (IRR) [50]. While mechanisms like green bonds, energy service companies (ESCOs), and carbon financing exist, uptake in the post-secondary sector remains limited due to procurement rules and institutional risk aversion [51].

Cold-climate conditions add another layer of complexity. In Ottawa, for example, heating degree days (HDD) regularly exceed 4,500, making space heating the dominant end-use. Improving envelope performance is critical, yet winter conditions introduce risks such as snow accumulation, freeze–thaw cycles, and thermal bridging. Solar PVs, effective in warmer climates, underperform in northern latitudes due to low winter solar incidence. Retrofits must therefore emphasize airtightness, high-efficiency heating systems, and advanced technologies such as HR ventilation (HRV) and ground-source heat pumps [52]. [53] recommend incorporating passive solar design, optimized window orientation, and winter-specific energy modeling to maximize retrofit performance.

Finally, data and modeling limitations hinder effective planning. Building energy simulations are indispensable for evaluating retrofit strategies, yet their accuracy often suffers from incomplete or unreliable inputs. Common gaps include outdated utility records, missing occupancy schedules, and insufficient sub-metering, all of which contribute to performance gaps between predicted and actual savings. [54], highlights the importance of improved calibration using on-site measurements, occupancy profiling, and continuous commissioning. Emerging approaches that combine Building Energy Modeling (BEM) with machine learning show promise in reducing these discrepancies by adapting models to observed building behavior. [51] further argues that investment in digital infrastructure, including sub-metering, IoT devices, and performance dashboards, is critical to bridging the gap between design intent and operational outcomes.

2.4. Classification of Retrofit Strategies: Passive, Active, and Renewable

Retrofit strategies in buildings are commonly grouped into three categories: passive, active, and renewable energy interventions. This tripartite classification provides a systematic approach to achieving energy savings in both new and existing buildings, particularly in cold climates where heating loads dominate [55].

Passive retrofit strategies aim to reduce energy demand by improving the thermal performance of the building envelope. Typical measures include upgrading insulation, improving airtightness, minimizing thermal bridging, reducing infiltration, and installing high-performance windows [56]. In cold climates, these interventions are prioritized because they directly lower baseline energy use and enhance the effectiveness of subsequent active and renewable upgrades [57]; [58]. For instance, exterior insulation and replacement of poorly sealed windows can reduce heating loads by up to 40% in older institutional buildings.

Active retrofit strategies target improvements in mechanical and electrical systems. Examples include upgrading HVAC systems with high-efficiency boilers and chillers, implementing DCV, converting constant air volume (CAV) to variable air volume (VAV) systems, and deploying advanced control strategies through building automation [59]; [32]. Lighting retrofits such as LEDs, occupancy sensors, and daylight harvesting also fall into this category. Active measures respond dynamically to occupancy and climate conditions and typically achieve the greatest impact when implemented after passive measures have already reduced thermal loads.

Renewable energy retrofits introduce on-site generation to decrease reliance on fossil fuels and grid electricity. Technologies include solar PV systems, solar thermal collectors, photovoltaic-thermal (PVT) hybrids, geothermal heat pumps, and biomass boilers [60]; [61]. In cold climates, however, their performance must be adjusted for challenges such as snow accumulation, reduced daylight hours, and seasonal variability [62]. Appropriate siting, tilt optimization, and de-icing strategies are therefore necessary to maximize yield.

The International Energy Agency [22] recommends a sequential retrofit pathway:

1. Implement passive measures to reduce energy demand.
2. Upgrade active systems to improve efficiency.
3. Apply renewable technologies to meet remaining loads.

This stepwise framework ensures cost-effectiveness, thermal comfort, and meaningful reductions in energy consumption.

For university buildings, this classification is particularly relevant due to their diverse space functions and operational patterns. Dormitories and offices may benefit most from passive upgrades, while laboratories or gymnasiums with high internal gains may require active or renewable solutions [63]. Beyond guiding technical interventions, this framework also supports multi-objective optimization studies, such as the present analysis of Montpetit Hall, where trade-offs between energy savings, cost, and comfort are systematically evaluated across passive, active, and renewable strategies.

2.5. Passive Envelope Retrofit Strategies

In cold climates, where heating dominates building energy demand, passive retrofitting represents the foundation of effective energy renovation. These strategies enhance envelope performance, reduce heat loss, and improve thermal comfort without relying on mechanical systems. They are often prioritized in retrofit frameworks due to their cost-effectiveness, durability, and ability to reduce both the capacity and operating requirements of active systems [64]; [14].

Insulation improvements in walls, roofs, floors are among the most impactful measures. In older institutional buildings, these upgrades can reduce heating energy demand by 30–50%, depending on climate severity and baseline conditions [65]. Better insulation also stabilizes indoor temperatures, limiting thermal drift and improving occupant comfort. Equally important is airtightness, since uncontrolled infiltration through aged windows, construction gaps, and poorly sealed joints significantly undermines energy performance. Blower door testing is commonly used to identify leakage points, which can then be treated with membranes, weatherstripping, and advanced sealing solutions [66].

While tighter buildings reduce infiltration, they must be paired with controlled ventilation to maintain indoor air quality. Heat recovery ventilators (HRVs) and energy recovery ventilators (ERVs) provide this balance by ensuring fresh air supply without excessive energy loss. Another critical consideration is the mitigation of thermal bridging in structural components such as floor slabs, window headers, and steel columns. Detailing that incorporates thermal breaks or continuous exterior insulation can reduce heating demand by 5–15% [59]; [67].

Windows are a particularly sensitive element of the envelope, often responsible for 25–30% of total heat loss in older institutional facilities [64]. Replacing outdated units with triple-pane glazing, low-emissivity (low-e) coatings, and argon or krypton fills can drastically improve U-values and reduce conductive losses. In cases where full replacement is restricted by heritage status or limited budgets, secondary glazing or low-e films offer cost-effective alternatives [23]. Performance also depends on sealing and installation quality, including the use of thermally broken frames and gaskets to minimize leakage. In addition to reducing losses, windows influence solar gain. While winter sunlight can offset heating demand, uncontrolled gains on south- and west-facing façades may cause overheating during transitional seasons. Spectrally selective coatings and dynamic shading systems help manage this balance, improving both thermal and visual comfort [68].

Beyond direct energy savings, passive envelope retrofits deliver co-benefits such as improved acoustics, fewer drafts, enhanced comfort, and increased property value. These outcomes strengthen the overall return on investment and support broader sustainability goals on university campuses [69]. Importantly, multiple reviews highlight that passive strategies should be implemented early in the retrofit process, as they reduce baseline loads and set the stage for more efficient active systems and renewable energy integration [64].

2.6 Active HVAC Retrofit Strategies

Heating, ventilation, and air-conditioning (HVAC) systems are among the most energy-intensive components in institutional buildings, often responsible for more than 50% of total energy use in cold climates such as Canada [70]. Retrofitting these systems is therefore a critical pathway to reducing operational energy demand, improving thermal comfort, and advancing institutional decarbonization goals. Numerous studies highlight HVAC retrofits as among the most cost-effective energy conservation measures, particularly when integrated into broader frameworks that also address envelope and passive upgrades [71]; [72] .

A widely applied strategy is DCV, which dynamically adjusts airflow according to occupancy and indoor air quality, typically measured by CO_2 sensors. By avoiding over-ventilation of underused spaces, DCV reduces unnecessary conditioning of outdoor air, a major thermal load in heating-dominated climates. Meta-analyses report HVAC energy savings of 20–40%, making DCV particularly effective in educational facilities with highly variable occupancy [73].

Another impactful measure is the conversion from CAV to VAV systems. Whereas CAV systems deliver fixed airflow regardless of demand, VAV systems modulate supply to meet zone-level requirements. This flexibility reduces fan energy, minimizes reheat loads, and enhances thermal zoning. [74] and [75] report fan energy savings of up to 50% in large, multi-zone buildings, making this strategy particularly relevant for complex facilities such as Montpetit Hall.

Economizer systems have become increasingly important in boosting energy efficiency for commercial and institutional buildings, especially within HVAC operations. Recent research highlights how using smart, data-driven controls can significantly improve their performance [76]. When integrated with building automation, economizers can adapt in real time to environmental changes, enhancing both energy savings and indoor comfort [77]. Still, their success largely depends on proper maintenance and how well the system matches local climate conditions [78].

Heat recovery systems in HVAC setups are increasingly used in commercial and institutional buildings to reduce energy consumption by reusing exhaust heat. Recent research emphasizes the integration of these systems with smart controls to enhance their efficiency. Advanced designs like rotary heat exchangers have shown strong potential in real-world case studies [79].

Crucially, HVAC retrofits are most effective when implemented within a multi-stage retrofit framework. When combined with passive envelope improvements and window upgrades, HVAC enhancements deliver synergistic benefits: lower baseline loads, opportunities for equipment downsizing, and extended system lifespans. [80] note that such integrated approaches not only maximize energy savings but also improve lifecycle cost-effectiveness and resilience.

In summary, HVAC modernization is a cornerstone of high-performance retrofits in institutional buildings. Its full potential is realized through advanced controls, high-efficiency components, and coordinated integration with passive measures and occupancy dynamics. As universities and other institutions pursue net-zero targets, HVAC retrofits will remain central to both energy and climate performance.

2.7. Renewable Solar-Based Renewable Strategies

Integration of solar-based renewable energy systems and green infrastructure provides a practical pathway toward decarbonization, grid independence, and long-term sustainability. When implemented alongside passive and active measures, technologies such as PV panels, PVT systems, solar thermal collectors, and green roofs can significantly enhance both building performance and campus-wide environmental objectives.

2.7.1. PV Systems

PVs are among the most widely adopted renewable technologies in institutional retrofits because of their scalability, modularity, and rapidly declining costs. In cold climates such as Canada, year-round effectiveness requires design strategies that address snow accumulation, low winter irradiance, and shading from nearby structures [81]. Recent research highlights that optimizing tilt angles and using bifacial modules can substantially improve winter performance by capturing reflected snow albedo [82]. Even under snow-prone conditions, PV installations in university buildings can offset 20–40% of annual electricity demand, with the greatest contributions during non-heating seasons when lighting and cooling loads dominate [83].

2.7.2. PVT Systems

Hybrid PVT systems maximize rooftop potential by generating both electricity and heat from solar radiation. In cold climates, this dual output provides a distinct advantage over PV-only systems, supplying electricity while also meeting domestic hot water (DHW) and preheating needs during sunny but cold conditions. PVT panels operate more efficiently because active cooling improves electrical performance while simultaneously delivering useful thermal energy [84]. Reported system efficiencies often exceed 60%, making them well suited to institutions with high, year-round energy demand [85], [86]. Integration with thermal storage and smart controls further enhances load shifting and carbon reduction potential.

2.7.3. Solar Thermal Collectors

Solar thermal collectors, including flat-plate and evacuated tube designs, are well established for DHW production and, in some cases, space heating. Although output is lower during peak winter months, these systems perform effectively during spring and fall when solar availability aligns with moderate heating requirements. Compared with PVT, stand-alone thermal collectors are simpler and generally less expensive, with efficiencies ranging from 40–70% depending on design and operating conditions [30]. In cold climates, reliability depends on insulated piping, freeze protection, and efficient heat exchangers. They are particularly cost-effective in buildings with high DHW demand such as residence halls, gyms, and dining facilities.

2.7.4. Green Roof Systems

While green roofs do not directly generate energy, they contribute indirectly to institutional retrofit performance. Benefits include enhanced roof insulation, reduced conductive heat loss in winter, mitigation of urban heat island effects, improved stormwater management, and extended roof membrane lifespans [87]. Green roofs also support PV and PVT performance by reducing rooftop temperatures in summer, which improves panel efficiency. Several Canadian universities have implemented green roofs not only for energy and environmental gains but also for co-benefits such as biodiversity, aesthetics, and student engagement [88].

2.8. Building Energy Modeling: Design Builder and Energy Plus

Recent literature increasingly positions the integration of Design Builder and Energy Plus at the forefront of building energy modeling (BEM), especially in the context of retrofit evaluations. Design Builder's intuitive interface, combined with Energy Plus's robust simulation engine, enables detailed analysis of thermal performance, HVAC systems, and energy consumption under varying retrofit conditions [89]. This combination has been widely adopted for assessing energy-saving interventions across diverse building types, including healthcare, residential, and office structures [90];[90]. Researchers emphasize the value of coupling these tools with sensitivity analysis and calibration procedures to enhance accuracy [91]. Moreover, the integration with BIM platforms is streamlining workflows, reducing manual inputs, and supporting automated data exchanges [92]. Despite their strengths, studies note that precise modeling still relies heavily on data quality and user expertise [93]. Together, Design Builder and Energy Plus provide a comprehensive toolkit for performance-based retrofit planning and decision-making. Their continued development supports the growing demand for low-carbon, high-efficiency building upgrades aligned with global sustainability goals. For this thesis, Design Builder and Energy Plus were selected for their complementary strengths, supporting robust and validated modeling of retrofit scenarios at Montpetit Hall.

2.9. Optimization Frameworks in Building Retrofit

Optimization frameworks have become central to the energy-efficient retrofit of buildings, particularly in institutional settings where diverse and often conflicting objectives must be reconciled. These include reducing energy consumption, minimizing costs, lowering emissions, and maintaining occupant comfort. Unlike sequential or heuristic approaches, optimization frameworks employ systematic methodologies to identify Pareto-optimal solutions, making trade-offs between objectives explicit and transparent [94].

Multi-objective optimization (MOO) methods, including the Non-Dominated Sorting Genetic Algorithm II (NSGA-II) and Multi-Objective Particle Swarm Optimization (MOPSO), have become prominent tools in building retrofit research, as they effectively capture the complexity and nonlinearity inherent in building performance analysis. For example, [95] developed a two-stage optimization framework for Chinese school buildings that combined an artificial neural network (ANN) meta-model with NSGA-II to optimize envelope design and PV systems. Their results demonstrated that meta-models significantly reduce simulation time while preserving solution accuracy.

[96] advanced this approach by integrating MOO with energy simulations to optimize retrofits in Canadian institutional buildings. Their framework evaluated multiple energy conservation measures (ECMs) and quantified trade-offs among energy, cost, and environmental performance. By linking evolutionary algorithms with simulation tools such as Energy Plus, the method captured seasonal and dynamic effects that are particularly important in cold climates.

The increasing complexity of building energy retrofits has encouraged the adoption of multi-stage optimization frameworks, which divide the decision-making process into manageable phases to improve both efficiency and accuracy. Early contributions by [18], [59] illustrated how two- and three-stage genetic algorithm approaches could progressively integrate envelope upgrades, HVAC improvements, and renewable energy systems, significantly reducing computation times without compromising the quality of retrofit decisions. Later studies emphasized the role of computational enhancements: for instance, [97] and [98] showed that parallelized multi-objective algorithms could accelerate optimization workflows for residential buildings while maintaining robust solutions. More recently [99] advanced this discourse by examining how different model simplifications such as thermal zoning, HVAC idealization, material R-value approximations, and geometric abstractions perform within a parallel NSGA-II framework. Their findings revealed that a three-zone model provided a practical balance, cutting optimization time by around 40% while keeping prediction errors within acceptable ranges. In contrast, aggressive simplifications, such as the shoebox model, drastically reduced computation time but at the expense of substantial inaccuracies. These outcomes align with previous evidence that zone aggregation can underestimate energy use by 10–35% and that simplified HVAC assumptions may produce errors exceeding 90% in cooling predictions. Collectively, this body of research demonstrates that multi-stage optimization, when complemented by careful model simplification and parallel computing, represents a promising pathway for scalable, cost-conscious, and reliable energy retrofits.

Optimization frameworks have also been applied to the integration of renewable energy systems. For instance, used NSGA-II to evaluate combinations of passive and active measures, including PV installations and window retrofits, balancing cost, energy efficiency, and thermal comfort. The strength of NSGA-II lies in its ability to maintain population diversity while converging toward optimal fronts, making it a standard tool in retrofit optimization research.

2.10. Economic and Environmental Assessment of Building Retrofits

Economic and environmental assessments are fundamental for determining the feasibility, prioritization, and long-term value of building retrofits. This is particularly relevant in cold climates, where heating demands dominate, and intervention costs can be substantial. Institutional buildings, including universities, face dual pressures of limited budgets and increasing sustainability mandates. Integrating cost–benefit analyses with environmental metrics provides a more balanced basis for decision-making [59].

In recent years, the financial evaluation of building retrofit strategies has increasingly adopted structured tools such as Net Present Value (NPV), IRR, and Life Cycle Cost Analysis (LCCA). NPV offers a measure of net financial gain by weighing future energy savings against both initial capital and recurring operational costs, while IRR serves as an indicator of investment attractiveness when compared to alternative financial [100]. LCCA further expands this analysis by incorporating the full cost trajectory of a retrofit project, including long-term elements such as maintenance, replacements, and energy cost escalation [101]. Recent findings highlight that even capital-intensive interventions, particularly those targeting envelope and HVAC systems can yield internal rates of return that meet or exceed market expectations, supporting their economic viability in institutional and commercial settings [102]. In cold climates, payback periods are often shorter because extended heating seasons amplify energy savings. Upgrades to insulation, airtightness, glazing, and HVAC systems can justify investments within 8 to 15 years in public-sector institutions [59].

In summary, combining economic and environmental assessments provides a comprehensive foundation for retrofit planning in cold-climate institutional buildings. This integrated approach supports fiscal responsibility while aligning with climate objectives, and it strengthens access to green financing, performance contracting, and incentive programs, thereby reinforcing the business case for deep retrofits.

3. Methodology

3.1 Methodology Overview

This thesis investigates a deep energy retrofit of a multifunctional institutional building situated in Ottawa, a heating-dominated climate. The extreme seasonal temperature variations present considerable challenges for energy efficiency, making the development of effective retrofit strategies particularly crucial. In this regard, the research adopts a structured framework integrating simulation and optimization tools, using Design Builder, Energy Plus, and MATLAB.

The process begins with the development of a detailed building energy model. Building geometry and spatial configuration are generated, and material properties and construction assemblies are defined using physical and architectural specifications. All modeling tasks are conducted in Design Builder, which provides a user-friendly interface for preparing inputs compatible with Energy Plus. Once the geometry and construction details are established, the model is exported to Energy Plus for dynamic simulation of baseline energy performance. These simulations incorporate local climatic conditions, occupancy schedules, internal loads, and system operations to provide a comprehensive assessment of current energy use

The research then advances to an optimization phase. Key design and operational variables are identified, and objective functions are defined with an emphasis on minimizing energy use intensity and life-cycle cost. A two-staged optimization process is applied. First, the NSGA-II is executed through MATLAB to conduct iterative simulations and extract Pareto-optimal solutions. This is followed by a scenario-based analysis that evaluates two major strategies: HVAC system retrofits and the integration of renewable energy technologies. Ultimately, the optimized scenarios are evaluated in comparison to determine the solutions that provide the greatest balance of effectiveness and economic feasibility. This ensures that selected retrofit strategies achieve energy performance targets while remaining consistent with practical constraints and long-term sustainability objectives (Figure 3.1).

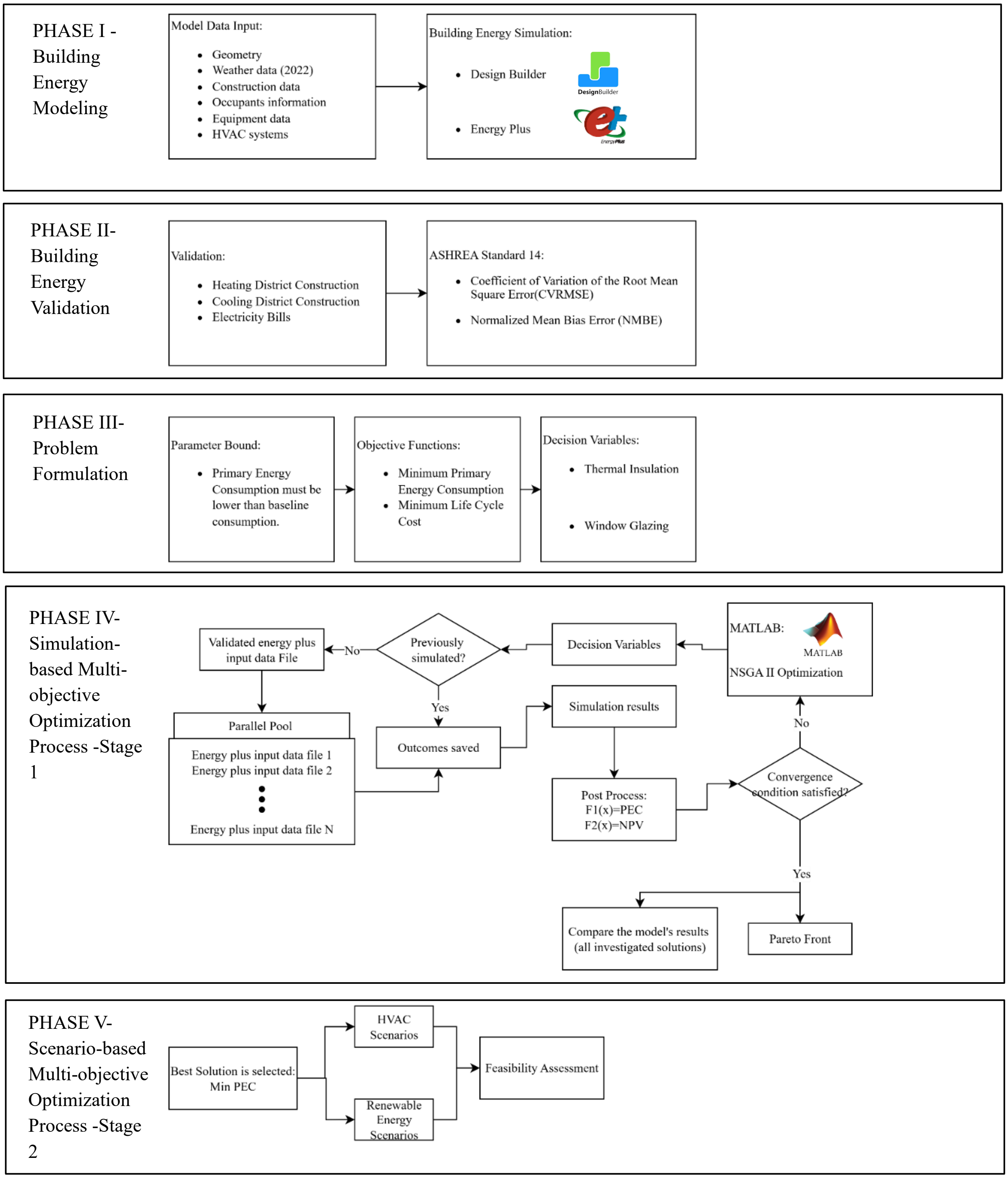

Figure 3. 1 Methodology Framework

3.2 Case Study Building

The case study for this research is Montpetit Hall, a mixed-use institutional facility situated on the University of Ottawa campus (see Figure 3.2). Completed in 1972, the building accommodates both academic and athletic functions, housing the Faculty of Health Sciences as well as the university's varsity athletic programs (Gee-Gees). It occupies a site of approximately 3,583 m² and provides a total floor area of 17,096 m².

Figure 3. 2 Montpetit Building and Site Outline

Montpetit Hall is a complex facility comprising four above-grade floors and two below-grade levels, with a maximum elevation of approximately 24 m. The building's L-shaped core structure is complemented by two adjoining bays that accommodate a double-height gymnasium and an Olympic-sized swimming pool, with elevations of 9 m and 13.5 m, respectively. In addition, the facility is physically integrated into the broader campus network, with enclosed walkways on the second level connecting it to the University Centre to the north and Lamoureux Hall to the east.

Architecturally, the building features a poured concrete exterior, with the south- and west-facing façades treated with solar-reflective paint to mitigate solar radiation heat gains. Half of the roof surface has been upgraded with a two-ply asphalt membrane as part of a partial roofing system replacement. The façade design incorporates fenestration strategies that reduce cooling demand in the summer and enhance passive heating in the winter. Specifically, windows on the south- and west-facing elevations are installed at a 23° inclination to minimize solar gain during summer when the incident sunlight angle reaches 68° (on July 21 in Ottawa), while allowing greater solar penetration during winter months when the angle drops to as low as 21°.

The south-facing elevation has a total surface area of 2,027 m^2, with 18% fenestration and 1% dedicated to mechanical openings and hatches. The west-facing façade spans 2,046 m^2 with 28% fenestration and 2% attributed to service access points. The east-facing wall measures 2,009 m^2 and includes 18% window coverage and 1% for openings. This façade includes a small sloped tin roof segment and is partially shaded by trees, which reduces solar gains. The north wall, approximately 2,027 m^2, contains 15% fenestration and 3% openings. Most of the windows are tinted or polarized to further control solar heat gains.

In terms of thermal behavior, façade absorptance varies by surface: the painted south and west façades absorb only 15% of incident solar radiation, whereas the untreated concrete façades absorb significantly more. With the exception of the inclined south and west glazing, all walls are vertically aligned at 90° to grade. Tin flashing, door and window frames, are painted dark brown to increase wintertime solar absorption and reduce ice accumulation risks.

Montpetit Hall is intensively used year-round. It supports approximately 4,100 occupants daily and includes space for around 1,500 students in classrooms and auditoriums. Athletic facilities include three basketball courts, a public gym, a dance studio, a martial arts room, and a high-performance training area adapted from former squash courts. During peak events, the building can accommodate up to 2,000 spectators. Internally, it includes large gender-specific changing rooms, steam-heated saunas, faculty offices, research laboratories, and two large auditoriums (each with 244 seats) added in the 1990s. The building also supports the academic needs of the nutrition and human kinetics departments within the Faculty of Health Sciences.

Figure 3. 3 South Facing Wall

Figure 3. 4 West Facing Wall

The sun path diagram (Figure 3.5) generated for Ottawa (latitude 45.42°N, longitude 75.7°W) reveals the substantial seasonal variation in solar altitude and azimuth, and its implications for passive solar building strategies. At the winter solstice, the solar elevation peaks at approximately 20° at local noon. This low-angle solar incidence is particularly conducive to deep penetration of sunlight through south-facing apertures, optimizing passive solar heat gains during periods of peak heating demand. Despite the reduced photoperiod, the alignment of solar access with thermal necessity renders winter solar geometry particularly advantageous for heating-dominated climates such as Ottawa's.

Conversely, during the summer solstice, solar elevations exceed 65° at noon, with extensive daylight duration. While this could lead to undesirable overheating, the high solar altitude facilitates effective mitigation via horizontal overhangs or fixed shading elements, reducing cooling loads without sacrificing daylight quality. At the equinoxes, the solar altitude stabilizes near 45° at midday, offering a balanced condition for transitional-season heating and lighting strategies.

This seasonal solar trajectory supports climate-responsive architectural design, emphasizing orientation, glazing optimization, and passive control mechanisms to maximize wintertime gains while curbing summertime overheating. The local solar geometry, as visualized in the sun path chart, informs envelope and fenestration strategies critical for energy-efficient building performance in Canadian climatic contexts.

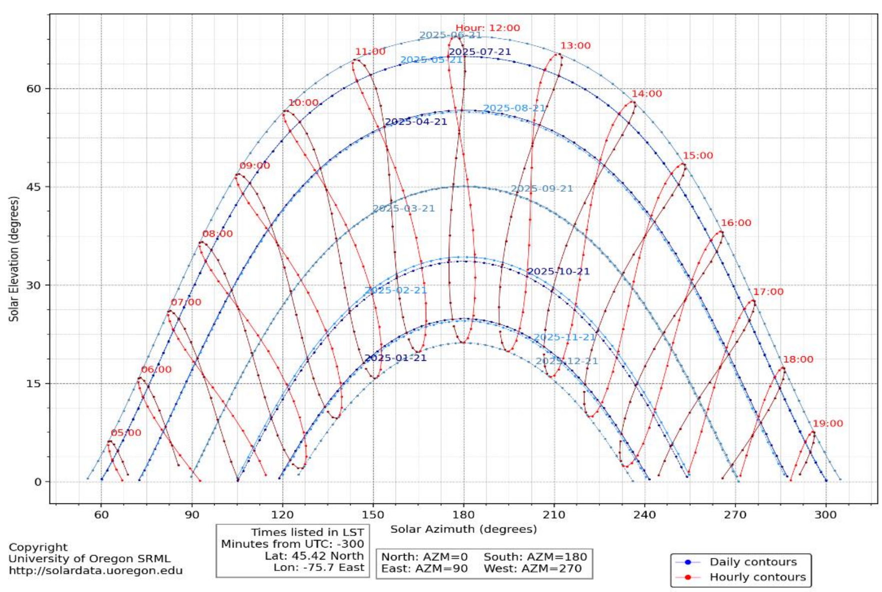

Figure 3. 5 The Sun Path Diagram of Ottawa

In the following, the reasons for selecting this building are outlined:

Montpetit Hall was chosen as the case study for this thesis due to a set of interconnected architectural, operational, and environmental factors that make it an ideal candidate for evaluating solar-based energy retrofits in a Canadian institutional context. The justification is presented below in numbered format, with each point elaborating a specific rationale for the selection:

1. High Energy Consumption Due to Building Function

Montpetit Hall houses a variety of energy-intensive facilities, including a large indoor swimming pool, fitness center, gymnasium, classrooms, and office spaces. These functional zones require extensive heating, ventilation, dehumidification, and lighting, particularly for the pool and gym areas. While official building-level consumption data is not publicly available, anecdotal and operational sources suggest that Montpetit Hall is among the highest energy consumers on campus, drawing a substantial load from the university's central power plant. High-occupancy recreational buildings typically exhibit energy use intensities (EUIs) that are 2–4 times greater than standard academic buildings [103].

2. Aging Building Envelope and System Inefficiencies

Constructed several decades ago, Montpetit Hall was built to legacy energy performance standards and is likely to have under-insulated walls, single or double glazing without low-e coatings, and limited air sealing. These outdated construction features contribute to heat loss, uncontrolled solar gains, and occupant discomfort, particularly in Ottawa’s winter climate. This makes the building a suitable target for envelope retrofits, HVAC upgrades, and solar optimization measures [104].

3. Architectural and Operational Complexity

The building’s geometry, functions, and systems make it one of the most complex facilities on campus. Its design integrates an L-shaped core with large-volume spaces for the gymnasium and Olympic pool, while also supporting academic functions such as classrooms, laboratories, and offices. This diversity results in highly variable internal loads, operating schedules, and ventilation requirements, which complicate both modeling and retrofit planning. Such complexity underscores the value of using Montpetit Hall as a testbed for simulation-based optimization, as insights gained here can be transferred to other large, multifunctional institutional buildings.

4. Favorable Orientation for Passive Solar Optimization

The building features a prominent south-facing façade, which enables effective implementation of passive solar strategies such as daylighting, winter solar gain, and seasonal shading control. This spatial orientation aligns well with solar path chart analysis and building envelope optimization simulations, making Montpetit Hall an excellent candidate for geometry-informed design evaluation.

5. Location in a Heating-Dominated Climate

Ottawa experiences long, cold winters with significant heating loads and relatively short summers, which makes the optimization of passive solar heat gain particularly valuable. In heating-dominated climates, buildings benefit from design strategies that maximize solar gain in winter while minimizing cooling demand in summer through appropriate shading [105]. This climatic context strengthens the relevance of solar path-based retrofitting for Montpetit Hall.

6. Broader Relevance

Over 60% of Ontario's educational buildings were constructed before 1980. Insights from this study can guide retrofits of similar mid-century institutional buildings across North America [106].

These factors make Montpetit Hall a high-value subject for deep energy retrofit analysis and simulation-based performance enhancement.

7. Alignment with Institutional Sustainability Goals

The University of Ottawa has declared goals to reduce greenhouse gas emissions and improve energy efficiency as part of its broader sustainability mandate. Selecting Montpetit Hall for retrofit investigation aligns with these institutional objectives and supports evidence-based decision-making toward achieving carbon neutrality.

3.3 Geometry Modeling

Accurate representation of a building's geometry forms the foundation of reliable energy modeling and performance analysis. For Montpetit Hall, the three-dimensional model was developed using Design Builder, a graphical user interface for Energy Plus, to capture the architectural and spatial characteristics essential for thermal simulation.

The modeling process began with the preparation and simplification of architectural drawings. Auto CAD file of the building layout was modified to eliminate extraneous elements and ensure compatibility with the Design Builder environment. The processed file was then imported into the software to generate a preliminary 3D representation of Montpetit Hall, as illustrated in Figures 3.6 through 3.11. This model reflects the actual spatial organization and elevation of the structure, including its complex L-shaped layout and various attached volumes.

Once the base geometry was established, building envelope and internal construction materials were defined within the software. These definitions included wall assemblies, roof types, window properties, and internal partitions, based on a combination of as-built documentation and engineering assumptions. Material properties were assigned to each surface element, ensuring consistency with real-world performance characteristics.

Following this, thermal zoning was carried out. The original architectural spaces were assessed and merged where appropriate to form thermally homogeneous zones. Zoning decisions were guided by functional use, orientation, and occupancy schedules, with the aim of reducing the total number of zones without sacrificing analytical granularity. This step is critical for reducing computational complexity while maintaining simulation accuracy, particularly in a building as functionally diverse as Montpetit Hall.

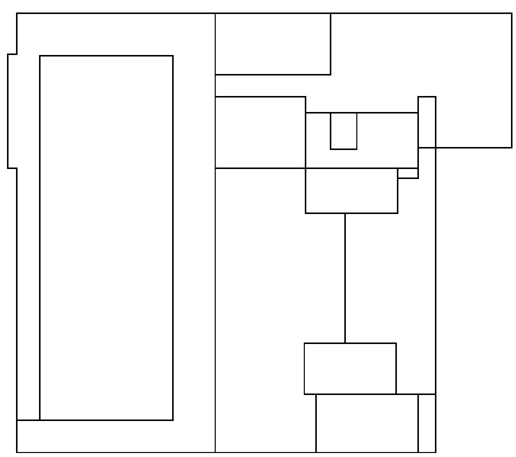

Figure 3. 6 Second basement plan (Underground)

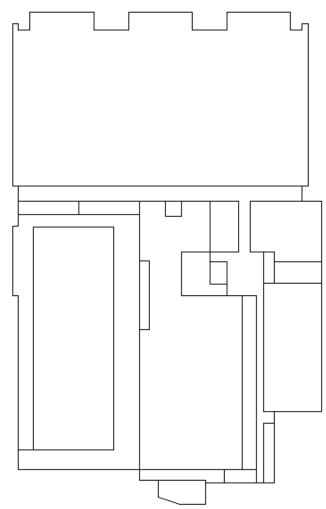

Figure 3. 7 First basement plan (Underground)

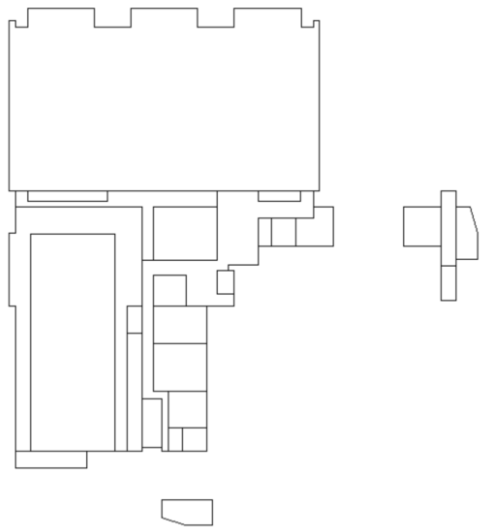

Figure 3. 8 First floor plan

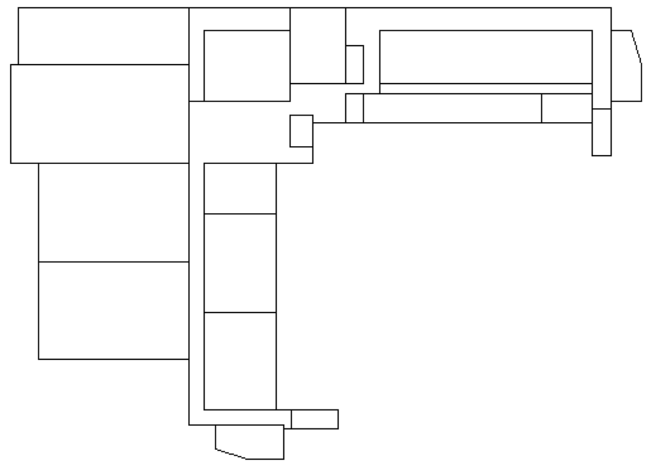

Figure 3. 9 Second floor plan

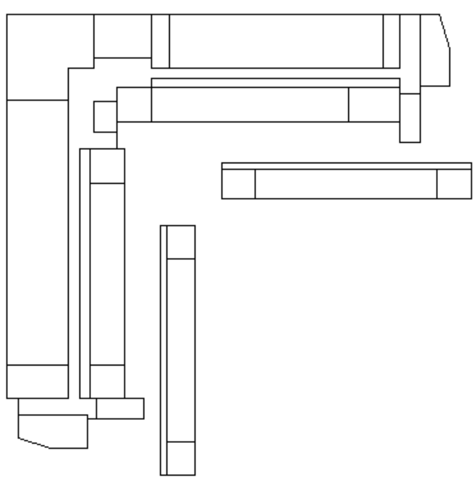

Figure 3. 10 Third floor plan and Second half floors

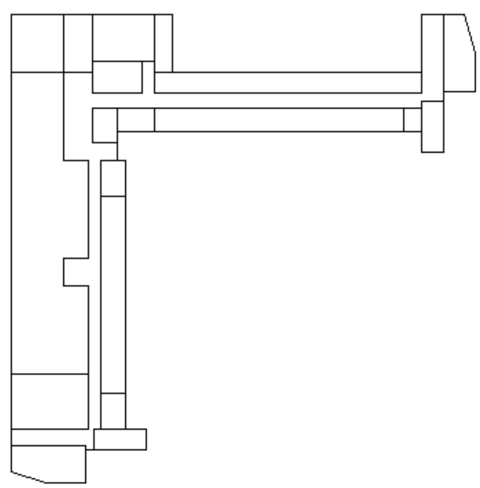

Figure 3. 11 Fourth floor plan

Figures from 3.12 to 3.15 provide views of the completed geometric model from the southern and northern perspectives, respectively. This detailed and coherent geometric setup forms the basis for the subsequent simulation tasks carried out using Energy Plus through the Design Builder platform.

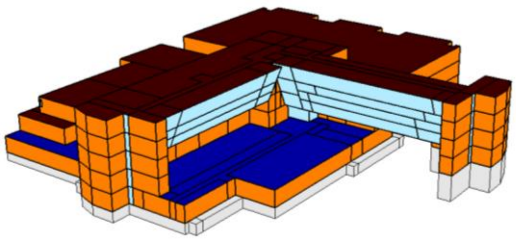

Figure 3. 12 Geometry model of Montpetit Hall (South View)

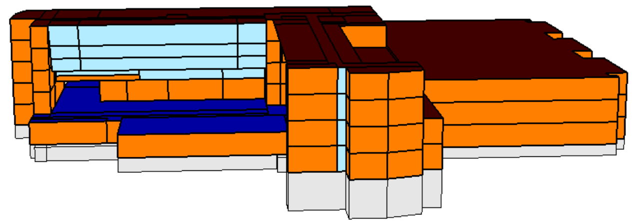

Figure 3. 13 Geometry model of Montpetit Hall (Eastern South View)

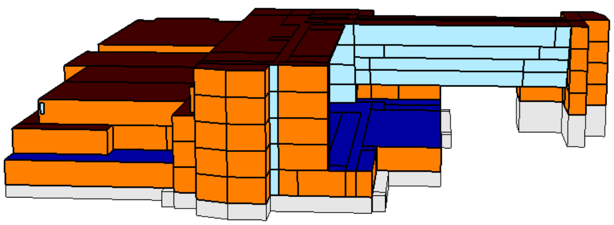

Figure 3. 14 Geometry model of Montpetit Hall (Western South View)

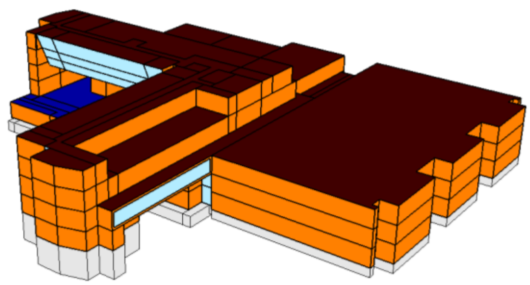

Figure 3. 15 Geometry model of Montpetit Hall (Eastern North View)

3.3.1 Thermal Zoning Strategy

The definition of thermal zones is a critical step in building energy modeling, as it directly influences the accuracy of heating, cooling, and ventilation load calculations. In this study, the zoning of Montpetit Hall was based on spatial orientation, occupancy type, and operational scheduling. These parameters reflect the actual usage patterns and thermal behavior of the building's spaces, thereby enabling more precise energy simulations.

Thermal zoning was carried out in Energy Plus after establishing the building's geometric framework. Each space was evaluated individually, and zones with comparable thermal characteristics, such as similar orientation, function, and schedule, were grouped to streamline simulation without compromising analytical accuracy. The final model contains a total of 128 thermal zones.

Each thermal zone is modeled using a transient energy balance equation based on the first law of thermodynamics. At every simulation timestep, the rate of change of zone air temperature is calculated as the result of all heat gains and losses, including internal gains (occupants, lighting, equipment), convective exchange with internal surfaces (walls, floors, ceilings, windows), airflows (infiltration, ventilation, and inter-zone mixing), and the heating or cooling provided by the HVAC system. In conceptual form, the model enforces that the change in heat stored in the air zone equals the sum of all heat inputs minus all heat losses, ensuring that the simulated zone temperature and loads are physically consistent with the building's envelope, internal loads, and system operation. Energy Plus models zone air temperature using a lumped-capacitance ordinary differential equation (ODE) in time, while heat transfer through opaque constructions is based on one-dimensional transient conduction equations derived from partial differential formulations and solved numerically.

The core zone air heat balance equation looks like this [107]:

$$C_z \frac{dT_z}{dt} = \sum Q_{internal} + \sum Q_{surface} + \sum Q_{airflow} + \sum Q_{HVAC} \tag{1}$$

Where:

C_z = thermal capacitance of the zone air

$T_{z=}$zone air temperature

$\frac{dT_z}{dt}$ = rate of change of zone temperature

$\sum Q_{internal}$ = internal gains (e.g. people, lights, equipment, etc.)

$\sum Q_{surface}$ = convective heat exchange between zone air and all inside surfaces (e.g. wall)

$\sum Q_{airflow}$ = heat gains/losses due to infiltration, ventilation, mixing with other zones

$\sum Q_{HVAC}$ = heating or cooling provided by the air system and terminals

In the Energy Plus formulation, the thermal behavior of each zone is determined not only by the zone air heat balance equation itself, but also by the boundary conditions imposed on the zone and its enclosing surfaces. For the zone air node, the boundaries are defined by convective heat exchange with all internal surfaces, mass and energy exchange through ventilation, infiltration, and inter-zone air mixing, and the sensible and latent loads supplied or removed by the HVAC terminals. For opaque and transparent constructions, the internal surface boundary condition is established by the adjacent zone air temperature, and the zone means radiant temperature, while the external surface boundary condition is driven by outdoor climatic variables such as external dry-bulb temperature, solar radiation, sky longwave radiation, wind speed, and, where applicable, ground temperature. Together, these boundary conditions ensure that the solution of the zone air energy balance and the transient one-dimensional heat conduction through building elements remains consistent with both the indoor environment and the external weather inputs used in the simulation.

As illustrated in Figures (3.15), (3.16), and (3.17) each zone is represented by a distinct color, providing a visual overview of the spatial distribution and zoning logic. For example, on the second basement level, mechanical and maintenance rooms with analogous operating schedules and thermal conditions were consolidated into a single zone. These schedules are consistent with the National Energy Code for Buildings (NECB) guidelines.

On the first basement floor, functionally similar spaces, such as the pool area, gymnasium, exercise rooms, and dance studios, were grouped into unified zones due to their shared environmental exposure and identical scheduling profiles. Similar consolidation was applied to classrooms and offices located on the first and second floors, with each zone formed based on matching orientation and function. The third and fourth floors, which house laboratories and additional offices, were similarly zoned. Where adjacent spaces such as corridors or washrooms had no unique occupancy schedule, they were included in the same zone lists as the associated office or mechanical areas in accordance with NECB conventions.

To facilitate further simulation in Energy Plus, spaces with identical use and scheduling were grouped into zone lists. For instance, all offices across multiple floors with similar conditions were compiled into shared lists, whereas classrooms with variable schedules were modeled as individual thermal zones. Table 3.1 presents the compiled list of zone groupings used in this analysis. This zoning approach ensures a balanced trade-off between model manageability and thermal performance fidelity, supporting robust energy use predictions and retrofit scenario evaluations.

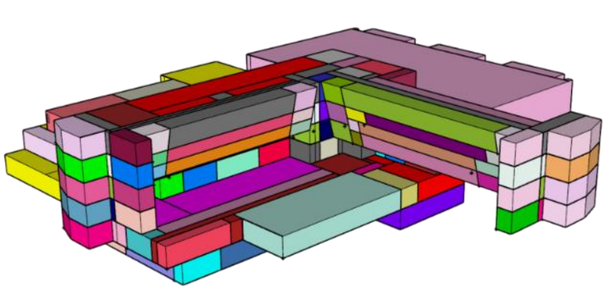

Figure 3. 16 Geometry rendered by thermal zones (South, west View)

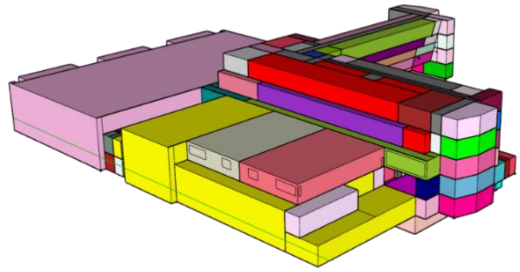

Figure 3. 17 Geometry rendered by thermal zones (South, West View)

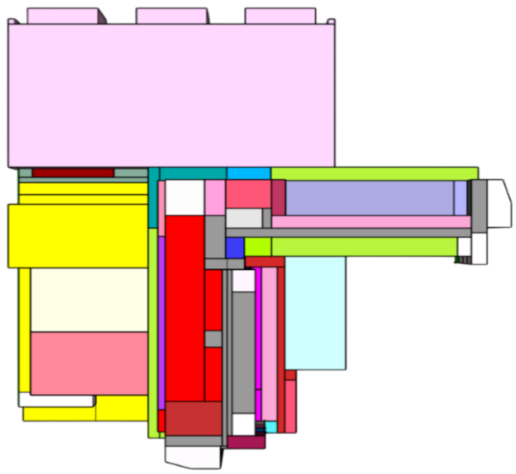

Figure 3. 18 Geometry rendered by thermal zones (Upside View)

Table 3.1. Thermal Zones Lists

Thermal zone lists according to Montpetit Hall building spaces	
LEVEL 00	Exercise Spaces- Storage Spaces- Mechanical Room
LEVEL 0	Gymnasium- Aquatic Centre- Fitness Centre- Locker Room
LEVEL 1	Classroom- Laboratories- Dance Studio- Offices
LEVEL 2	Classrooms- Offices
LEVEL 3	Laboratories- Offices
LEVEL 4	Offices- Meeting room- Laboratories

3.3.2. Construction Element Profiling

Upon completion of the geometric model, the next step involved defining material properties and incorporating them into the building's construction assemblies directly within Design Builder.

Each construction layer was assigned based on its thermal characteristics to accurately represent the building envelope.

Table 3.2 through 3.9 outlines the material configurations used in the constructions of the building envelopes, including layered assemblies for exterior walls, floors, and ceilings and roof. These material definitions were derived based on documentation provided by the university, which served as the primary reference for reconstructing the building's envelope on a layer-by-layer basis.

Table 3.2. Materials and Construction Features of Montpetit Hall Underground Floor

Material	**Roughness**	**Thickness (m)**	**Conductivity** $(W/m.K)$	**Density** (Kg/m^3)	**Specific Heat** $(J/Kg.K)$
Cement Topping	Medium Smooth	0.05	1.4	2000	840
Structural Slab	Medium Rough	0.2032	1.95	2400	880
Lean Concrete	Medium Rough	0.0508	1	2000	880
Waterproof Membrane	Medium Smooth	0.003	0.2	1350	1800
Lean Concrete	Medium Rough	0.0508	1	2000	880
Crushed Stone	Rough	0.1524	1.7	1900	800

Table 3.3. Materials and Construction Features of Montpetit Hall Interior Floor

Material	**Roughness**	**Thickness (m)**	**Conductivity** $(W/m.K)$	**Density** (Kg/m^3)	**Specific Heat** $(J/Kg.K)$
Vinyl Asbestos Tile	Smooth	0.003	0.25	1600	1300
Cement Topping	Medium Smooth	0.05	1.4	2000	840
Structural Slab	Medium Rough	0.2032	1.95	2400	880

Table 3.4. Materials and Construction Features of Montpetit Hall Exterior Floor

Material	**Roughness**	**Thickness (m)**	**Conductivity** $(W/m.K)$	**Density** (Kg/m^3)	**Specific Heat** $(J/Kg.K)$

Cement Topping	Medium Smooth	0.05	1.4	2000	840
Insulation Board	Medium Rough	0.0508	0.0288	43.25	1214.17
Gravel	Rough	0.1	1.6	1900	900
Membrane Protection	Smooth	0.004	0.2	1200	1500
Waterproof Membrane	Medium Smooth	0.003	0.2	1350	1800
Sloping Concrete	Medium Rough	0.1	1	2000	880
Structural Slab	Medium Rough	0.2032	1.95	2400	880

Table 3.5. Materials and Construction Features of Montpetit Hall Semi-Exposed Floor

Material	**Roughness**	**Thickness (m)**	**Conductivity** $(W/m.K)$	**Density** (Kg/m^3)	**Specific Heat** $(J/Kg.K)$
Carpet	Medium Smooth	0.012	0.06	288	1400
Cement Topping	Medium Smooth	0.05	1.4	2000	840
Structural Slab	Medium Rough	0.2032	1.95	2400	880
Concrete Exposed	Medium Rough	0.2032	1.4	2400	880

Table 3.6. Materials and Construction Features of Montpetit Hall Roof

Material	**Roughness**	**Thickness (m)**	**Conductivity** $(W/m.K)$	**Density** (Kg/m^3)	**Specific Heat** $(J/Kg.K)$
Built-Up Roofing Bitumen	Rough	0.007	0.17	1120	1460
Roof Insulation	Medium Smooth	0.0508	0.048967	265	836.79
Sloping Concrete	Medium Rough	0.1	1	2000	880
Structural Slab	Medium Rough	0.2032	1.95	2400	880

Table 3.7. Materials and Construction Features of Montpetit Hall Exterior Wall

Material	**Roughness**	**Thickness (m)**	**Conductivity** $(W/m.K)$	**Density** (Kg/m^3)	**Specific Heat** $(J/Kg.K)$

Concrete Exposed	Medium Rough	0.2032	1.4	2400	880
Glass Fiber	Medium Smooth	0.0254	0.0353	32.84	837.36
Gypsum Board	Medium Smooth	0.012	0.16	800	1090

Table 3.8. Materials and Construction Features of Montpetit Hall Interior Wall

Material	**Roughness**	**Thickness (m)**	**Conductivity** $(W/m.K)$	**Density** (Kg/m^3)	**Specific Heat** $(J/Kg.K)$
Gypsum Board	Medium Smooth	0.012	0.16	800	1090
Metal Stud with Air Gap	Smooth	0.09	0.025	1.2	1005
Gypsum Board	Medium Smooth	0.012	0.16	800	1090

Table 3.9. Materials and Construction Features of Montpetit Hall Underground Wall

Material	**Roughness**	**Thickness (m)**	**Conductivity** $(W/m.K)$	**Density** (Kg/m^3)	**Specific Heat** $(J/Kg.K)$
Gypsum Board	Medium Smooth	0.012	0.16	800	1090
Structural Slab	Medium Rough	0.2032	1.95	2400	880
Glass Fiber	Medium Smooth	0.0254	0.0353	32.84	837.36
Waterproof Membrane	Medium Smooth	0.003	0.2	1350	1800

All physical and thermal properties of materials (Table 3.10) and constructions (Table 3.11) were established using validated reference sources. Key attributes such as thickness, thermal conductivity, surface roughness, and material density were specified for each layer.

Table 3.10. Material Properties of the Building Envelope

Material	Roughness	Thickness (m)	Conductivity $(W/m.K)$	Density (Kg/m^3)	Specific Heat $(J/Kg.K)$
Structural Slab	Medium Rough	0.2032	1.95	2400	880
Sloping Concrete	Medium Rough	0.1	1	2000	880
Precast Concrete	Medium Rough	0.1	0.14	2400	1050
Cement Topping	Medium Smooth	0.05	1.4	2000	840
Gypsum Board	Medium Smooth	0.012	0.16	800	1090
Rigid Insulation	Medium Smooth	0.05	0.03	32	1400
Lean Concrete	Medium Rough	0.0508	1	2000	880
Crushed Stone	Rough	0.1524	1.7	1900	800
Concrete Exposed	Medium Rough	0.2032	1.4	2400	880
Waterproof Membrane	Medium Smooth	0.003	0.2	1350	1800
Vinyl Asbestos Tile	Smooth	0.003	0.25	1600	1300
Built-Up Roofing Bitumen	Rough	0.007	0.17	1120	1460
Carpet	Medium Smooth	0.012	0.06	288	1400
Metal Stud with Air Gap	Smooth	0.09	0.025	1.2	1005
Gravel	Rough	0.1	1.6	1900	900
Membrane Protection	Smooth	0.004	0.2	1200	1500
Roof Insulation	Medium Smooth	0.0508	0.048967	265	836.79
Insulation Board	Medium Rough	0.0508	0.0288	43.25	1214.17
Glass Fiber	Medium Smooth	0.0254	0.0353	32.84	837.36

Table 3.11. Constructions of Montpetit Hall

Layer	Underground Floor	Interior Wall	Underground Wall	Roof	Exterior Wall	Interior Floor	Exterior Floor	Semi-exposed Floor
Layer 1	Crushed Stone	Gypsum board	Waterproof Membrane	Built-Up Roofing Bitumen	Concrete Exposed	Structural Slab	Cement Topping	Carpet
Layer 2	Lean Concrete	Metal Stud with Air Gap	Glass Fiber	Roof Insulation	Glass Fiber	Cement Topping	Insulation Board	Cement Topping
Layer 3	Waterproof Membrane	Gypsum board	Structural Slab	Sloping Concrete	Gypsum board	Vinyl Asbestos Tile	Gravel	Structural Slab
Layer 4	Lean Concrete	Gypsum board	Gypsum board	Structural Slab			Membrane Protection	Carpet
Layer 5	Structural Slab						Waterproof Membrane	Concrete Exposed
Layer 6	Cement Topping						Sloping Concrete	
Layer 7							Structural Slab	

For glazing components, additional parameters were defined, including solar and visible transmittance, as well as reflectance values for both the front and rear surfaces. These detailed characteristics are presented in Tables 3.12.

Table 3.12. Glazing window material characteristics

Thickness (m)	Solar transmittance	Front-side solar reflectance	Back-side solar reflectance	Visible transmittance	Front-side visible reflectance	Back-side visible reflectance
0.006	0.5	0.1	0.1	0.55	0.08	0.08

The windows are configured as double-glazed units, incorporating an air-filled cavity, with the interlayer thickness treated as a key performance parameter (see Table 3.13). This specification is based on typical construction materials and glazing practices commonly used in Canada during the early 1970s.

Table 3.13. Gas window material characterization

Gas window material	Thickness (m)
Air	0.012

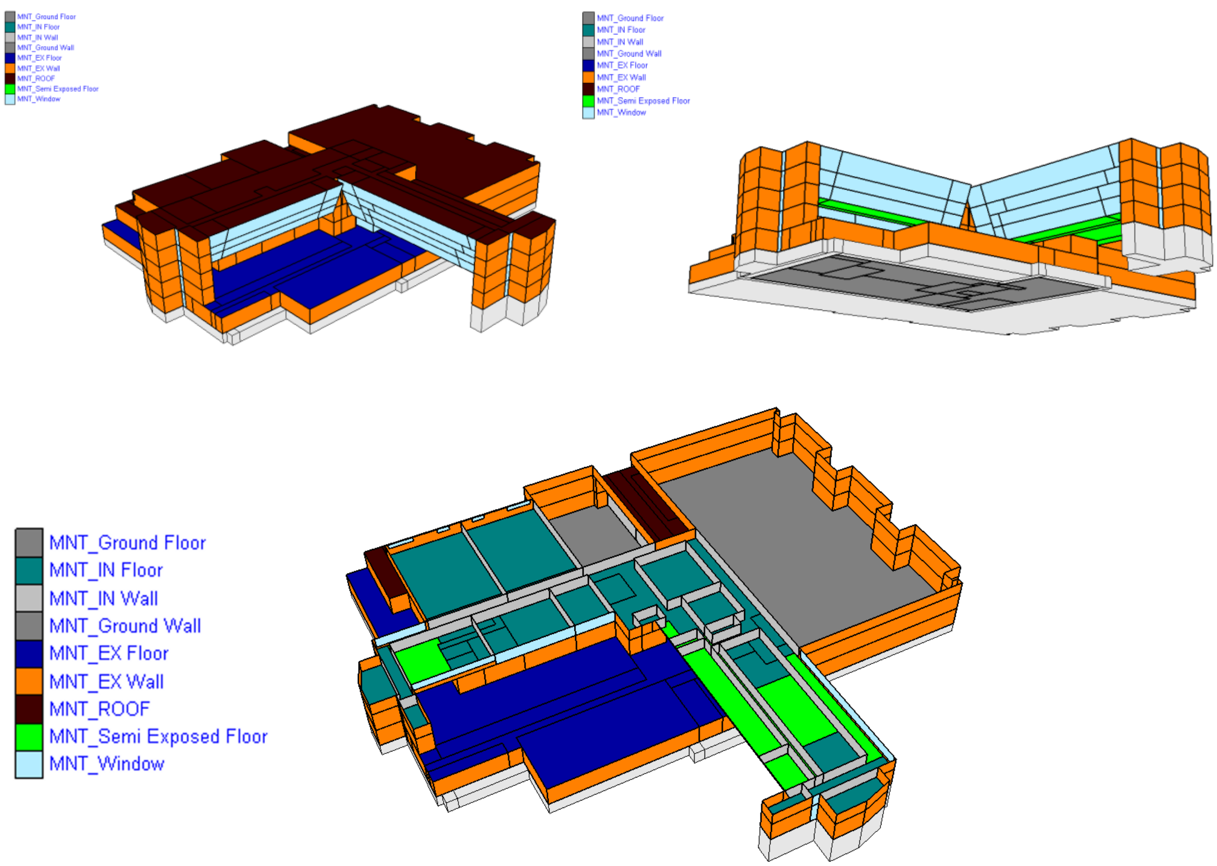

Figure 3. 19 Geometry rendered by construction

3.4 Energy Modeling

The fourth stage of this process involved the development of a comprehensive energy model to simulate the performance of Montpetit Hall under typical operational conditions. The objective was to understand how various components of the building and its systems interact and contribute to overall energy consumption.

Following the completion of the building geometry in Design Builder, the model was exported into Energy Plus using the Input Data File (IDF) format. At this stage, detailed data inputs were incorporated into the simulation model to ensure an accurate representation of the building's energy behavior. These inputs included:

- **Weather data:** Climatic conditions derived from a Actual Weather File (AWF) file for Ottawa.
- **Occupancy data:** Number of occupants and their distribution across different zones.
- **Lighting systems:** Lighting power density, control strategies, and usage schedules.
- **Electrical equipment:** Internal loads from plug-in devices and specialized equipment.
- **Mechanical systems:** Power plant, HVAC system, and Pool configurations and operational settings.
- **Schedules:** Time-based operational schedules assigned to different space types.
- **Infiltration rates:** Estimated air leakage values [108].

Information for these inputs was obtained from various sources, including university-provided documentation and Canadian building standards such as the NECB. For components with missing or incomplete data, standard engineering assumptions were applied.

To validate the accuracy of the model, simulation results were compared against actual energy consumption records retrieved from utility bills supplied by the facility office. Where discrepancies were identified, iterative adjustments were made to calibrate the model until it achieved satisfactory alignment with measured data.

This stage of the study serves as a foundation for identifying energy inefficiencies and developing retrofit strategies. The insights gained from the modeling process are instrumental in guiding efforts to reduce energy consumption, lower operational costs, and improve the overall environmental performance of Montpetit Hall.

3.4.1 Weather File

Accurate representation of local climate conditions is critical for reliable energy simulation. In this study, a customized weather file was prepared in the Energy Plus Weather (EPW) format for the Ottawa region (Ontario, Canada). The data was compiled using multiple sources, including typical meteorological year datasets from the Energy Plus database, historical solar and meteorological records from the National Solar Radiation Database [109], and supplementary data provided by the university.

The year 2022 was selected as a representative climatic period for the location, based on its consistency with historical temperature and solar radiation averages. Initial datasets were processed in spreadsheet format to allow for data cleansing and restructuring. After completing necessary adjustments, the dataset was recompiled into EPW format for compatibility with Energy Plus simulations.

Table 3.14 presents an overview of the data points extracted and translated from the NSRDB source into the final EPW file, including parameters such as dry-bulb temperature, relative humidity, global horizontal irradiance, wind speed, and atmospheric pressure.

Table 3.14. Data Transferred from NSRDB to Energy Plus Weather File

1-	Dry Bulb Temperature (C)
2-	Dew Point Temperature (C)
3-	Relative Humidity (%)
4-	Atmospheric Pressure (Pa)
5-	Global Horizontal Radiation (Wh/m^2)
6-	Direct Normal Radiation (Wh/m^2)
7-	Diffuse Horizontal Radiation (Wh/m^2)
8-	Wind Direction (deg)
9-	Wind Speed (m/s)

3.4.2 Schedule

Occupancy and operational schedules play a critical role in accurately simulating internal loads and energy usage patterns. For this study, scheduling data was derived from two primary sources: class schedules were obtained directly from the University of Ottawa, while standard operational schedules for other building functions were based on the National Energy Code of Canada for Buildings [110].

Two schedule formats were implemented in Energy Plus: Compact and Constant. The compact format represents typical annual behavior through time-dependent fractional values ranging from 0 to 1, enabling precise control over occupancy, equipment usage, and lighting patterns. In contrast, the constant schedule format applies a uniform value throughout the simulation period, typically used for elements that remain unchanged over time, such as continuous equipment operation or base ventilation loads. Schedules were assigned to all major internal loads, including occupancy, lighting, plug loads (electrical equipment), and mechanical systems. To manage these assignments efficiently, specific thermal zones with similar usage patterns were grouped into zone lists, facilitating streamlined data input and improved simulation coherence. The development and application of these zone lists are detailed in the subsequent section.

3.4.2.1 Schedule Constant

Several schedules are presented in this section, among which the activity level schedule is identified as a critical component of the occupant-related inputs. The definition of this parameter is essential, as it directly affects the calculation of internal loads within the model. Considering that students in the dormitory participate in a variety of daily activities, the activity levels were established based on the Energy Plus reference (Table 3.15). This schedule is particularly relevant to the present study, as it ensures that the modeled occupancy patterns in Montpetit Hall accurately reflect variations in metabolic rates associated with different student activities.

Table 3.15. The Metabolic Rates for Various Activities based on Energy Plus reference

Activity	Activity Level Schedule Value (W/ Person)
Class (considered filling seated)	130
Office (considered seated typing)	120
Exercise	350
Laboratory	140
Corridor (considered walking 3.2 km/h)	200

3.4.2.2 Schedule Compact

A schedule was developed for each section, encompassing occupants, lighting, and miscellaneous equipment. Since the available information from the University of Ottawa was incomplete, direct student surveys, though desirable for improved accuracy, were not conducted. Instead, all compact schedules were established based on the National Energy Code of Canada for Buildings [110]. Each schedule differentiates between weekdays and weekends; with weekend patterns derived from the Saturday schedule to ensure consistency with standard NECB assumptions.

3.4.3 Occupancy

Occupant density data for Montpetit Hall was sourced directly from university-provided records, detailing the number of individuals present on each floor (Table 3.16). For integration into the Energy Plus simulation environment, this information was normalized and expressed in terms of people per square meter of floor area. This metric enables the modeling engine to assign realistic internal heat gains and ventilation loads based on occupancy distribution throughout the building.

Table 3.16. Building Occupancy [111]

Level	Occupancy	Area (m^2)
Total Level 00	43	3656.25
Total Level 0	2266	6783.73
Total Level 1	432	1646.94
Total Level 2	917	2795.09
Total Level 3	205	2895.09
Total Level 4	254	1625.76

The occupancy schedules were developed by zone type, classrooms, laboratories, exercise facilities, and offices, and differentiated across the Fall, Winter, and Spring/Summer semesters. In general, classroom and office zones exhibit two peak periods during weekdays, corresponding to morning and afternoon activities, with noticeably lower fractions during weekends. Laboratory zones follow a similar trend, although they demonstrate slightly earlier start times and more extended afternoon usage compared to classrooms. Exercise zones, by contrast, show broader activity spans that extend into the evening, particularly during weekends, reflecting the flexible nature of recreational use. Seasonal variation is also evident: the Winter semester tends to present higher weekday occupancy fractions in classrooms and offices compared to the Spring/Summer semester, while laboratories and exercise zones maintain more consistent patterns across terms. These results highlight both the temporal (hourly and daily) and seasonal dynamics of building occupancy, which are crucial for accurately modeling internal loads and energy demand. The schedules are provided in Figures A.10 to A.13.

3.4.4 Lighting

Accurate representation of lighting loads is essential for simulating internal heat gains and electricity consumption. In this study, lighting data was compiled by aggregating the total number of lamps installed across all functional spaces, organized on a per-floor basis. Figures A.14 through A.17 presents the estimated lighting schedule for each categorized zone.

To enable integration with the Energy Plus simulation engine, lighting power density was calculated in terms of Watts per square meter of zone floor area (W/m²). This was achieved by dividing the total annual lighting power for each floor by its respective floor area. These values were then used to define lighting loads in the model's IDF file, ensuring alignment with actual building conditions.

Table 3.17. lighting load per floor [111]

Level	T8 Fixture Count	Load (kW)	Annual consumption (kWh)	Annual consumption (GJ)
Level 00	417	10.4	60,882	219
Level 0	1367	34.2	199,582	718
Level 1	340	8.5	49,640	179
Level 2	826	20.7	120,596	434
Level 3	690	17.3	100,740	363
Level 4	446	11.2	65,116	234
Penthouse	5	0.1	730	3
Total	102.3		597,286	2,150

3.4.5 Other Equipment

In the absence of detailed equipment load data from the university, electrical equipment inputs were modeled using standardized values from the National Energy Code of Canada for Buildings

[110]. These loads fall under the "Electric Equipment" category within the IDF file structure of Energy Plus. For each thermal zone, the Peak Receptacle Load per unit floor area (W/m²) was applied based on NECB recommendations. This approach ensures consistency with recognized national benchmarks while allowing for a realistic estimation of internal gains associated with plug loads, appliances, and miscellaneous equipment. The schedule for equipment is presented in Tables from A.18 to A.21.

3.4.6. HVAC System

3.4.6.1 System Configuration

Montpetit Hall employs a centralized HVAC system with thirteen air handling units (AHUs), most operating under CAV control. These systems serve diverse functional areas, academic, athletic, and research, through heating and cooling coils. Although much of the infrastructure dates to the 1972 construction, partial upgrades, such as variable frequency drives (VFDs), have improved fan efficiency under part-load conditions. However, no Building Automation System (BAS) is in place; operation remains reliant on local controls and thermostats.

3.4.6.2 Heating and Cooling Sources

Heating and cooling are provided by the University of Ottawa's district energy system. Upgrades in 2010 and 2015 introduced two-way control valves, enabling variable flow and pump energy savings. Heating water supply temperature is adjusted via an outdoor air reset strategy, ranging from 85°C at –20°C outdoor to 45°C at 13°C. Indoor heating and cooling setpoints are 21°C and 24°C, respectively. The chilled water loop supplies 5°C and returns at 9°C, serving as the baseline for coil performance modeling.

3.4.6.3 Ventilation System

Fresh air is delivered through the AHUs, equipped with MERV 7 pre-filters and MERV 12 bag filters, achieving over 95% efficiency. Return fans maintain slightly negative pressure, supporting ASHRAE fresh air standards. Dedicated exhaust and makeup air systems serve high-moisture zones, including saunas and showers.

3.4.6.4 Zone Grouping and Distribution

Each AHU serves distinct functional zones. Three units supply the gymnasium, while local fan coils support laboratories and IT rooms with high internal loads. AHU-14, serving the Decelles Auditorium, integrates a reversible "flip/flop" HR module with up to 90% efficiency. The pool is conditioned by a standalone system installed in 2020, incorporating DX refrigeration, dry coolers, and HR from the refrigerant cycle. This diversity in age and configuration necessitated detailed modeling to represent both legacy and retrofitted systems. Centralized plant loops in the model deliver heating and cooling to each AHU.

3.4.6.5 Air Handling Units (AHU)

Without a BAS, controls are limited to fixed setpoints (21°C heating, 24°C cooling) and predefined schedules. Heating water supply is reset according to outdoor air temperature, while VFD-equipped fans typically operate at 90% of capacity. Each AHU was individually modeled in Design Builder to reflect specific system characteristics.

A comprehensive summary of each AHU, including its type, associated equipment, and the zones it serves, is presented on the accompanying table (Table 3.18).

AHU Summaries

- **AHUs 1–3 (Gymnasium):** 100% outdoor air systems meeting high ventilation demands. Lack of energy recovery increases thermal loads. Negative pressure design prevents cross-contamination, consistent with ASHRAE 62.1.
- **AHU 4 (Pool):** Serves the natatorium with a standalone DX system, rooftop dry coolers, and HR. Provides strict humidity control but raises electrical demand.
- **AHU 5 (Central Core):** Dual-deck makeup air unit (MUA) supplying corridors and lobbies with outdoor air only, increasing ventilation effectiveness but limiting energy recovery.
- **AHU 6 (Offices):** 100% outdoor air system serving administrative areas, operating at fixed ventilation rates with limited efficiency.
- **AHU 7 (Athletic Zones):** Dual-duct system allowing simultaneous heating/cooling but with high energy penalties. Supplemental fan coils address overheating.
- **AHU 8 (Locker Rooms):** CAV system with heating and cooling coils to manage humidity and odor but lacking variable airflow control.
- **AHU 9 (Mechanical Room):** CAV unit using return air from AHU-6 for improved efficiency, supplemented with glycol heating and chilled water cooling.
- **AHU 12 (Computer Labs):** Incorporates a run-around loop HR system, reducing heating loads by recovering exhaust heat.
- **AHU 13 (Auditorium):** Conventional heating and cooling coils connected to district systems.
- **AHU 14 (Auditorium):** Features a reversible "flip/flop" HR system, significantly reducing heating demand in winter.
- **AHU 15 (Dance Studio):** Single-zone CAV unit with glycol heating and chilled water cooling, supplying 100% outdoor air at a fixed rate.

Table 3.18. Montpetit AHU and Exhaust detail Information

Equipment		Daily Runtime (hr)	Fan Air Capacity (m^3/s)	Fan Power (KW)	System Type	Zone
AHU 1	Supply	16	13.215	15	Packaged Unit with DX Cooling and DOAS Unit	Gymnasium
	Return	16	13.498	6		
AHU 2	Supply	16	13.215	15	Packaged Unit with DX Cooling and DOAS Unit	Gymnasium
	Return	16	13.498	6		
AHU 3	Supply	16	13.215	15	Packaged Unit with DX Cooling and DOAS Unit	Gymnasium
	Return	16	13.498	6		
AHU 4	Supply	16	15.574	40	Packaged Unit with Cool –Reheat Dehumidification control	Pool
	Return	24	5.191	30		
AHU 5	Supply	16	1.537	1.12	Dual Deck	Centre Core
	Return	16	1.472	0.56		
AHU 6	Supply	10	2.53	2.24	Make-up Air Unit	Administration & Cubicle Areas
	Return	10	2.671	1.12		
AHU 7	Supply	16	8.023	7.46	Dual Deck	Fitness Area
	Return	16	9.543	5.59		
AHU 8	Supply	16	5.05	5.59	CAV System with Central Hydronic Coils	Locker Rooms
	Return	16	6.135	2.24		
AHU 9	-	24	4.012	1.49	CAV System with Central Hydronic Coils	Mechanical Room
AHU 12	Supply	16	0.944	2.24	CAV System with Heat Recovery Ventilator	Computer Laboratory
	Return	16	0.755	0.56		
AHU 13	Supply	16	2.36	5.59	CAV System with Central Hydronic Coils	Decelles Auditorium
	Return	16	2.195	1.49		
AHU 14	Supply	16	2.36	5.59	Reversible-flow Heat Recovery Unit	Decelles Auditorium
	Return	16	2.195	1.49		
AHU 15	-	16	1.416	1.49	CAV System with Central Hydronic Coils	Dance Studio
Exhaust Fan 1	-	24	0.142	0.19	Dedicated Exhaust	General Exhaust
Exhaust Fan 2	-	24	0.42	0.25	Dedicated Exhaust	General Exhaust
Exhaust Fan 3	-	24	0.642	0.56	Dedicated Exhaust	General Exhaust
Exhaust Fan 4	-	24	-	-	Dedicated Exhaust	General Exhaust
Exhaust Fan 5	-	24			Dedicated Exhaust	General Exhaust
Exhaust Fan 6	-	24	1.657	0.75	Dedicated Exhaust	EF for Dryers
Exhaust Fan 7	-	24	-	-	Dedicated Exhaust	General Exhaust
Exhaust Fan 8	-	24	-	-	Dedicated Exhaust	General Exhaust
Exhaust Fan 10	-	24	1.331	0.37	Dedicated Exhaust	Washrooms West Wing
Exhaust Fan 11	-	24	1.331	0.37	Dedicated Exhaust	Washrooms South Wing
Exhaust Fan 12	-	24	0.127	0.19	Dedicated Exhaust	Room 321A
Exhaust Fan 13	-	24	0.212	0.19	Dedicated Exhaust	Room 307 (A, B, C, D, E)
Exhaust Fan 14	-	24	0.566	0.25	Dedicated Exhaust	Locker Rooms (Women)
Exhaust Fan 15	-	24	0.708	0.37	Dedicated Exhaust	Locker Rooms (Men)
Exhaust Fan 16	-	24	0.127	0.19	Dedicated Exhaust	Room 306
Exhaust Fan 17	-	24	0.354	0.19	Dedicated Exhaust	Washrooms 120, 122
Exhaust Fan 18	-	24	1.657	0.75	Dedicated Exhaust	Stockrooms 007, 007A, 007B
Exhaust Fan 19	-	24	0.127	0.19	Dedicated Exhaust	Room 0033
Exhaust Fan 20	-	24	1.133	1.49	Dedicated Exhaust	Shower Exhaust

3.4.6.6 Standalone and Local Systems

In addition to central AHUs, select areas (labs, IT rooms, small offices) use standalone units or fan coils for localized control. While these improve comfort, their fragmented operation complicates centralized energy monitoring.

3.4.6.7 Domestic Hot Water (DHW) System

DHW is supplied via the district heating network and distributed through a closed-loop recirculation system. The network uses DN 50 mm copper piping with 0.31 L/s continuous circulation, primarily serving showers and pool facilities. Wastewater heat is unrecovered, representing a loss of reclaimable energy. At the campus level, DHW generation uses flue-gas HR supplemented by a steam shell-and-tube exchanger. For modeling, it was conservatively assumed that 100% of DHW is provided by steam at 90% efficiency. Limitations include the absence of submeters and greywater recovery, indicating future retrofit potential.

3.4.7 Base Model Evaluation

To assess the accuracy of the energy simulation model developed in Energy Plus, the predicted energy consumption of the base case model was compared against actual utility data obtained from the University of Ottawa. The simulation was conducted using Actual Weather Data (AWD) for the year 2022, ensuring alignment between environmental inputs and the historical consumption period under evaluation.

3.4.7.1 Model Accuracy Evaluation Metrics

The statistical indices Normalized Mean Bias Error (NMBE) and Coefficient of Variation of the Root Mean Square Error (CVRMSE) are widely recognized as standard measures for the calibration of building energy simulation models. According to ASHRAE Standard 14 and the International Performance Measurement and Verification Protocol (IPMVP), these indices provide quantitative benchmarks for assessing model accuracy. Specifically, ASHRAE 14 prescribes that for monthly calibration data, the NMBE should remain within ±5%, while the CVRMSE should not exceed 15%. For models calibrated at an hourly resolution, the corresponding thresholds are ±10% for NMBE and 30% for CVRMSE [112]. These performance limits ensure that the simulation results are both reliable and representative of actual building energy performance. In this study, the model calibration was performed using monthly utility data.

Normalized Mean Bias Error (NMBE):

$$NMBE\ (\%) = \frac{\frac{1}{n}\sum_{i=1}^{n}(M_i - S_i)}{\bar{M}} \times 100 \tag{2}$$

Coefficient of Variation of the Root Mean Square Error (CV(RMSE)):

$$CV(RMSE)(\%) = \frac{\sqrt{\frac{1}{n}\sum_{i=1}^{n}(M_i - S_i)^2}}{\bar{M}} \times 100 \tag{3}$$

Where:

• M_i = Measured (observed) data at time step i

• S_i = Simulated (predicted/modelled) data at time step i

• $\bar{M}$= Mean of the measured data

• n = Number of data points

In the case of Montpetit Hall, the electricity billing system operates under a flat-rate structure, in which the university is charged a fixed amount based on projected demand or historical usage, rather than actual monthly metered consumption. Although monthly electricity usage values are recorded, they do not reflect real-time building-level consumption and are instead derived from standardized flat estimates applied uniformly across the billing cycle. This billing approach, often used in institutional settings, simplifies utility accounting but introduces limitations for energy modeling validation.

Because the available monthly electricity data is not based on actual meter readings, it does not meet the accuracy or resolution requirements needed to apply standard validation metrics such as the NMBE and CV(RMSE). These metrics require time-resolved and reliable measured data for comparison, which is not available in this case.

To address this constraint, a percentage error method was adopted using the annual simulated electricity consumption compared against the total annual billed electricity data. This allowed for a reliable overall evaluation of the model's accuracy. In addition, a monthly disaggregation of end-use categories, such as lighting, equipment, and cooling, was analyzed to verify that the simulated patterns align with expected seasonal behavior. Internal load assumptions, including lighting power density and plug load intensities, were also cross-referenced with values recommended by the National Energy Code of Canada for Buildings [110] to ensure consistency with accepted standards. This combined approach offers a practical and transparent validation framework under conditions where detailed electricity metering is not available.

$$\text{Percentage Error (\%)} = \frac{E_a - E_s}{E_s} \times 100 \quad (4)$$

Where:

• E_a = Annual electricity consumption of actual model

• E_s = Annual electricity consumption of simulation model

3.5 Optimization Process

This research employs a simulation-based, multi-objective optimization framework to evaluate both the accuracy and the computational efficiency of simplified building energy models. At the same time, the framework is applied to identify optimal Energy Conservation Measures (ECMs) for retrofitting purposes. The optimization process is designed to balance two competing goals: reducing primary energy consumption (PEC) and minimizing the Net Present Value (NPV) of retrofit investments. These objectives are evaluated under a constraint ensuring that the proposed retrofit strategies lead to energy performance improvements compared to the baseline scenario (i.e., $PEC \leq PEC_0$). To solve this multi-objective problem, the Non-dominated Sorting Genetic Algorithm II (NSGA-II) is employed, owing to its demonstrated effectiveness in building energy optimization applications and its ability to balance computational efficiency with solution robustness [113] [114].

The optimization framework is developed in MATLAB and integrated with Energy Plus to conduct detailed energy performance simulations. The exchange of data between the two platforms is facilitated via text-based input and output formats, ensuring a seamless coupling. One of the key computational enhancements leveraged in this framework is MATLAB's parallel computing capability, which significantly accelerates the optimization process. By decomposing the computational workload into parallel tasks across multiple processors, the optimization runtime is notably reduced.

The optimization process employs the NSGA-II algorithm, which begins with a population of candidate solutions, each corresponding to a distinct retrofit configuration defined by a set of decision variables. Evolutionary research is driven by genetic operators, including crossover and mutation, while elitism and diversity-preservation mechanisms ensure solution quality and convergence stability. For every candidate, Energy Plus simulations is conducted to assess building energy performance and compute the objective functions, namely, primary energy consumption (PEC) and NPV. A parametric Energy Plus model is used as the baseline template, which is iteratively updated according to the decision-variable values of each retrofit scenario. (See Figure 3.1).

To enable seamless integration, a dedicated coupling interface connects NSGA-II with Energy Plus by converting decision variables into simulation input files and automating the execution process. Following each simulation, essential output parameters are extracted, and a post-processing module calculates the objective values, which are subsequently transferred back to the optimization engine. Through this iterative exchange, NSGA-II progressively refines the candidate solutions across generations, ultimately converging toward a Pareto-optimal front that illustrates the trade-offs between reducing PEC and minimizing NPV. This structured workflow ensures both methodological robustness and practical applicability in evaluating retrofit strategies.

3.5.1. First Stage: Simulation-Based Performance Evaluation

As discussed in earlier sections, building energy consumption can be effectively optimized through a combination of active and passive strategies aimed at enhancing overall performance. In this study, the optimization process is specifically designed to improve the energy efficiency of the building envelope as a passive design intervention. The development and application of this approach are elaborated in the subsequent sections.

3.5.1.1 Identifying Decision Variables for Multi-Objective Optimization

In multi-objective optimization for building energy performance, identifying relevant decision variables is a foundational step that significantly influences the quality of solutions. These variables represent the parameters that can be manipulated during the optimization process, such as envelope insulation levels, glazing ratios, HVAC system types, and building orientation. Unlike single-objective optimization, where a single criterion is optimized in isolation, multi-objective problems require the concurrent evaluation of multiple often conflicting goals (e.g., minimizing energy use and investment cost). Hence, decision variables must be chosen to reflect the trade-off space effectively. Several studies have emphasized the importance of sensitivity analysis and simulation-based parametric modeling to isolate high-impact variables, ensuring the optimization framework remains computationally efficient and practically relevant [115]; [116]; [117].

This study centers on enhancing building energy efficiency through the optimization of key envelope components. The selection of decision variables is guided by factors such as building energy performance, local climate conditions, stakeholder priorities, and market availability. These variables are broadly categorized into insulation and glazing systems. For insulation, the evaluation criteria include material type, thickness, cost-effectiveness, thermal performance, and environmental impact. Similarly, window configurations are assessed based on their thermal transmittance (U-value), solar heat gain coefficient (SHGC), and glazing types specifically whether double or triple-pane systems are employed.

3.5.1.2 Objective Functions

In this methodology, particular emphasis is placed on the definition and formulation of objective functions, which establish the criteria for the optimization process. These functions are typically structured around two primary dimensions: environmental and economic. The environmental objective targets the reduction of primary energy consumption, reflecting the ecological performance of retrofit strategies, while the economic objective focuses on minimizing total costs. Each is discussed in detail in the subsequent sections.

Following the definition of objectives, optimization algorithms are systematically applied to evaluate and improve the performance of candidate solutions. These algorithms, designed to navigate complex decision spaces, facilitate the identification of trade-offs and synergies between conflicting objectives. By conducting a comparative analysis of the resulting solutions, the process seeks to determine the most favorable outcome. This dual-objective framework enables a balanced integration of environmental and financial priorities, supporting more comprehensive and rational decision-making.

3.5.1.2.1 Environmental Objective Function

In the adopted methodological framework, the environmental evaluation of building energy retrofits is primarily based on total energy consumption (EC). Heating and cooling demands are converted into primary energy use by applying appropriate primary energy factors. To accurately quantify these demands, dynamic energy simulations were conducted using Energy Plus, which provided detailed monthly energy consumption profiles. Within this framework, insulation upgrades are categorized as a retrofit intervention aimed at reducing thermal loads. Additionally, any on-site energy generation is deducted from the total energy consumption, thereby reflecting a net reduction in building energy demand.

3.5.1.2.2 Economic Objective Function

The economic objective of an energy retrofit project is to minimize the total cost over the building's operational life by strategically investing in appropriate Energy Retrofit Measures (ERMs). These interventions aim to reduce expenditures related to electricity, natural gas, and renewable energy systems. By optimizing the initial capital investment, the project seeks to achieve long-term financial benefits through lowered operational energy costs.

3.5.1.2.2.1 Net Present Value

The Net Present Value (NPV) is a core financial metric employed to evaluate the economic viability of energy retrofit projects. It reflects the trade-off between the initial capital expenditure and the projected cost savings realized over the building's service life. The NPV is calculated using the following expression:

$$NPV = IC + EC + GC \tag{5}$$

Here, IC represents the upfront investment cost required to implement the retrofit measures, while EC and GC refer to the present value of cumulative savings from reduced electricity and natural gas consumption, respectively [118]. These components are evaluated over the analysis period and discounted to their present values. A more comprehensive explanation of the NPV calculation process is presented in Section 3.6.

3.5.1.2.2.2 Investment Cost

To conduct a reliable economic assessment, it is necessary to quantify the total capital required to implement the selected retrofit measures. The investment cost (IC) is defined by the following equation:

$$IC = \sum_{i=0}^{1} \sum_{j=0}^{1} C_i^j \,.\, K_i^j \tag{6}$$

In this formulation, C_i^j denotes the cost associated with implementing the i option of the j retrofit measure, while K_i^j is a binary indicator variable. A value of 1 signifies that a specific measure has been selected, whereas a value of 0 indicates its exclusion from the retrofit strategy. This structure ensures that only the costs of actively implemented measures are included in the total investment calculation [119].

3.5.1.2.2.3 Present Value of Electricity and Natural Gas Costs

To evaluate the financial savings resulting from reduced energy consumption, it is necessary to calculate the present value of future electricity and natural gas costs over the building's operational lifespan. These calculations consider both the time value of money and projected energy price escalation.

The present value of electricity and natural gas costs is calculated as [118]:

$$q = \begin{cases} \dfrac{[1 - \left(\dfrac{1+g}{1+d_r}\right)^t]}{d_r - g} & if\ d_r \neq g \\ \dfrac{t}{1+d_r} & if\ d_r = g \end{cases} \tag{7}$$

Where:

- q is present value factor
- d_r is the actual discount rate (discount future cash flows to present value, accounting for time value of money)
- t is lifespan
- g represents the annual energy price escalation rate (expected percentage increase in energy prices per year)

Which the actual discount rate can be calculated as [118]:

$$d_r = \frac{1 + d_n}{1 + e} - 1 \tag{8}$$

Where:

- e represents inflation rate
- d_r denotes nominal discount

In life cycle cost analysis, accurately capturing the impact of inflation and discounting is essential. In this study, a real discount rate of 3 % is adopted in accordance with Canadian federal guidance for economic evaluation [120]. Adjusting for the disparity between the discount rate and the rate of energy price escalation provides a more realistic estimate of the NPV of energy cost savings, thereby improving the reliability of the financial assessment for retrofit projects.

3.5.1.3 Multi-Objective Optimization

Following the definition of the objective functions, the multi-objective optimization problem can be formally structured as follows:

- **Objective 1: Environmental Performance**

  $Energy\ Consumption: [Min]F_1(x) = PEC$

Where PEC denotes the annual primary energy consumption of the retrofitted building.

- **Objective 2: Economic Performance**

  $Price\ of\ \{Investment\ Cost, Cost\ of\ Energy\}$:$[Min]\ F_2(x) = NPV$

Where NPV represents the present value of total lifecycle costs, including both investment and operational savings.

These objectives are subject to the following constraints:

$x \epsilon X$

$F_1(x) \leq PEC_0$

$IC(x) \leq Available\ Budget$

Here, x refers to the vector of decision variables, each representing a specific combination of retrofit measures, while X defines the domain of feasible solutions. The term PEC_0 denotes the baseline primary energy consumption of the existing building in its unmodified state.

To ensure the viability and performance of proposed retrofit strategies, the optimization framework excludes configurations that increase energy consumption relative to the base case. Financial constraints, such as high capital costs, rising energy prices, and limited funding, also pose significant barriers to implementation.

A simulation-based multi-objective optimization approach is adopted to identify retrofit scenarios that minimize both Primary Energy Consumption (PEC) and NPV. This study employs the Non-dominated Sorting Genetic Algorithm II (NSGA-II) for its robustness in handling complex, non-analytical objective functions and its ability to explore diverse solution spaces efficiently.

The framework integrates four key components (Figure 3.20):

- **Optimization Engine**: NSGA-II iteratively evolves populations of decision vectors to identify Pareto-optimal solutions.
- **Parametric Model Input**: An Energy Plus `.idf` file allows automated variation in retrofit parameters.
- **Communication Module**: Interfaces MATLAB with Energy Plus to modify simulation inputs, execute runs, and extract results.
- **Post-Processing**: Evaluates each solution's PEC and NPV based on Canadian utility prices (0.129 CAD/kWh electricity, 0.045 CAD/kWh natural gas).

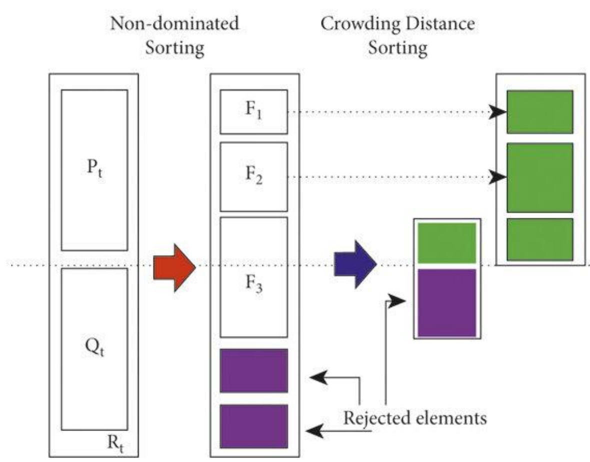

Figure 3. 20 Sorting of the Answers in the NSGA-II Algorithm, 2022 [121]

NSGA-II, implemented in MATLAB and linked with Energy Plus, classifies solutions into Pareto fronts via a non-dominated sorting mechanism. Each individual, representing a retrofit configuration, is evaluated based on its trade-offs between PEC and NPV. To maintain solution diversity, the algorithm uses a crowding distance metric, favoring individuals in less-populated regions of the objective space.

Unlike single-objective methods, NSGA-II returns a set of optimal trade-off solutions rather than a single best one. Its selection process is guided by two operators:

- **Non-Dominated Sorting**: Ranks individuals based on dominance hierarchy.
- **Crowding Distance**: Promotes diversity by prioritizing isolated solutions.

To improve efficiency, a result caching system stores previously evaluated configurations, preventing redundant simulations. The optimization proceeds until a stopping criterion (e.g., maximum generations) is met, after which the final Pareto front provides a range of retrofit options that balance environmental and economic goals.

The optimization technique employed in this study NSGA II is a population-based, evolutionary algorithm that seeks to approximate the global Pareto-optimal front rather than converging to a single local optimum. Unlike traditional gradient-based methods that are prone to getting trapped in local optima due to the deterministic nature of their search trajectory, NSGA II utilizes stochastic operators such as selection, crossover, and mutation to diversify the search process and escape local minima. This enhances its ability to explore a broader solution space and approach the global optimum across multiple conflicting objectives [122]. In the context of this research, the application of NSGA II enabled the identification of a set of trade-off solutions that capture the best compromises between energy reduction and economic performance, rather than settling on a single sub-optimal point. This characteristic is particularly valuable in building retrofit problems where the solution space is highly non-linear and multi-modal due to complex interactions between envelope parameters, HVAC systems, and occupancy profiles. In optimization theory, a local optimum is a solution that is better than all neighboring solutions but not necessarily better than all possible solutions in the entire domain. In contrast, a global optimum is the best possible solution over the entire feasible space. Metaheuristic algorithms like NSGA II are designed to approximate global optima by avoiding premature convergence to local optima.

3.5.1.4 Multi-Criteria Decision-Making

The solutions obtained from the Pareto front represent alternative retrofit strategies that offer optimal trade-offs between conflicting objectives, such as reducing energy consumption and minimizing financial cost. While all points on the Pareto front are mathematically non-dominated, practical implementation often requires selecting a single solution that best aligns with project priorities and contextual constraints. To facilitate this selection, a multi-criteria decision-making (MCDM) approach is applied. This method enables the evaluation of Pareto-optimal solutions based on additional qualitative or quantitative preferences, ensuring that the final choice reflects a balanced consideration of technical, economic, and possibly environmental priorities. The MCDM process thus bridges the gap between computational optimization and real-world decision-making.

3.5.1.5 Identification of Energy Efficiency Measures

A curated set of Energy Efficiency Measures (EEMs) was established through a two-stage process involving an in-depth market analysis and structured engagement with key project stakeholders. Insights gathered from supplier data, building codes, and current retrofit practices were combined with input from a focused expert panel to ensure that selected measures were both practical and contextually appropriate.

These EEMs were then formulated as discrete decision variables within the Energy Plus simulation framework and incorporated into the MATLAB-based optimization model. This integration allowed each measure to be evaluated under a consistent simulation-optimization workflow. The selected measures include a mix of passive and active strategies, ranging from thermal envelope upgrades to HVAC retrofits and on-site renewable energy systems.

In this study, both the population size and the number of generations (iterations) were set to 50 during the NSGA II optimization process. These values were determined after performing several trial runs aimed at balancing computational efficiency and solution quality. Preliminary tests using larger parameters, such as population sizes of 60 and 60 iterations, showed only marginal improvements in solution diversity and convergence while significantly increasing total computational time. Specifically, the gain in performance was minimal compared to the 50×50 configuration, with changes in objective function values remaining within a narrow range. On the other hand, reducing the parameters below 50 (e.g., 30×30) led to unstable results, limited Pareto front coverage, and weaker convergence behavior. Therefore, the 50×50 configuration was selected as an efficient and practical trade-off, offering a reliable set of optimization solutions while keeping the simulation workload within manageable limits.

A complete list of the selected EEMs and their corresponding parameterizations is presented in Table 3.19, forming the basis for scenario development within the multi-objective optimization process.

An essential starting point in developing energy retrofit strategies is the establishment of a baseline energy profile against which proposed improvements can be measured. This performance reference enables a clear assessment of how different interventions affect the building's thermal behavior. A major contributor to energy inefficiency in buildings is heat loss through the envelope, including transmission through opaque elements and infiltration through gaps and joints.

Table 3.19. Strategies for Energy Efficiency Measures (EEMs)

Construction	Type	Number of discrete options	Type of Retrofit
Wall	Exterior	10	Add Insulation Layer
Wall	Underground	10	Add Insulation Layer
Floor	Semi-exposed	10	Add Insulation Layer
Floor	Exterior	10	Changing Insulation Layer
Floor	Underground	10	Changing Insulation Layer
Roof	Roof	10	Changing Insulation Layer
Window	East Side	6	Changing Glaze
Window	West Side	6	Changing Glaze
Window	North Side	6	Changing Glaze
Window	South Side	6	Changing Glaze
Window	East-tilted Side	6	Changing Glaze
Window	South-tilted Side	6	Changing Glaze

To mitigate these losses, one of the most effective and widely applicable approaches is the enhancement of the building envelope through the installation of thermal insulation. By increasing the resistance to heat flow, insulation helps stabilize indoor temperatures and reduce the demand for mechanical heating and cooling. In this context, several insulation materials and thickness configurations were identified and analyzed for their potential application. These alternatives are summarized in Table 3.20, and each was treated as a configurable input within the simulation and optimization framework.

Table 3.20. Insulation variables

Insulation Modeling Name	Component	Type	RSI	Thickness (m)	Conductivity $(W/m.K)$	Price/ m^2
Insulation 1	Extruded Polystyrene	Rigid Insulation SM XPS	0.882	0.0254	0.0288	$20.33
Insulation 2	Expanded Polystyrene	Isoform Rigid Insulation Panel	0.987	0.0381	0.0386	$91.20
Insulation 3		Rigid Mineral Wool Insulation	1.058	0.0381	0.0360	$21.53
Insulation 4	Extruded Polystyrene	rigid insulation Panel-XPS 20	1.323	0.0381	0.0288	$29.04
Insulation 5		Rigid Mineral Wool Insulation	1.411	0.0508	0.0360	$30.81
Insulation 6	Extruded Polystyrene	Rigid Insulation SM XPS	1.764	0.0508	0.0288	$42.57
Insulation 7		Rigid Mineral Wool Insulation	2.116	0.0762	0.0360	$46.07
Insulation 8	Extruded Polystyrene	Rigid Insulation SM XPS	2.646	0.0762	0.0288	$66.54
Insulation 9		Rigid Mineral Wool Insulation	2.822	0.1016	0.0360	$61.54
Insulation 10	Extruded Polystyrene	rigid insulation Panel-XPS 30	3.528	0.1016	0.0288	$93.18

Glazing systems represent a critical component of the building envelope, with significant influence on both energy consumption and occupant comfort. Beyond their role in admitting natural daylight, which can substantially reduce lighting energy use, windows also act as thermal bridges that permit heat gain or loss, depending on seasonal conditions and solar exposure. Their impact on thermal performance is governed by characteristics such as insulation value, solar control capacity, and optical clarity. As part of this study, a range of high-performance window alternatives was examined, incorporating variations in glazing type, frame construction, and thermal properties. These options were incorporated into the optimization framework as discrete design variables and are systematically outlined in Table 3.21.

Table 3.21. Window Variables

Glass material	Gas	U value $(W/m^2 \cdot K)$	SHGC	Price/m^2
Insulated Dual Clear Air-Filled High Altitude	Air	2.73	0.69	$673.53
Insulated Dual Clear Air-Filled High-Altitude Upgrade To 4mm	Air	2.67	0.67	$745.44
Insulated Dual Low-E Advanced Low-E Insulating Glass Air-Filled High-Altitude Upgrade To 5mm	Air	1.82	0.32	$745.44
Insulated Dual Low-E Natural Sun Low-E Insulating Glass Argon Non-High-Altitude Upgrade To 6mm	Argon	1.65	0.57	$804.16
Insulated Dual Low-E Sun Defense™ Low-E Insulating Glass Argon Non-High-Altitude Upgrade To 6mm	Argon	1.53	0.24	$840.11
Insulated Dual Low-E Advanced Comfort Low-E Insulating Glass Argon Non-High-Altitude Upgrade To 6mm	Argon	1.31	0.31	$876.06

3.5.2 Second Stage: Scenario-Based Performance Evaluation

Following the envelope optimization phase, which identified high-performing design configurations through a multi-objective algorithmic process, the second stage of this study adopts a scenario-based approach to further improve the building's energy performance. In this stage, the optimized envelope serves as a fixed baseline condition, upon which a series of targeted retrofit strategies are systematically evaluated. Unlike the first phase, which relied on evolutionary optimization, this phase emphasizes practical feasibility and comparative analysis across predefined retrofit packages. These scenarios are designed to reflect real-world upgrade pathways and include two main categories: (1) HVAC system optimization, which explores improvements in mechanical system design and control, and (2) Renewable Energy integration, which investigates the impact of distributed energy solutions such as solar PV systems and green roofs.

Each scenario is assessed using dynamic simulation to quantify its impact on energy consumption, economic performance, and carbon footprint, enabling a comprehensive evaluation of its retrofit potential.

3.5.2.1 HVAC Optimization

This study focuses on HVAC optimization by analyzing key variables such as heating, cooling, and electricity usage. Three individual retrofit scenarios and two combined approaches are evaluated to enhance system efficiency. Optimization is carried out with an emphasis on improving energy performance and reducing operational costs. The methodology integrates scenario-based analysis to support cost-effective and sustainable HVAC operations.

3.5.2.1.1 HVAC Retrofit Scenario 1: Conversion from Constant Air Volume (CAV) to Variable Air Volume (VAV) System

In the baseline, air distribution relied on CAV systems, which supply fixed airflow regardless of demand, often leading to excessive energy use. To improve efficiency, this scenario evaluates conversion to VAV. These systems dynamically adjust airflow and, when necessary, supply air temperature, thereby reducing fan energy, improving zone-level comfort, and facilitating integration with advanced controls such as DCV and economizers.

All applicable AHUs were reconfigured from fixed- to variable-speed fans, enabling demand-responsive operation. Simulations compared baseline CAV and retrofit VAV performance under identical conditions, focusing on annual electricity, heating, and cooling consumption.

3.5.2.1.2 HVAC Retrofit Scenario 2: Integration of Heat Recovery System

This scenario investigates adding a sensible HR system to the AHUs. A flat plate exchanger transfers thermal energy from exhaust to incoming outdoor air without mixing, lowering heating and cooling loads while avoiding cross-contamination. Advantages include reduced central plant energy demand, low maintenance, and compliance with ASHRAE 90.1.

The retrofit is particularly effective in winter, when exhaust air preheats cold outdoor air, and offers some pre-cooling benefits in summer. Energy savings were quantified by comparing annual heating and cooling loads before and after implementation.

3.5.2.1.3 HVAC Retrofit Scenario 3: Integration of an Economizer Control Strategy

An economizer strategy was modeled to provide "free cooling" by increasing outdoor air intake when conditions are favorable. Dampers modulate based on outdoor temperature or enthalpy, reducing reliance on mechanical cooling and lowering peak demand.

In Ottawa's cold climate, economizer operation is restricted to transitional and cooling seasons. A low-limit cutoff of 4°C prevents unnecessary heating penalties in winter. Simulation results compare annual cooling and fan electricity use before and after retrofit.

3.5.2.1.4 HVAC Retrofit Scenario 4: Implementation of Demand-Controlled Ventilation (DCV)

DCV modulates outdoor air intake according to occupancy or indoor CO_2 levels, avoiding over-ventilation common in constant-rate systems. Ventilation is reduced when CO_2 is below thresholds (e.g., 1000 ppm) and increased during high occupancy, maintaining air quality while reducing energy use.

This strategy is especially effective in classrooms, offices, and meeting areas with variable occupancy. The retrofit was modeled in relevant zones, and its impact on ventilation load, heating, cooling, and overall HVAC performance was evaluated against baseline operation.

3.5.2.1.5 Combined HVAC Retrofit Scenario

To evaluate the potential synergy among multiple energy-saving HVAC measures, two combined retrofit scenarios were developed in this study. The first scenario integrates DCV, HR, and economizer control strategies. The second scenario combines VAV systems with HR and economizer integration. These combinations aim to assess whether the simultaneous implementation of previously evaluated individual retrofits can deliver greater reductions in energy consumption than the sum of their standalone effects. Comparative simulations were performed to quantify the cumulative impact of these integrated strategies on annual heating, cooling, and electricity demands.

3.5.2.2 Renewable Energy Integration for Load Reduction and On-Site Generation

In this study, a green roof was evaluated as a retrofit strategy to improve the building's thermal and environmental performance. The installation of a vegetated roof system introduces additional layers of insulation and thermal mass, which help reduce conductive heat transfer through the roof assembly. This results in lower heating loads during the winter and decreased cooling demand during the summer months. Furthermore, the presence of vegetation reduces rooftop surface temperatures by limiting solar radiation absorption, thereby contributing to the mitigation of urban heat island effects. Beyond energy benefits, green roofs offer supplementary advantages, including improved stormwater retention and extended membrane lifespan, as the vegetation layer protects the underlying waterproofing from ultraviolet radiation and thermal stress. Incorporating a green roof also aligns with broader sustainability goals and performance frameworks such as LEED and net-zero energy initiatives. Within the Energy Plus modeling environment, the green roof assembly was defined using layered construction inputs for soil and vegetation, allowing for a detailed simulation of its thermal impact on annual energy consumption.

The final stage explores renewable technologies to offset remaining loads after envelope and HVAC optimization. Rooftop surfaces (38 in total) were modeled at a fixed 40° tilt to match Ottawa's solar geometry. Scenarios include PV panels, solar thermal collectors, PVT hybrids, and a green roof system. Each is assessed for energy contribution, impact on reducing grid reliance, and economic feasibility.

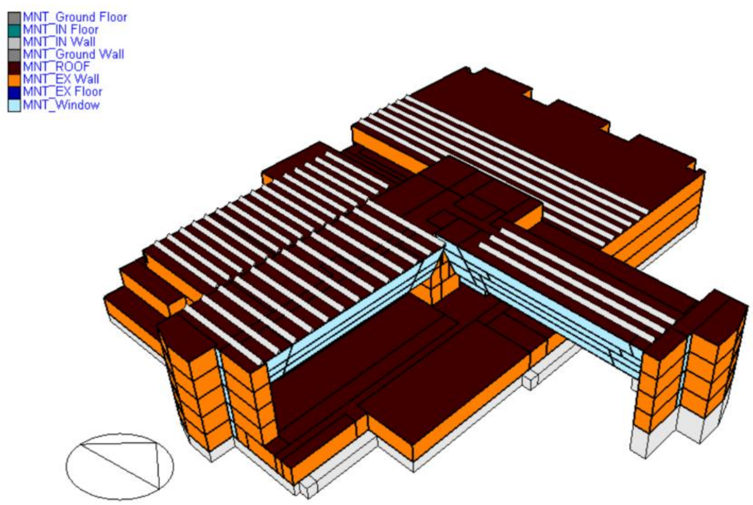

Figure 3. 21 Layout of surfaces on the roof of Montpetit Hall

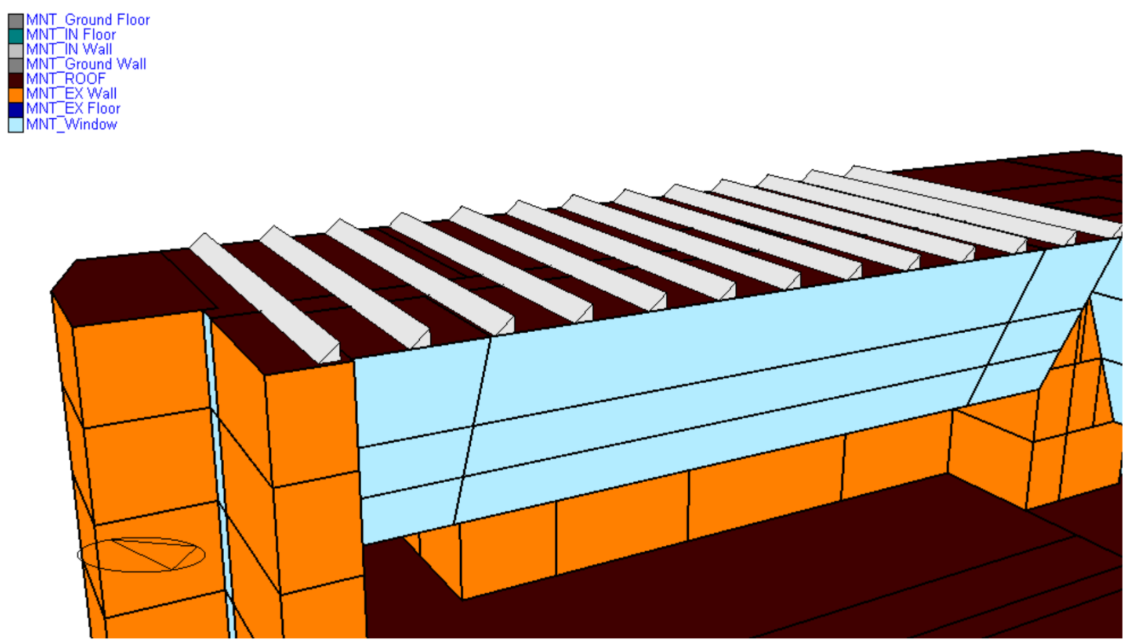

Figure 3. 22 layout and angle of rooftop surfaces

3.5.2.2.1 Renewable Energy Scenario 1: Integration of PV Panels

PV technology was selected as the first renewable option due to its maturity and declining costs. The REC Alpha Pro M 640W module, featuring heterojunction half-cut cell technology and a rated efficiency of 22.5%, was modeled. Its high conversion efficiency makes it well suited to limited rooftop space.

PV modules were deployed across all 38 available roof surfaces, oriented at a 40° tilt. Simulations accounted for local climate and insolation conditions to estimate annual electricity generation. Outputs were compared against total building electricity demand to determine offset potential and quantify reductions in reliance on the university's central energy supply. This scenario also evaluated the effect on peak electrical demand and long-term operational carbon reductions.

3.5.2.2 Renewable Energy Scenario 2: Integration of Solar Thermal Collectors

Solar thermal collectors were modeled to supplement the building's heating requirements. Unlike PV, these systems directly convert solar radiation into usable heat, reducing reliance on district-supplied hot water.

The AE-32 flat plate solar collector (2.88 m² gross area), designed for commercial applications, was selected. The collector incorporates a black chrome absorber, tempered glass glazing, and insulated casing, ensuring efficient solar gain and reduced losses. Collectors were installed at a 40° tilt to maximize seasonal efficiency.

Thermal output simulations quantified the contribution of the system to space heating and domestic hot water loads. Annual energy yield was compared to baseline heating demand to evaluate reductions in natural gas use, district energy consumption, and operating costs.

3.2.2.3 Renewable Energy Scenario 3: Integration of PVT Systems

The PVT system represents an advanced hybrid technology that combines PV cells with a thermal collector mounted on the rear surface. This configuration allows simultaneous electricity and heat generation, with two primary benefits:

1. **Enhanced PV performance**: extracting heat lowers PV surface temperature, improving electrical efficiency.
2. **Additional thermal recovery**: captured heat can be applied to domestic hot water or space heating.

The modeled PVT unit included a fluid-based heat exchanger for continuous heat removal. Simulations assessed annual combined outputs, reductions in grid electricity, and offsets to district heating. This scenario highlights the potential of PVT systems to achieve higher total solar conversion efficiency compared to stand-alone PV or solar thermal, making them particularly relevant for buildings with limited roof space but high energy demands.

3.5.2.2.4 Renewable Energy Scenario 4: Implementation of a Green Roof System

A green roof system was investigated for its potential to improve building thermal performance through shading, evapotranspiration, and additional insulation. The modeled configuration included four layers:

1. **Vegetation layer**: sedum species, selected for drought tolerance and low maintenance.
2. **Soil substrate**: providing both thermal mass and growing medium.

3. **Drainage layer**: ensuring water runoff management.
4. **Waterproofing membrane**: protecting the structural roof.

The system was modeled with key vegetation parameters: leaf area index, reflectivity, emissivity, and minimum stomatal resistance, which govern shading, radiation balance, and evapotranspiration.

Simulations assessed the impact on roof surface temperature, heat flux, and seasonal heating/cooling loads. Results indicate significant reductions in cooling energy during peak summer periods and moderate winter insulation benefits. Secondary benefits include extended roof lifespan, stormwater management, and contributions to urban biodiversity, though the focus remained on quantifiable energy performance.

1. **Leaf Area Index:** one-sided green leaf area per unit ground surface area.
2. **Leaf Reflectivity**: The fraction of incident solar radiation that is reflected by the individual leaf surfaces. Solar radiation includes the visible spectrum as well as infrared and ultraviolet wavelengths.
3. **Leaf Emissivity**: This field is the ratio of thermal radiation emitted from leaf surfaces to that emitted by an ideal black body at the same temperature. This parameter is used when calculating the long wavelength radiant exchange at the leaf surfaces.
4. **Minimum Stomatal Resistance:** The resistance of the plants to moisture transport. Plants with low values of stomatal resistance will result in higher evapotranspiration rates than plants with high resistance.

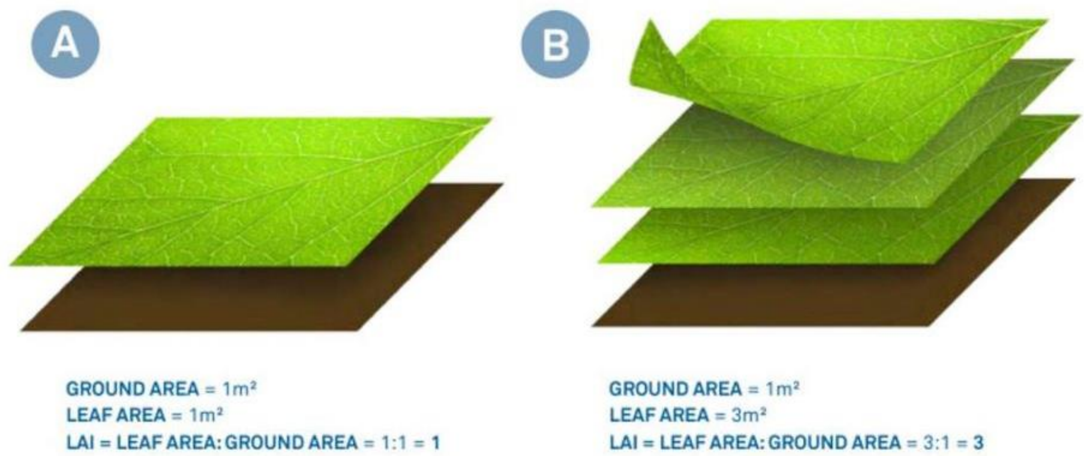

Figure 3. 23 Conceptual visualization of Leaf Area Index (LAI)

Table 3.22. Characteristics of the vegetation

Vegetation Name	Height of Plants (m)	Leaf Area Index	Leaf Reflectivity	Leaf Emissivity	Minimum Stomatal Resistance (s/m)
Sedum Species (Yellow green leaves)	0.1	3.75	0.25	0.95	250

Figure 3. 24 Vegetation with high leaf density (Sedum Species)

Table 3.23. The materials and their features of Green Roof

Material	Roughness	Thickness (m)	Conductivity $(W/m.K)$	Density (Kg/m^3)	Specific Heat $(J/Kg.K)$
Vegetation	-	-	-	-	-
Soil	Rough	0.1	0.35	800	1200
Drainage	Medium Rough	0.025	0.45	950	2200
Waterproof Membrane (EPDM)	Medium Rough	0.025	0.3	880	1700

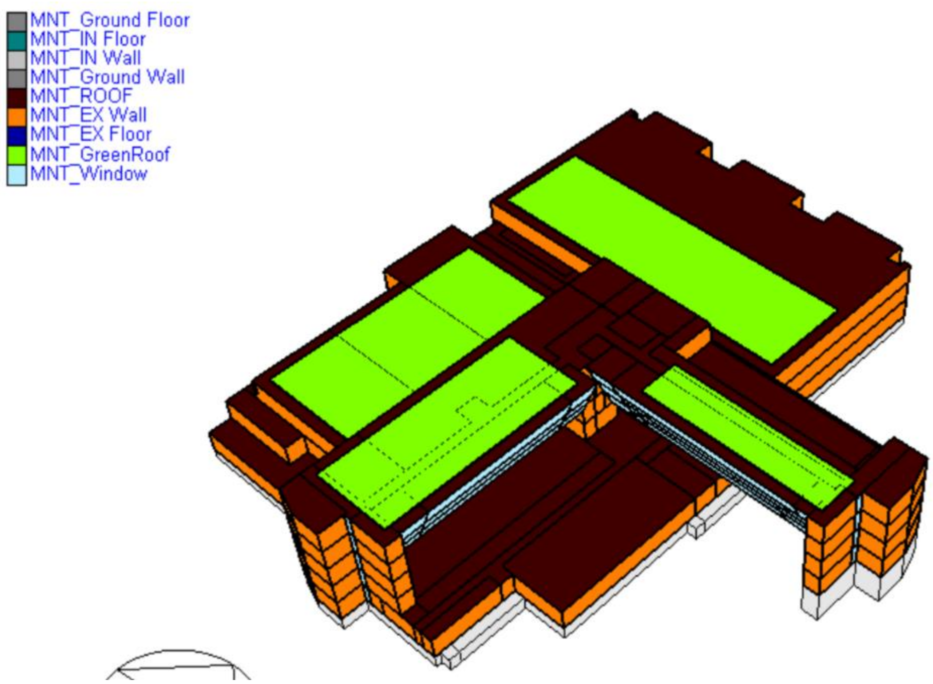

Figure 3. 25 Geometry model of Montpetit Hall after green roof implementation

In this study, PV panels and a green roof were investigated as separate retrofit scenarios rather than as a combined system. This decision was made for several methodological and practical reasons. First, from a research design perspective, modelling the two measures independently allows for a clear attribution of their individual impacts on heating, cooling, and electricity consumption, as well as on economic performance. A combined PV–green roof configuration would introduce interaction effects (e.g., mutual shading, modified roof surface temperatures, changes in convective and radiative heat transfer) that are more complex to represent accurately in simulation and would complicate the interpretation of results within a single master's thesis. Second, implementing both systems simultaneously on Montpetit Hall would require a detailed structural and architectural assessment to verify load-bearing capacity, wind uplift resistance, and compatibility with existing roof assemblies, especially given the building's age and history of partial roof replacement. These structural and durability questions are beyond the scope of the present work and would more appropriately fall under a dedicated building envelope or structural engineering study.

In addition, a combined PV–green roof system would necessitate a careful optimization of roof use: PV modules typically require specific tilt, spacing, and setback conditions to avoid self-shading and to maximize annual yield, whereas green roofs require sufficient exposure, irrigation, and maintenance access to sustain vegetation health. Balancing these competing requirements on a constrained roof area would demand a more advanced multi-domain optimization (energy, structure, horticulture, maintenance) than was feasible within the timeframe and objectives of this thesis. Finally, reliable performance data and cost information for integrated PV–green roof systems in cold climates such as Ottawa are still limited compared to conventional PV and extensive green roofs considered separately, which would introduce additional uncertainty into both the energy and economic evaluation. For these reasons, PV and green roof retrofits were modeled and assessed independently in this work, while the analysis of a fully integrated PV–green roof system is identified as a promising avenue for future research.

3.6 Economic Feasibility Assessment

Evaluating the economic performance of retrofit measures is essential to determine whether projected energy savings justify the required investments. In this study, four standard financial indicators, NPV, Lifecycle Cost (LCC), IRR, and Payback Period, were employed to assess the feasibility of HVAC and renewable energy retrofits for Montpetit Hall. These indicators were selected because they provide complementary perspectives: NPV and IRR capture overall profitability, LCC reflects the comprehensive cost of ownership, and payback periods highlight the speed of capital recovery. The following subsections describe these indicators and outline the methodology adopted in this research.

3.6.1 Net Present Value (NPV)

The NPV expresses the difference between the present value of benefits and costs over the analysis period, discounted at a given rate. It accounts for the time value of money by reducing future savings and costs to today's equivalent [123].In this study, NPV was used to evaluate whether the monetary savings generated by each retrofit exceeded the associated investment and operating costs.

$$NPV = \sum_{t=0}^{n} \frac{(B_t - C_t)}{(1+r)^t} \tag{9}$$

Where B_t represents benefits such as avoided energy expenditures and residual value in year t, C_t denotes costs including capital, maintenance, and replacement, r is the real discount rate, and n is the analysis horizon. For Montpetit Hall, the analysis was conducted over a 20-year period using a 3% discount rate, which aligns with Canadian public-sector investment guidelines [124], [125];

[70]. A positive NPV indicates that a retrofit provides net financial benefits compared to the baseline.

3.6.2 Lifecycle Cost (LCC)

The LCC method estimates the total cost of owning and operating a system throughout its life span, expressed in present value terms. Unlike NPV, which emphasizes net profitability, LCC captures the cumulative financial burden of each alternative [126].

$$LCC = C_{cap} + \sum_{t=1}^{n} \frac{C_{op,t} + C_{maint,t} + C_{rep,t}}{(1+r)^t} - \frac{RV}{(1+r)^n} \tag{10}$$

Here, C_{cap} denotes initial capital investment, $C_{op,t}$ refers to annual energy expenditures, $C_{maint,t}$ is annual maintenance, $C_{rep,t}$ represents replacements, and RV is the residual value at the end of the analysis period. For this project, both the baseline system and each retrofit alternative were assessed using LCC. A retrofit was considered cost-effective if its LCC was lower than that of the baseline case ([127]; [128]).

3.6.3 Internal Rate of Return (IRR)

IRR is defined as the discount rate (r) at which the NPV of an investment equals zero. It reflects the annualized return generated by a retrofit, expressed as a percentage [129].

$$\frac{C_0}{(1+r)^0} + \frac{C_1}{(1+r)^1} + \frac{C_2}{(1+r)^2} + \cdots + \frac{C_n}{(1+r)^n} = 0 \tag{11}$$

$$NPV = \sum_{t=0}^{n} \frac{C_t}{(1+r)^t} \quad (12)$$

Where:

- C_t is cash flow at time t (with C_0 usually being the initial investment, a negative value)
- r is IRR
- n = number of periods

In practice, the IRR allows for a direct comparison between a retrofit and the selected discount rate. In this study, if the IRR exceeded 3%, the retrofit was deemed financially attractive. This approach is consistent with common decision-making practices in building energy retrofits [130].

3.6.4 Payback Period

The payback period measures the time required for cumulative savings to equal the initial investment. Two variations were applied:

Simple Payback Period (SPP): based solely on undiscounted annual savings.

Discounted Payback Period (DPP): accounts for the time value of money by discounting future savings [125].

$$SPP = \frac{C_{cap}}{Annual\ Net\ Savings} \quad (13)$$

Although payback is less comprehensive than NPV or LCC, it provides a straightforward indication of risk and liquidity, which is particularly relevant for institutional budgeting decisions [110].

3.6.5 Methodology Applied in This Study

The economic evaluation followed a systematic approach:

In this study, a feasibility analysis was carried out for each retrofit scenario using a life-cycle cost (LCC) framework over a 20-year horizon. For every option, the cash flow was constructed to include the initial capital cost at year zero, the annual expenditures for energy and operation and maintenance (O&M), the replacement costs scheduled at year ten, and the residual (salvage) value credited at the end of year twenty. These cash flows were then discounted using a real discount rate of 3% to obtain the NPV of each scenario. The NPV indicates the economic viability of a project, where a positive value confirms that the retrofit is financially justified, and a higher NPV reflects greater profitability. In addition, the IRR was calculated, which represents the effective return on investment; this value must exceed the discount rate, and the larger it is, the more profitable the project becomes. Finally, the LCC was determined for both the baseline and the retrofit scenarios by summing all discounted costs and subtracting the residual value, allowing for a direct comparison of long-term ownership costs to assess whether the proposed retrofit measures reduce total expenditures relative to the existing system.

Energy simulation outputs: Energy Plus models of Montpetit Hall were developed and calibrated against utility data. Baseline and retrofit scenarios (VAV, DCV, economizer, HR, and their combinations) as well as renewable strategies (PV, PVT, solar collectors, green roof) were simulated to determine annual heating, cooling, and electricity consumption.

Conversion to energy costs: Simulated consumption was translated into costs using Ottawa utility rates: electricity at 0.1105 CAD/KWh, heating energy equivalent at 0.0249 CAD/kWh_{th}, and cooling energy at 0.0268 CAD/kWh_{th}.

Decision-making criteria: Retrofits with NPV>0, IRR>3%, or lower LCC than baseline were considered economically viable. Additionally, institutional decision-makers may prioritize measures with shorter payback periods, especially when budget cycles are constrained [130].

This framework ensured a comprehensive and comparable assessment of each retrofit and renewable strategy, balancing long-term financial viability with short-term budgetary concerns.

4. Discussion and Results

4.1 Model Measured Data

To establish the reliability of the baseline model, the simulated energy consumption of Montpetit Hall was calibrated against measured utility data obtained from the University of Ottawa's central energy plant for the year 2022. Table 4.1 presents the monthly actual energy consumption for heating, cooling, and electricity, expressed in gigajoules (GJ). The annual energy cost breakdown was also provided by the university, amounting to $213,055 CAD for electricity, $144,755 CAD for heating hot water, and $40,174 CAD for chilled water, for a total annual energy expenditure of $397,984 CAD.

Table 4. 1. Monthly measured energy consumption for Montpetit Hall (2022)

Month	Heating (GJ)	Cooling (GJ)	Electricity (GJ)
January	2209.9	125.98	390.41
February	1711.38	114.72	384.65
March	1451.51	137.04	442.18
April	982.03	200.44	407.74
May	392.41	486.26	415.74
June	206.72	555.68	628.31
July	128.34	820.57	675.59

August	141.64	833.35	715.08
September	384.13	537.60	681.28
October	648.47	267.06	570.69
November	1200.00	132.00	541.00
December	1600.00	128.00	539.00
Total	**10,056.5**	**4,338.7**	**6,391.7**

The annual totals indicate that heating demand dominates the energy profile of Montpetit Hall, accounting for 10,056 GJ in 2022. Cooling energy consumption is also significant, with 4,339 GJ annually, reflecting the high ventilation and cooling requirements during the summer months. Electricity use amounted to 6,392 GJ annually, primarily associated with plug loads, fans, pumps, and auxiliary systems.

The monthly distribution highlights clear seasonal patterns. Heating demand peaks in January (2209.9 GJ) and declines to a minimum in the summer months (July: 128.3 GJ), consistent with Ottawa's cold climate. Cooling demand is negligible in winter but rises sharply in summer, with the highest values in August (833.3 GJ) and July (820.6 GJ). Electricity consumption is more evenly distributed throughout the year but exhibits a noticeable increase during cooling-intensive months (June–September) due to higher fan and pump operation.

These measured energy use profiles serve as the benchmark for calibrating the baseline simulation model. The next step involves comparing simulated results against these actual data to assess the accuracy of the model through calibration metrics such as Normalized Mean Bias Error (NMBE) and Coefficient of Variation of the Root Mean Square Error (CVRMSE), following ASHRAE Guideline 14 standards.

4.2 Model Calibration

To ensure the reliability of the baseline simulation model, the results were calibrated against measured utility data provided by the University of Ottawa's central energy plant for Montpetit Hall in 2022. Table 4.2 summarizes the comparison of simulated and measured monthly energy consumption for heating, cooling, and electricity. (Figure 4.1)

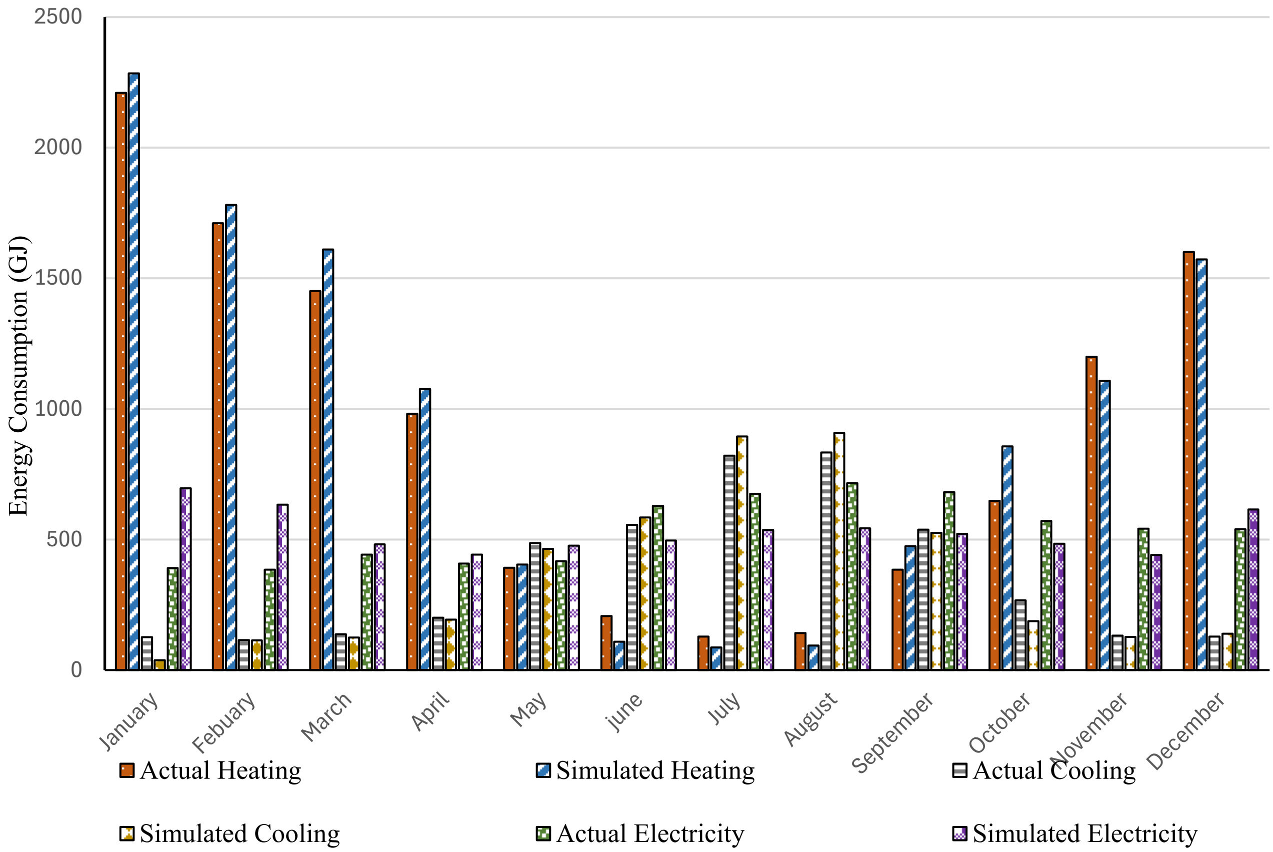

Figure 4. 1 Actual and Simulation Energy Consumption of Montpetit Hall In 2022

The annual totals indicate strong agreement between simulated and measured data. Heating demand was slightly overpredicted by the model (10,282 GJ vs. 10,056 GJ, an error of –3.6%), while cooling demand was reproduced with excellent accuracy (4,296 GJ vs. 4,339 GJ, +0.97%).

Electricity use showed a very small deviation of only –0.41% from actual consumption. (Table 4.3)

Calibration accuracy was further assessed using Normalized Mean Bias Error (NMBE) and the Coefficient of Variation of the Root Mean Square Error (CVRMSE), in accordance with ASHRAE Guideline 14.

Table 4. 2. Comparison of measured and simulated monthly energy consumption (2022)

Month	Heating (Actual)	Heating (Simulated)	Cooling (Actual)	Cooling (Simulated)	Electricity (Actual)	Electricity (Simulated)
January	2209.9	2284.8	125.98	37.51	390.41	696.46
February	1711.38	1780.7	114.72	113.87	384.65	633.16
March	1451.51	1610.3	137.04	124.89	442.18	481.29
April	982.03	1075.3	200.44	192.70	407.74	442.27
May	392.41	404.2	486.26	463.60	415.74	476.44
June	206.72	108.5	555.68	584.15	628.31	496.40
July	128.34	86.8	820.57	894.00	675.59	537.08
August	141.64	94.5	833.35	908.14	715.08	542.34
September	384.13	473.7	537.60	525.53	681.28	521.15
October	648.47	856.8	267.06	186.77	570.69	484.00
November	1200.00	1107.9	132.00	126.67	541.00	440.77
December	1600.00	1572.8	128.00	138.89	539.00	614.38
Total	**10,056.5**	**10,281.8**	**4,338.7**	**4,296.0**	**6,391.7**	**6,563.3**

Table 4. 3. Calibration error indicators

End-Use	NMBE (%)	CVRMSE (%)	Simple Error (%)
Heating	–3.62	10.80	–

Cooling	+0.97	13.13	–
Electricity	–	–	–0.41

According to ASHRAE Guideline 14, acceptable thresholds for monthly calibration are ±5% for NMBE and ±15% for CVRMSE. The simulation results for heating and cooling both fall well within these limits, confirming that the baseline model is adequately calibrated. For electricity, due to variability in monthly billing and non-modeled plug loads, the simple annual error was used instead of statistical indicators. The deviation was only –0.41%, which is negligible.

Overall, the calibration results demonstrate that the baseline model provides a reliable representation of Montpetit Hall's energy performance and can be confidently used to evaluate retrofit strategies.

4.3 Solutions for Envelops and Windows

The outcomes of the optimization process are presented through the Pareto front, the selected decision variables, and the resulting evaluations of the objective functions. Figure 4.2 illustrates the Pareto front generated under prevailing utility price conditions through a simulation-based, multi-objective optimization using the NSGA-II algorithm. The process yielded 50 optimal solutions, providing a diverse set of feasible alternatives. The two-dimensional representation of the Pareto front highlights the trade-off between economic performance, measured by NPV, and environmental performance, represented by total primary energy demand. As the figure indicates, improvements in one objective are generally accompanied by compromises in the other. In the graphical representation, the red stars denote the solutions located on the Pareto front, which reflect the set of non-dominated optimal trade-offs, whereas the blue stars represent non-selected options, excluded from the Pareto set due to inferior performance in at least one of the objectives.

Displaying the blue stars is still valuable, as it demonstrates the broader solution space explored during the optimization process and emphasizes the superior performance of the Pareto-optimal solutions.

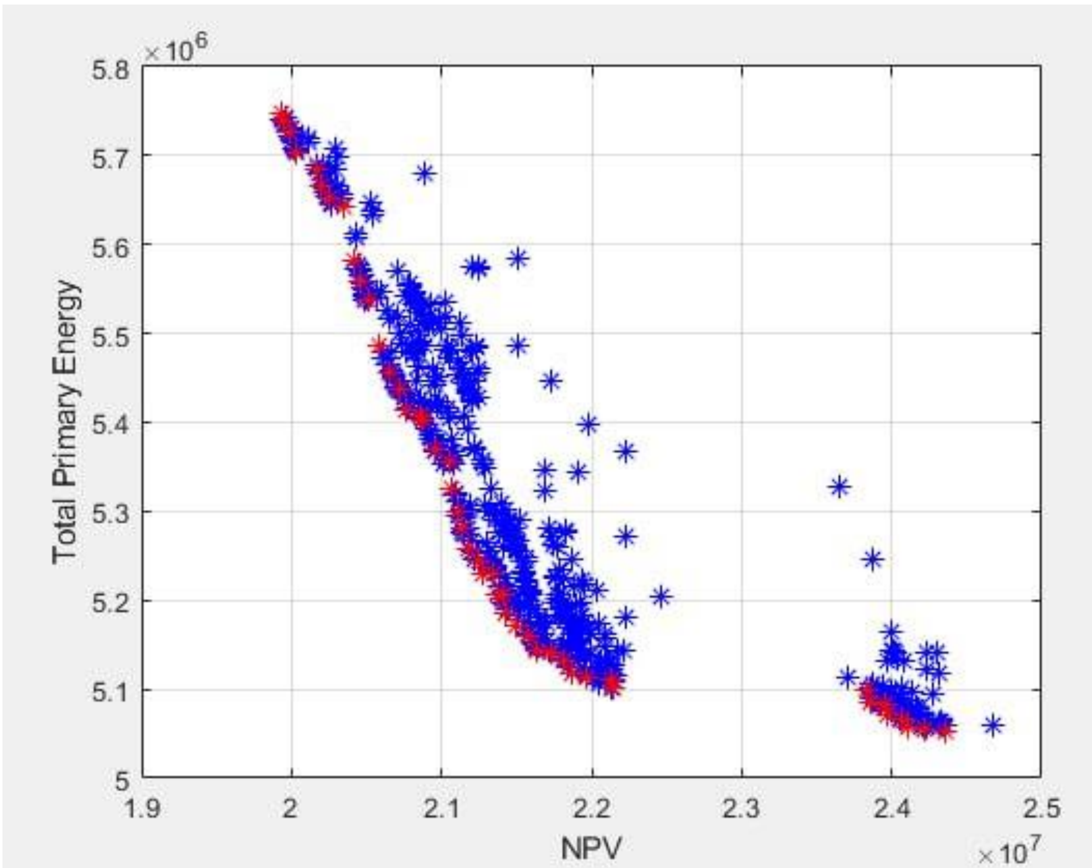

Figure 4. 2 Pareto Front and non-selected variables

The range of primary energy consumption among the evaluated solutions varies from 24,062 GJ to 26,967 GJ, reflecting the influence of different material types and properties applied in the retrofits. All fifty solutions represented on the Pareto front demonstrate improved performance compared to the original case. However, two criteria warrant closer examination: the highest reduction in primary energy consumption and the lowest associated capital cost.

As illustrated in Figure 4.3, the green dots indicate the most energy-efficient solutions. In this case, the total primary energy consumption is 24,062 GJ. Under this condition, the natural gas consumption for district heating is 11,131 GJ, while the electricity consumption for district cooling is 7,065 GJ. These values correspond to reductions of 19% in heating demand and 6% in cooling demand, respectively, compared with the baseline.

Conversely, the red dot represents the least effective solution in terms of primary energy savings. Here, the total primary energy consumption is 26,967 GJ, with district heating demand reaching 13,127 GJ and district cooling demand 7,567 GJ. These outcomes reflect only a 3% reduction in both heating and cooling consumption relative to the baseline. Detailed comparative reductions for each solution are presented in Table 4.4.

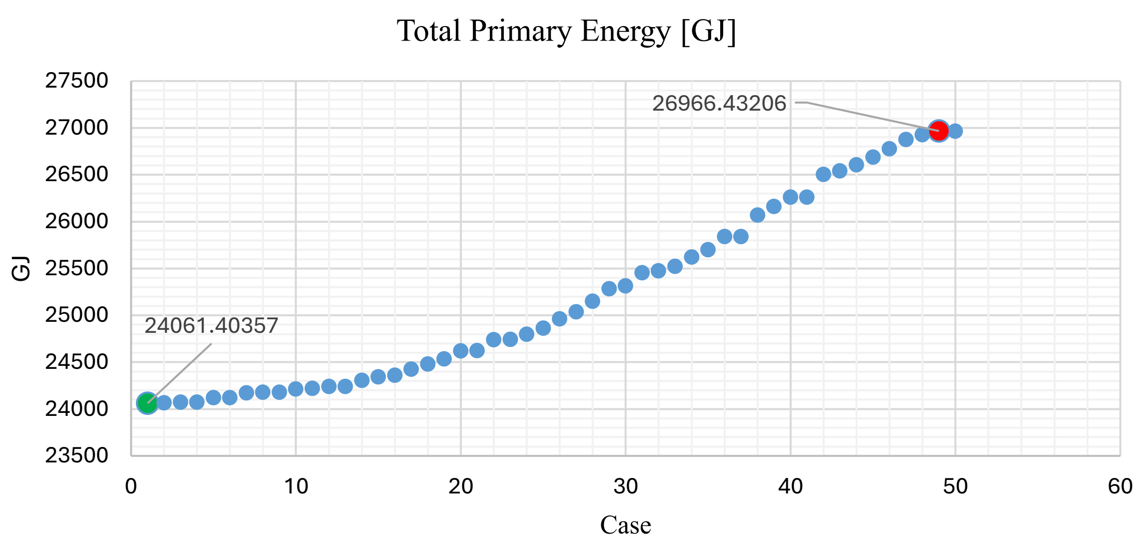

Figure 4. 3 Primary Energy Consumption of solutions

Table 4. 4. Detailed Information of Highest and Lowest Primary Energy Consumption Solutions

Case	Heating Consumption (GJ)	Heating reduction	Cooling consumption (GJ)	Cooling reduction	Electricity Consumption (GJ)	Electricity reduction

Case 1 – Green Point	9640	19%	1425	6.5%	7065	9%
Case 2- Red Point	1200	3.15%	1530	3.23%	7780	2.8%

From an economic perspective, the green dot solution demonstrates the lowest total utility cost, amounting to CAD 276,509.87. This includes CAD 199,207.26 for electricity consumption in the cooling district and CAD 77,302.62 for natural gas in the heating district. Notably, this retrofit achieves an overall utility cost reduction of approximately CAD 125,000, the greatest among the evaluated alternatives. However, this option is associated with a capital cost of CAD 6,556,034.07, which ranks among the three highest investment levels across fifty solutions. The elevated cost results from employing high-performance envelope and window materials, which maximize energy savings. While this option yields the greatest energy reduction, the financial indicators, including NPV, IRR, and payback period, do not demonstrate profitability. Nonetheless, this case was selected for further optimization because the primary objective at this stage is to maximize reductions in district heating, cooling, and electricity demand.

In contrast, the red dot solution represents the least effective case in terms of utility cost reduction. The total utility expenditure amounts to approximately CAD 304,000, reflecting a modest saving of around CAD 96,000 compared with the baseline. This value is distributed as CAD 213,228.44 for electricity consumption in the cooling district and CAD 91,156.54 for natural gas consumption in the heating district. The capital investment required for this retrofit is comparatively low at CAD 489,796.94. Consequently, the financial performance is favorable, with an NPV of CAD 1,980,260.40. This outcome is largely attributable to the relatively low capital cost, as the retrofit involves only window replacements. Therefore, although this solution is more profitable from an economic perspective, it is not the most effective in terms of energy performance.

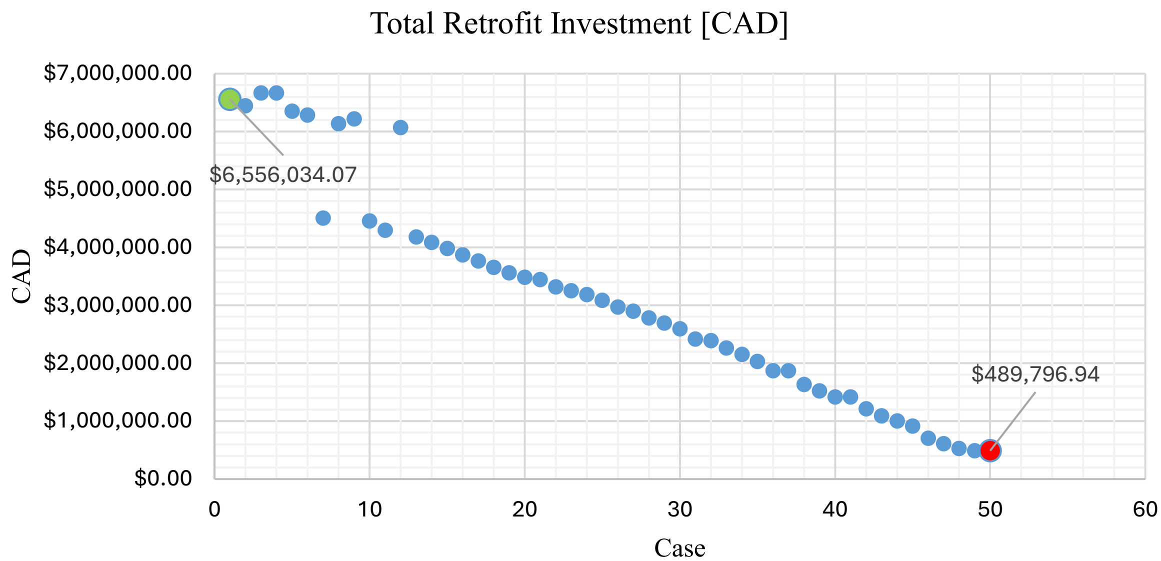

Figure 4. 4 Total Retrofit Investment of solutions

4.3.1. Selected Cases Analysis

In this section of the thesis, we present two selected scenarios: one scenario optimized primarily for economic feasibility, and another optimized for maximum energy efficiency. We then analyze the materials and construction methods utilized in each scenario. For the economically optimal case, we will describe the construction approaches and materials chosen, highlighting their features. For the energy-optimized scenario, we will similarly outline the selected materials and construction techniques, explaining how these choices enhance energy performance.

For the maximum energy efficiency scenario (Green Point) (See Tables 4.5 and 4.6) , all envelopes and window constructions were replaced with alternatives designed to minimize energy loss and enhance overall building performance. The results indicate that the Rigid Insulation Panel–XPS

30 was the most effective material, incorporated in four of the selected constructions. Following this, the Rigid Insulation Panel–XPS 20 and Rigid Insulation SM XPS also demonstrated significant contributions to energy efficiency. In contrast, in the economically optimal scenario (Red Point), the majority of envelope constructions remained in their original form, with the exception of one element and certain window types, as detailed in (Tables 4.7 and 4.8).

Table 4. 5. Selected Envelop with Lowest PEC in Pareto Front (Case1- Green Point)

Construction Type	Chosen Construction	Layer 1 (Outside)	Layer 2	Layer 3	Layer 4	Layer 5	Layer 6	Layer 7 (Inside)
Underground Wall	Underground Wall 8	Waterproof Membrane	Rigid Insulation	Structural Slab	Rigid Insulation SM XPS	Gypsum board		
Underground Floor	Underground Floor 4	Crushed Stone	Lean Concrete	Waterproof Membrane	Rigid Insulation Panel– XPS 20	Structural Slab	Cement Topping	
Exterior Wall	Exterior Wall 10	F06 EIFS Finish	Rigid Insulation Panel– XPS 30	Concrete Exposed	Rigid Insulation	Gypsum board		
Exterior Floor	Exterior Floor 10	Cement Topping	Rigid Insulation Panel– XPS 30	Gravel	Membrane Protection	Waterproof Membrane	Sloping Concrete	Structural Slab
Semi-exposed Floor	Semi Exposed Floor 10	Concrete Exposed	Rigid Insulation Panel– XPS 30	Carpet				
Roof	Roof 10	Built-Up Roofing Bitumen	Rigid Insulation Panel– XPS 30	Sloping Concrete	Structural Slab			

Table 4. 6. Selected Window with Lowest PEC in Pareto Front (Case 1- Green Point)

Construction Type	Chosen Construction	Window Material
West Window	SimpleWindow4	Insulated Dual Low-E Natural Sun Low-E Insulating Glass, Argon, Upgrade to 6 mm
East Window	SimpleWindow6	Insulated Dual Low-E Advanced Comfort Low-E Insulating Glass, Argon, Upgrade to 6 mm
South Window	SimpleWindow4	Insulated Dual Low-E Natural Sun Low-E Insulating Glass, Argon, Upgrade to 6 mm

North Window	SimpleWindow6	Insulated Dual Low-E Advanced Comfort Low-E Insulating Glass, Argon, Upgrade to 6 mm
West Tilted Window	SimpleWindow5	Insulated Dual Low-E Sun Defense™ Low-E Insulating Glass, Argon, Upgrade to 6 mm
South Tilted Window	SimpleWindow6	Insulated Dual Low-E Advanced Comfort Low-E Insulating Glass, Argon, Upgrade to 6 mm

Table 4. 7. Selected Envelop with Highest PEC in Pareto Front (Case 2- Red Point)

Construction Type	Chosen Construction	Layer 1 (Outside)	Layer 2	Layer 3	Layer 4	Layer 5	Layer 6	Layer 7 (Inside)
Underground Wall	Base construction	Waterproof Membrane	Glass Fiber	Structural Slab	Gypsum board			
Underground Floor	Base construction	Crushed Stone	Lean Concrete	Waterproof Membrane	Lean Concrete	Structural Slab	Cement Topping	
Exterior Wall	Base construction	F06 EIFS Finish	Glass Fiber	Concrete Exposed	Rigid Insulation	Gypsum board		
Exterior Floor	Base construction	Cement Topping	Insulation Board	Gravel	Membrane Protection	Waterproof Membrane	Sloping Concrete	Structural Slab
Semi-exposed Floor	Semi Exposed Floor 7	Concrete Exposed	Rigid Mineral Wool Insulation	Carpet				
Roof	Base construction	Built-Up Roofing Bitumen	Roof Insulation	Sloping Concrete	Structural Slab			

Table 4. 8. Selected Window with Highest PEC in Pareto Front (Case 2- Red Point)

Construction Type	Chosen Construction	Window Material
West Window	SimpleWindow4	Insulated Dual Low-E Natural Sun Low-E Insulating Glass, Argon, Upgrade to 6 mm
East Window	Base construction	-
South Window	SimpleWindow4	Insulated Dual Low-E Natural Sun Low-E Insulating Glass, Argon, Upgrade to 6 mm
North Window	Base construction	-
West Tilted Window	SimpleWindow5	Insulated Dual Low-E Sun Defense™ Low-E Insulating Glass, Argon, Upgrade to 6 mm
South Tilted Window	Base construction	-

The physical properties of selected insulation in green point and red point are preset in Table 4.9.

Table 4. 9. Physical Properties of Insulations in Selected Constructions

Name	Insulation Modeling Name	Case	RSI	Thickness (m)	Conductivity $(W/m.K)$
Rigid Insulation Panel-XPS 30	Type 10	1	3.528	0.1016	0.0288
Rigid Insulation Sm Xps	Type 8	1	2.646	0.0762	0.0288
Rigid Insulation Panel-XPS 20	Type 4	1	1.323	0.0381	0.0288
Rigid Mineral Wool Insulation	Type 7	2	2.1168	0.0762	0.0360

4.3.2. Envelopes Assessment

The analysis of construction modifications reveals distinct patterns depending on the level of investment. At the outset, the semi-exposed floor emerged as the primary target for intervention, representing 100% of the initial selections. This indicates that in all cases, the first modification choice was consistently directed toward this element. The rationale lies in the fact that semi-exposed floors act as thermal bridges between conditioned and unconditioned spaces, such as parking garages or partially exposed slabs. Unlike underground components, which benefit from the stabilizing effect of soil temperatures, semi-exposed floors are directly influenced by outdoor conditions. Consequently, they contribute significantly to heat losses in winter and heat gains in summer, making their retrofit both impactful and cost-effective. Following this, the roof (68%) and exterior wall (62%) were prioritized, reflecting their large surface exposure to outdoor climate and strong influence on thermal performance.

From the perspective of insulation performance, insulation type 10 was the most frequently selected option, accounting for 20% of cases. With an RSI value of 3.528 and a low thermal conductivity of 0.0288 W/m·K, this insulation offers the highest thermal resistance among all alternatives. Although it requires greater thickness (0.1016 m) and higher upfront cost, its superior insulation capacity maximizes energy savings, particularly when higher budgets are available. Following this, insulation type 9 (9%) and insulation type 8 (7%) were commonly adopted, both of which provided strong performance-to-cost ratios and thus represented practical choices under constrained investment conditions.

By contrast, the underground floor and underground wall experienced the least modifications, deviating from the baseline in only 18% of cases. This outcome is consistent with the scientific understanding that sub-surface building components are naturally less exposed to thermal exchanges with the external environment. The soil surrounding these elements maintains a relatively stable temperature (around 8–12 °C in Ottawa), thereby reducing fluctuations and mitigating heat losses. As a result, the potential energy savings from retrofitting underground elements is limited, and substantial investments in these areas are typically not justified in cost–benefit analyses.

When the investment was below 1.2 million CAD, the construction largely remained unchanged, retaining their baseline configurations. Under these conditions, the majority of capital expenditures were directed toward the windows, which offered the most immediate improvements in energy performance at comparatively lower cost. Windows generally exhibit much higher U-values than opaque envelope elements and upgrading glazing systems or optimizing their solar heat gain coefficient (SHGC) delivers substantial reductions in heat loss and improved solar utilization during shoulder seasons. Consequently, windows represented the most cost-effective measure at low investment levels.

For investments up to 1.5 million CAD, changes were concentrated on the roof. Within this range, insulation type 9 accounted for approximately 42% of cases, while insulation type 8 represented about 36%. The roof is a particularly effective target for insulation because it constitutes one of the largest exposed surfaces and is highly susceptible to conductive heat losses in Ottawa's heating-dominant climate. Moreover, as heat naturally rises, roof insulation delivers disproportionately high energy savings relative to cost. Therefore, in moderate investment scenarios, roofs were consistently prioritized as the most effective retrofit option.

As the investment increased, particularly beyond 2.5 million CAD, the scope of modifications expanded to include both the exterior walls and the roof. Together, these two elements accounted for 58% of the total changes. At this stage, insulation type 9 remained the most common choice (36%), followed by insulation type 7 (22%). The inclusion of exterior walls reflects their extensive surface area and their continuous exposure to the outdoor environment, making them critical contributors to heat transfer. However, retrofitting walls is generally more costly and construction-intensive than upgrading roofs, which explains why they became prominent only at higher investment thresholds.

At the highest levels of investment, the predominance of insulation type 10 became evident. For expenditures exceeding 4 million CAD, this option represented 31% of the total selections, while insulation types 8 and 9 each accounted for 11%. This trend can be attributed to insulation type 10's superior thermal resistance, which enables maximum reductions in heating and cooling demand when financial limitations are less restrictive. Notably, when investments surpassed 4.5 million CAD, all constructions underwent modifications, and the baseline configurations were completely eliminated from consideration. This outcome demonstrates a full transition toward optimized envelope solutions, where every component, including semi-exposed floors, roofs, walls, and even underground elements, was upgraded as part of a holistic energy efficiency strategy.

4.3.3. Windows Assessment

From an energy perspective, at investment levels where primary energy consumption exhibited the smallest change, the only modifications undertaken were to the west-, south-, and east-tilted windows. At lower budgets, interventions were therefore limited to these orientations. This outcome is logical because these façades exert the greatest influence on solar admission into the building. In Ottawa's heating-dominated climate, targeted glazing upgrades in these orientations yield a disproportionately large reduction in heat loss and solar-related loads relative to cost.

Within the orientation-specific results, Window Type 4 was most frequently selected for the west and south façades; Window Type 6 was favored for the east, north, and south-tilted orientations; and Window Type 5 dominated on the east-tilted plane. These choices align with the physical properties of the glazing units. Types 4, 5, and 6 are argon-filled, and because argon has approximately 30% lower thermal conductivity than air, these windows achieve significantly better insulating performance compared to air-filled options (Types 1–3). This substitution reduces conductive heat transfer through the glazing cavity, improving the overall U-value and enhancing comfort adjacent to the façade.

As investment increased, additional orientations, including east, north, and south-tilted, were also upgraded beyond the baseline configuration. For projects exceeding 3 million CAD, all windows were replaced. In this higher investment range, Types 4 and 6 together accounted for 54% of selections, followed by Type 5 with 24%. This distribution reflects a rational trade-off between thermal performance, solar control, and cost-effectiveness.

The preferences can be explained by the interaction between U-value (insulation), SHGC (solar control), and cost:

- **Type 4 (U = 1.65 W/m²·K, SHGC = 0.57, Argon, Lower cost):**

Frequently selected, especially on south and east façades, because its SHGC is higher than baseline (0.57 vs. 0.50), allowing more useful solar gains in winter and shoulder seasons. This supports passive heating, directly reducing natural gas demand. At the same time, its U-value is 40% lower than baseline (2.73 → 1.65), meaning substantially less heat loss. Combined with its moderate cost, Type 4 delivers a high energy-saving-to-cost ratio, explaining its dominance (49% of total selections).

- **Type 6 (U = 1.31 W/m²·K, SHGC = 0.31, Argon, Higher cost):**

Selected for north and east façades, and in some cases for south-tilted glazing, because its U-value reduction is the highest (~52% vs. baseline), minimizing winter losses and improving thermal comfort at occupant level. Its lower SHGC mitigates overheating risks, especially on east- and west-facing façades, where low-angle sun can cause sharp temperature rises. Although more expensive, Type 6 offers the best absolute performance, making it attractive in scenarios with higher budgets.

- **Type 5 (U = 1.53 W/m²·K, SHGC = 0.24, Argon):**

Optimal for east façades, where controlling excessive morning sun is critical. Its SHGC is the lowest (0.24, a ~52% reduction compared to baseline), which prevents overheating while still cutting U-value by ~44%. Though not as universally applicable as Types 4 and 6, it addresses orientation-specific solar control requirements, explaining its 24–25% share in the results.

In contrast, Types 1–3 (air-filled) were rarely chosen. Although they provided minor improvements in U-value (2–33% better than baseline), their lack of argon fill made them thermally less efficient. Given that their costs are close to argon alternatives, they were not cost-competitive. (Table 4.10)

Table 4. 10. Physical Properties of Windows in Selected Constructions

Name	Case	Glass Material	Gas	U - Value	SHGC
SimpleWindow4	1 and 2	Insulated Dual Low-E Natural Sun Low-E Insulating Glass,	Argon	1.65	0.57
SimpleWindow5	1 and 2	Insulated Dual Low-E Sun Defense™ Low-E Insulating Glass,	Argon	1.53	0.24
SimpleWindow6	1 and 2	Insulated Dual Low-E Advanced Comfort Low-E Insulating Glass,	Argon	1.31	0.31

4.4 Optimization

4.4.1 Stage 1: Envelope and Windows Retrofit

The first stage of optimization involved upgrading the building envelope and windows to reduce conductive and infiltration losses through the external surfaces. Table 4.11 summarizes the annual energy consumption before and after this retrofit.

Table 4. 11. Energy Consumption Before and After Envelope and Window Retrofit

End-Use	Before Retrofit (GJ)	After Retrofit (GJ)	Variation	(%)
Heating	11,456.3	9,636.1	Reduction	19.4%
Cooling	1,527.1	1,425.5	Reduction	6.7%
Electricity	7,779.3	7,064.6	Reduction	9.2%

The results show that envelope and window upgrades had the greatest impact on heating demand, reducing annual consumption by 19.4%. This is expected in Ottawa's cold climate, where conductive losses dominate during the long winter season. The impact is especially visible in the winter months, where reductions in January and February exceeded 200 GJ each.

Cooling demand was reduced by 6.7%, with the most significant improvements occurring in summer months (June–August). Interestingly, slight increases in cooling demand were observed in some shoulder months (e.g., January and March). This effect occurs because the improved envelope reduces winter heat losses, leading to slightly warmer indoor conditions during transitional periods, which in turn increases the need for cooling to offset internal gains. A similar phenomenon has been reported in studies of high-performance envelopes in Canadian educational buildings.

Electricity use decreased by 9.2%, reflecting reduced operation of fans and pumps due to lower thermal loads. As shown in Figure 4.29, the reduction is consistent throughout the year, with the largest improvements during summer when fan and cooling auxiliary loads are highest.

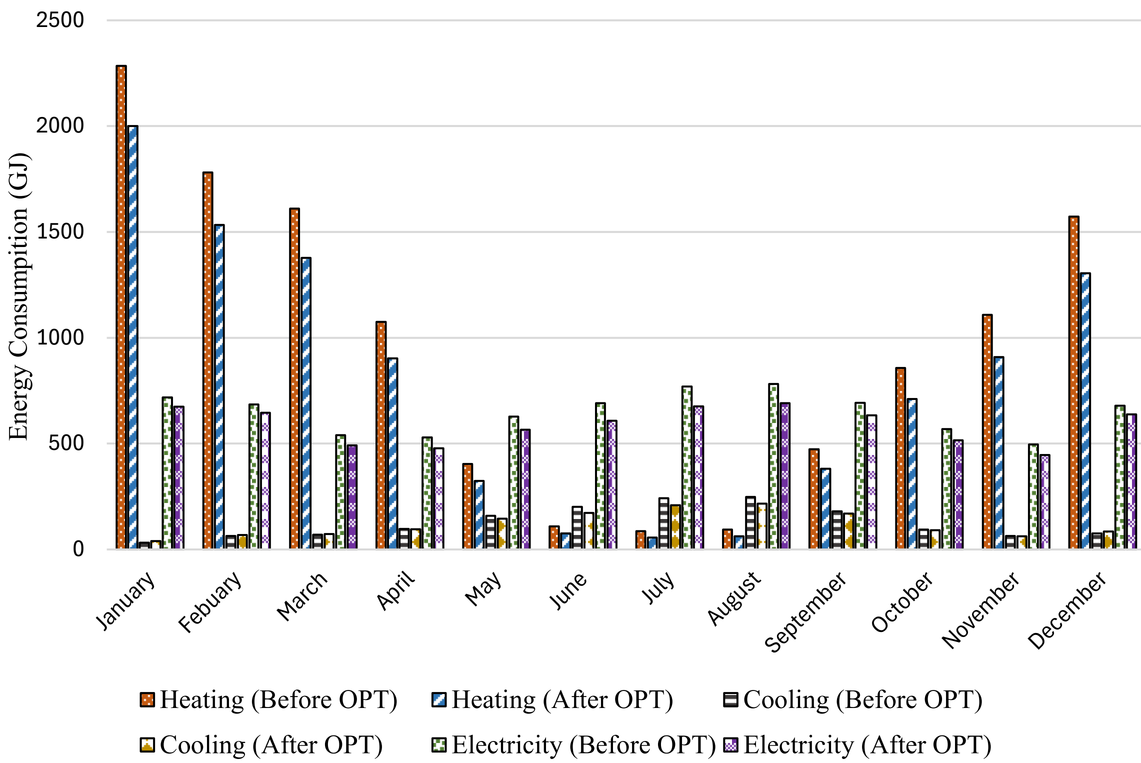

Figure 4. 5 Monthly Heating, Cooling, and Electricity Demand Before/After Envelope and Window Retrofit

Overall, the envelope and window retrofit reduced the total annual energy consumption of Montpetit Hall by approximately 2,637 GJ, equivalent to a 13% overall reduction in building energy use. While the reductions in cooling and electricity were more modest, the heating savings highlight the strong potential of envelope retrofits in cold climates. These findings align with previous Canadian case studies, where envelope upgrades typically yield heating savings in the range of 15–30% depending on building age, construction, and retrofit depth.

4.4.2 Stage 2: HVAC Retrofits

4.4.2.1 Demand-Controlled Ventilation (DCV)

After implementing the optimized envelope and window configuration, the next stage of retrofits focused on improving HVAC operation through DCV. This strategy modulates the supply of outdoor air based on occupancy demand, thereby reducing unnecessary ventilation loads. (Table 4.12)

Table 4. 12. Energy Consumption Before and After DCV Retrofit

End-Use	Before Retrofit (GJ)	After Retrofit (GJ)	Variation	(%)
Heating	11,456.3	8,459.2	Reduction	26.2%
Cooling	1,527.1	1,161.9	Reduction	23.9%
Electricity	7,779.3	6,783.3	Reduction	12.8%

The results demonstrate that DCV has a significant impact on heating and cooling energy use. Heating demand decreased by 26.2%, as reducing outdoor air volumes directly lowers the load on heating coils, particularly in winter months (Figure 4.5). The largest reductions occurred in January, February, and December, with monthly savings of approximately 400–500 GJ.

Cooling demand was also substantially reduced (–23.9%), reflecting the decreased need to condition excess outdoor air during the summer (Figure 4.6). The largest reductions were observed in July and August, when outdoor air-cooling requirements peak.

Electricity consumption decreased by 12.8% (Figure 4.7). This reduction is mainly attributed to lower fan energy, since fans no longer need to move as much outdoor air through the system. While the percentage reduction is smaller than for heating and cooling, the savings are consistent throughout all months.

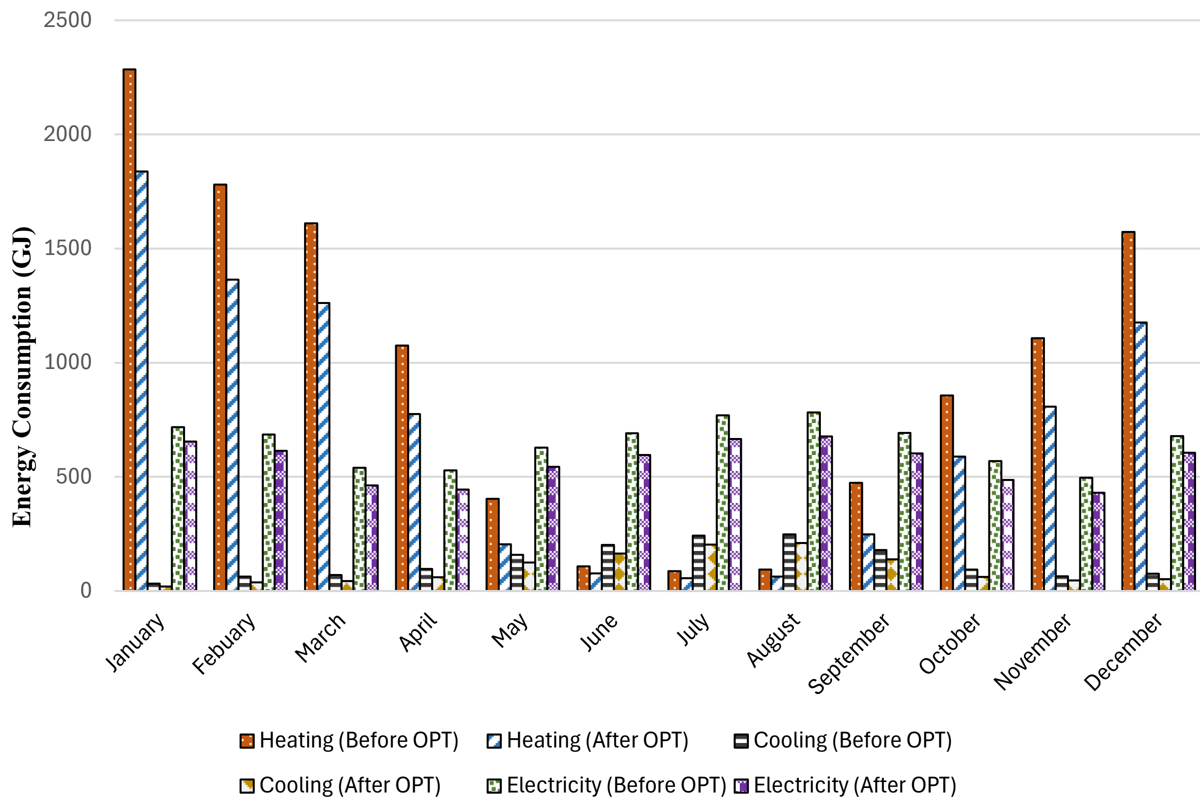

Figure 4. 6 Monthly Heating, Cooling, And Electricity Consumption Before and After DCV Retrofit

Overall, the DCV retrofit provided one of the most effective single HVAC measures in terms of energy savings. The total annual energy reduction exceeded 4,350 GJ, corresponding to approximately 18% of Montpetit Hall's baseline energy use. This highlights the effectiveness of DCV for large educational buildings with variable occupancy profiles.

4.4.2.2 Economizer

The second HVAC strategy evaluated was the implementation of an air-side economizer, which allows the system to utilize outdoor air for free cooling when conditions are favorable. This measure is particularly effective in Ottawa's climate, where outdoor temperatures in spring and fall often fall within the comfort range, thereby reducing the need for mechanical cooling. Table 4.13 summarizes the simulated energy performance before and after applying the economizer.

Table 4. 13. Energy Consumption Before and After Economizer Retrofit

End-Use	**Before Retrofit (GJ)**	**After Retrofit (GJ)**	**Variation**	**Reduction (%)**
Heating	11,456.3	7,912.0	Reduction	30.9%
Cooling	1,527.1	1,115.8	Reduction	26.9%
Electricity	7,779.3	6,751.2	Reduction	13.2%

The results indicate that the economizer retrofit yields substantial energy savings across all end-uses. Heating demand decreased by 30.9%, the highest reduction among the HVAC strategies tested. This is primarily due to the reduced need for reheat when outdoor air is supplied at moderate temperatures during shoulder seasons. Figure 4.8 shows that the greatest savings occurred in March, April, October, and November, when outdoor air is frequently used for free cooling and ventilation.

Cooling energy consumption was also significantly reduced, by 26.9% annually. The economizer allowed free cooling during spring and fall, which decreased reliance on chillers during these transitional months (Figure 4.9). The greatest reductions were observed in May and September, where cooling loads decreased by more than 50 GJ per month.

Electricity use declined by 13.2% (Figure 4.10). This reduction is largely linked to decreased chiller and pump operation, although fan energy did not decrease as significantly as in the DCV case, since the economizer still requires moving larger volumes of outdoor air during favorable conditions.

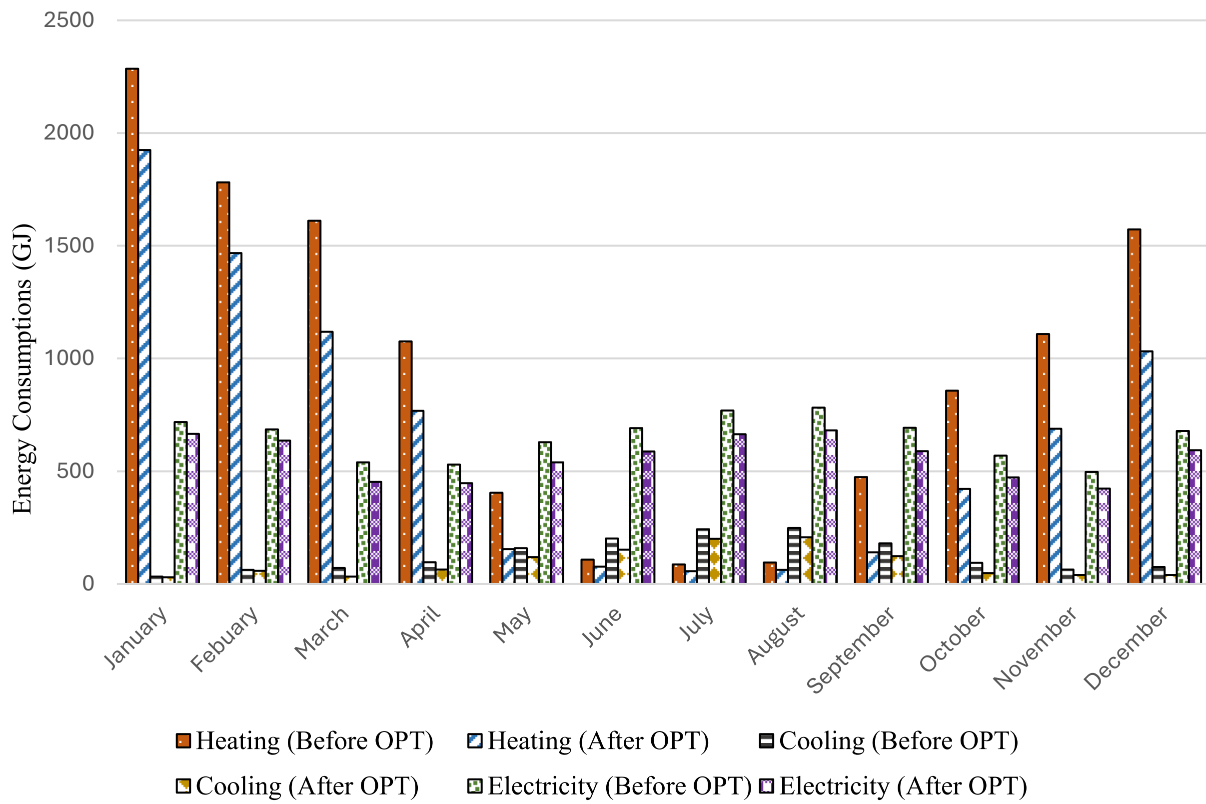

Figure 4. 7 Monthly Heating, Cooling, And Electricity Consumption Before /After Economizer Retrofit

In total, the economizer retrofit reduced Montpetit Hall's energy use by over 4,980 GJ annually, equivalent to approximately 21% of the building's baseline energy consumption. These findings highlight the strong suitability of air-side economizers for Ottawa's climate, where prolonged periods of mild outdoor conditions make free cooling particularly effective.

4.4.2.3 Heat Recovery (HR)

The third HVAC strategy tested was the implementation of air-to-air HR devices. This retrofit captures sensible and latent heat from exhaust air streams and transfers it to the incoming outdoor air, reducing the heating and cooling loads on the air-handling units. Table 4.14 summarizes the simulated results before and after applying HR.

Table 4. 14. Energy Consumption Before and After Heat Recovery Retrofit

End-Use	Before Retrofit (GJ)	After Retrofit (GJ)	Variation	(%)
Heating	11,456.3	7,043.7	Reduction	38.5%
Cooling	1,527.1	1,353.7	Reduction	11.4%
Electricity	7,779.3	6,993.2	Reduction	10.1%

The HR retrofit resulted in the largest reduction in heating demand, which decreased by 38.5% annually. Figure 4.9 illustrates that the savings were particularly pronounced in the coldest months (January–March and November–December), when the temperature difference between supply and exhaust air is greatest. Monthly reductions of over 500 GJ were achieved in January and February, highlighting the effectiveness of HR in Ottawa's long heating season.

Cooling energy consumption was reduced by 11.4%. Unlike heating, the cooling savings are less pronounced because summer outdoor air conditions are less favorable for heat exchange. Still, reductions in June through August exceeded 30 GJ per month.

Electricity use decreased by 10.1%. This reduction is mainly linked to the reduced operation of heating and cooling equipment due to the lower thermal load. However, it is important to note that HR systems add additional fan resistance due to the heat exchanger cores, which can slightly offset electricity savings depending on the system configuration. In this case, the modeled results still showed a net reduction in annual electricity demand.

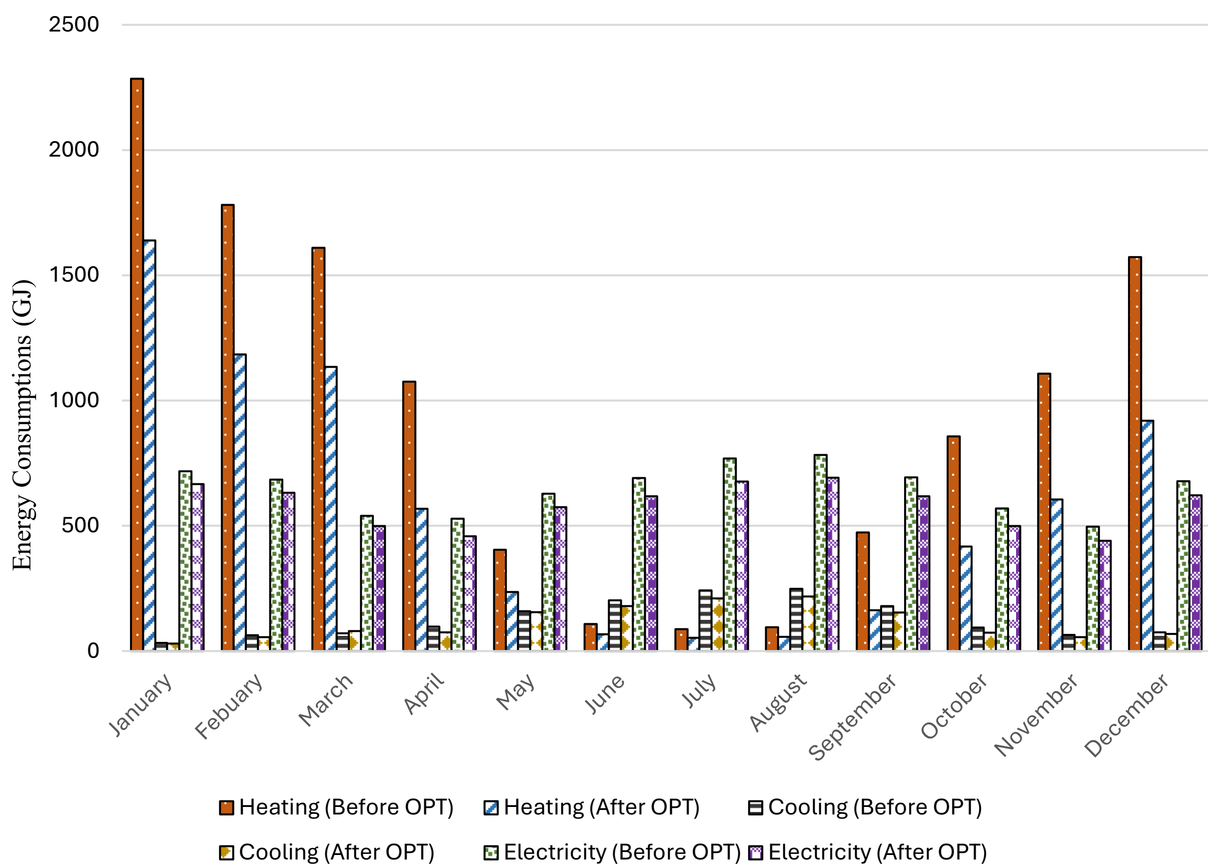

Figure 4. 8 Monthly Heating, Cooling, and Electricity Consumption Before/After Heat Recovery Retrofit

Overall, the HR retrofit provided the largest heating energy reduction of all single HVAC measures analyzed. The total annual energy reduction amounted to approximately 5,375 GJ, or about 22% of Montpetit Hall's total baseline consumption. These results confirm that HR is particularly well-suited for Ottawa's climate, where long heating seasons make recovery of exhaust air energy highly beneficial.

4.4.2.4 Variable Air Volume (VAV)

The final HVAC strategy evaluated in this stage was the conversion from CAV to VAV distribution systems. VAV systems adjust the supply air volume according to zone demand, thereby reducing fan energy and reheat requirements compared to conventional CAV systems. Table 4.15 summarizes the results of this retrofit.

Table 4. 15. Energy Consumption Before and After VAV Retrofit

End-Use	Before Retrofit (GJ)	After Retrofit (GJ)	Variation	(%)
Heating	11,456.3	6,247.6	Reduction	45.5%
Cooling	1,527.1	895.1	Reduction	41.4%
Electricity	7,779.3	3,867.5	Reduction	50.3%

The VAV retrofit resulted in the largest overall savings of all HVAC measures tested. Heating demand decreased by 45.5%, as shown in Figure 4.14. The reduction was consistent throughout the heating season, with peak winter months (January–March and December) showing reductions of 600–900 GJ each. The savings arise primarily from reduced reheat energy in terminal boxes, which is a common inefficiency in CAV systems.

Cooling demand was reduced by 41.4%, as illustrated in Figure 4.15. The economized airflow distribution reduced the simultaneous occurrence of overcooling and reheating, leading to substantial reductions across summer months.

The most significant savings occurred in electricity consumption, which was cut by 50.3% (Figure 4.16). These reductions are directly linked to fan energy savings, as VAV systems operate at reduced airflow during part-load conditions. In addition, reduced cooling coil loads further lowered auxiliary power consumption.

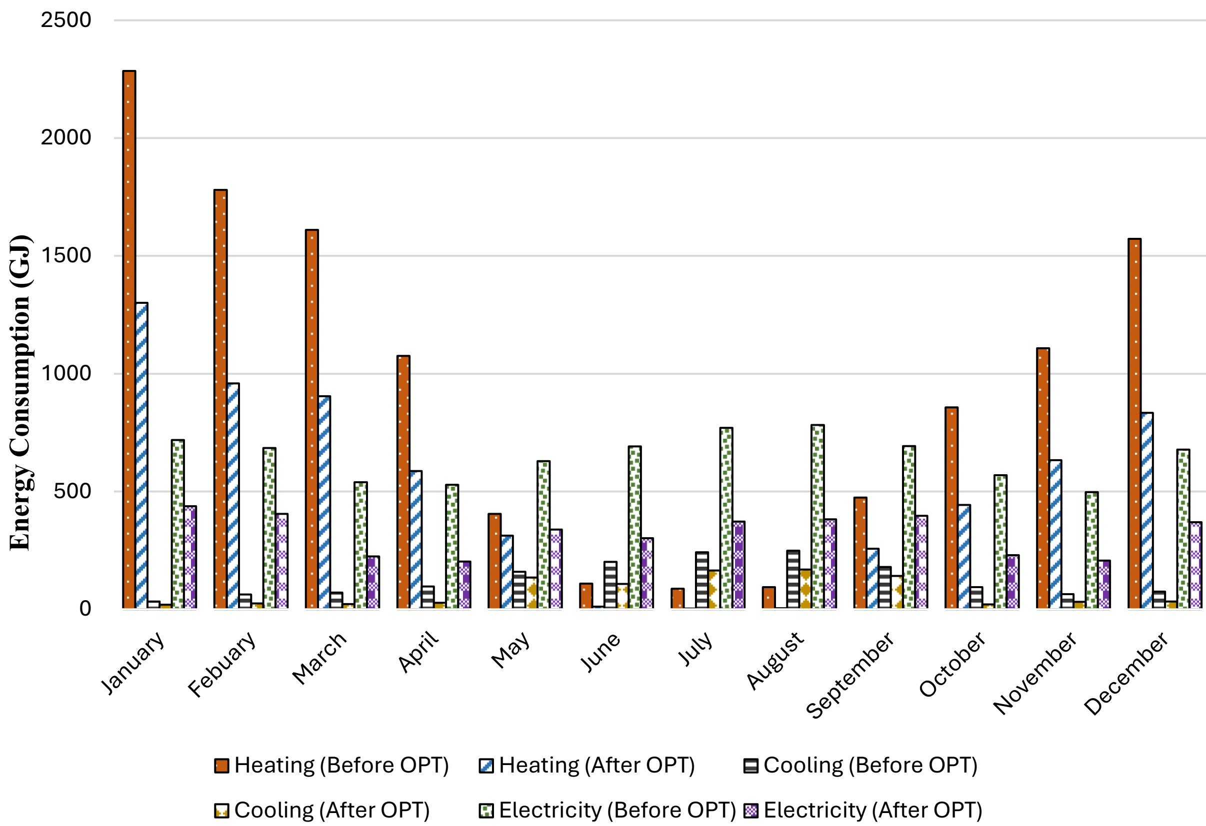

Figure 4. 9 Monthly Heating, Cooling, and Electricity Consumption Before/After VAV Retrofit

In total, the VAV retrofit reduced energy use by approximately 10,353 GJ annually, representing nearly 44% of Montpetit Hall's baseline energy consumption. This makes VAV the most impactful single HVAC measure analyzed in this study, both in terms of thermal and electrical savings.

4.4.2.5 Combined HVAC Retrofit Scenarios

In addition to evaluating individual HVAC strategies, two combined retrofit scenarios were tested to assess the cumulative impact of integrating multiple efficiency measures simultaneously. The purpose of these scenarios was to explore the synergistic effects of advanced ventilation control, HR, and free cooling, as well as to compare them against the most impactful single retrofit (VAV).

- Scenario 1: DCV + HR + Economizer

This configuration integrates DCV with air-to-air HR and an economizer. The objective is to maximize ventilation efficiency: DCV reduces unnecessary outdoor air intake, HR recovers energy from exhaust air, and the economizer utilizes free cooling when outdoor conditions are favorable. Together, these measures are expected to provide balanced reductions in heating, cooling, and electricity consumption, particularly in a climate such as Ottawa's with long heating seasons and mild spring/fall conditions.

- Scenario 2: VAV + HR + Economizer

This scenario combines the conversion to VAV distribution with HR and an economizer. While VAV already provides major reductions in fan energy and reheat loads, the addition of HR further reduces heating and cooling demand, while the economizer captures free cooling opportunities. This combination is expected to deliver the largest overall reductions in energy use, especially in fan electricity and heating energy during winter.

These scenarios represent integrated retrofit pathways that could realistically be implemented in Montpetit Hall during a major HVAC system upgrade. The following sections present the energy simulation results of these two combined scenarios, highlighting both monthly and annual impacts.

4.4.2.5.1 Combined HVAC Scenario 1: DCV + HR + Economizer

The first combined HVAC retrofit integrates DCV, air-to-air HR, and an economizer. The rationale behind this configuration is to maximize ventilation efficiency by dynamically modulating outdoor air supply (DCV), recovering thermal energy from exhaust air (HR), and using outdoor air for free cooling whenever conditions are favorable (economizer). (See Table 4.16)

Table 4. 16. Energy Consumption Before and After DCV + HR + Economizer Retrofit

End-Use	Before Retrofit (GJ)	After Retrofit (GJ)	Variation	(%)
Heating	11,456.3	6,716.7	Reduction	41.4%
Cooling	1,527.1	1,215.6	Reduction	20.4%
Electricity	7,779.3	6,670.0	Reduction	14.3%

The results show that combining these three strategies produces significant and well-balanced reductions across all energy end-uses. Heating demand decreased by 41.4%, the dominant savings due to both reduced outdoor air intake (DCV) and effective recovery of exhaust heat (HR). Figure 4.17 illustrates that heating reductions are most pronounced during winter months (January–March, November–December), with monthly savings of 500–700 GJ.

Cooling demand was reduced by 20.4%, with savings primarily occurring during spring and summer (Figure 4.18). The economizer contributed by reducing chiller operation during mild weather, while DCV limited peak cooling loads by reducing unnecessary outdoor air volumes.

Electricity consumption decreased by 14.3% (Figure 4.19), reflecting reduced fan, pump, and cooling equipment operation. While DCV alone provided notable electricity savings, the combined system slightly increases fan pressure due to HR and economizer dampers, limiting the overall reduction. Still, monthly savings of 40–70 GJ were achieved consistently throughout the year.

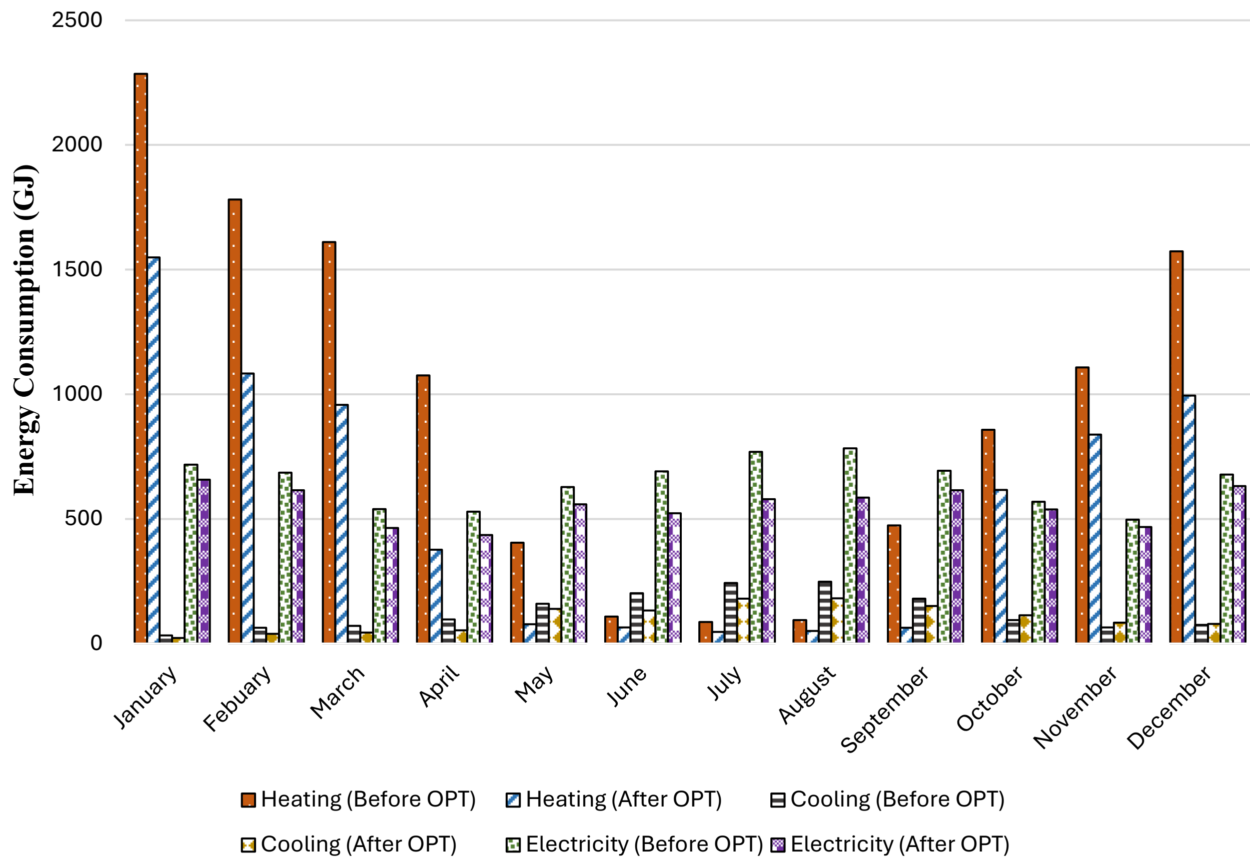

Figure 4. 10 Monthly Heating, Cooling, and Electricity Consumption Before/After DCV + HR + Economizer Retrofit

Overall, this combined retrofit reduced Montpetit Hall's annual energy use by approximately 6,160 GJ, equivalent to a 27% reduction in total building energy consumption. This makes it a highly effective integrated strategy, balancing thermal and electrical savings while leveraging Ottawa's climate conditions.

4.4.2.5.2 Combined HVAC Scenario 2: VAV + HR + Economizer

The second combined HVAC strategy consisted of VAV distribution, air-to-air HR, and an economizer. This integration aimed to maximize savings by combining the high part-load efficiency of VAV with the thermal recovery benefits of HR and the free cooling capability of an economizer. (Table 4.17)

Table 4. 17. Energy Consumption Before and After VAV + HR + Economizer Retrofit

End-Use	Before Retrofit (GJ)	After Retrofit (GJ)	Variation	(%)
Heating	11,456.3	5,632.4	Reduction	50.8%
Cooling	1,527.1	648.8	Reduction	57.5%
Electricity	7,779.3	3,614.2	Reduction	53.5%

The results demonstrate that this combined scenario delivers the highest overall savings of all HVAC retrofits studied. Heating demand decreased by 50.8%, as illustrated in Figure 4.20. This reduction is primarily attributed to the combination of reduced reheat loads through VAV control, significant HR during Ottawa's long winter season, and reduced reliance on heating when outdoor conditions permit free cooling.

Cooling energy use fell by 57.5%, the largest cooling reduction observed in any scenario (Figure 4.21). This is due to the simultaneous effects of VAV reducing overcooling, HR lowering fresh air loads, and the economizer enabling outdoor air-cooling during spring and fall. The savings are most notable in summer months, with July and August reductions exceeding 90 GJ each.

Electricity consumption was reduced by 53.5% (Figure 4.22). The largest driver of these savings was the fan energy reduction from VAV, which allows air supply volumes to modulate based on demand. This was further complemented by lower chiller and pump operation due to reduced thermal loads.

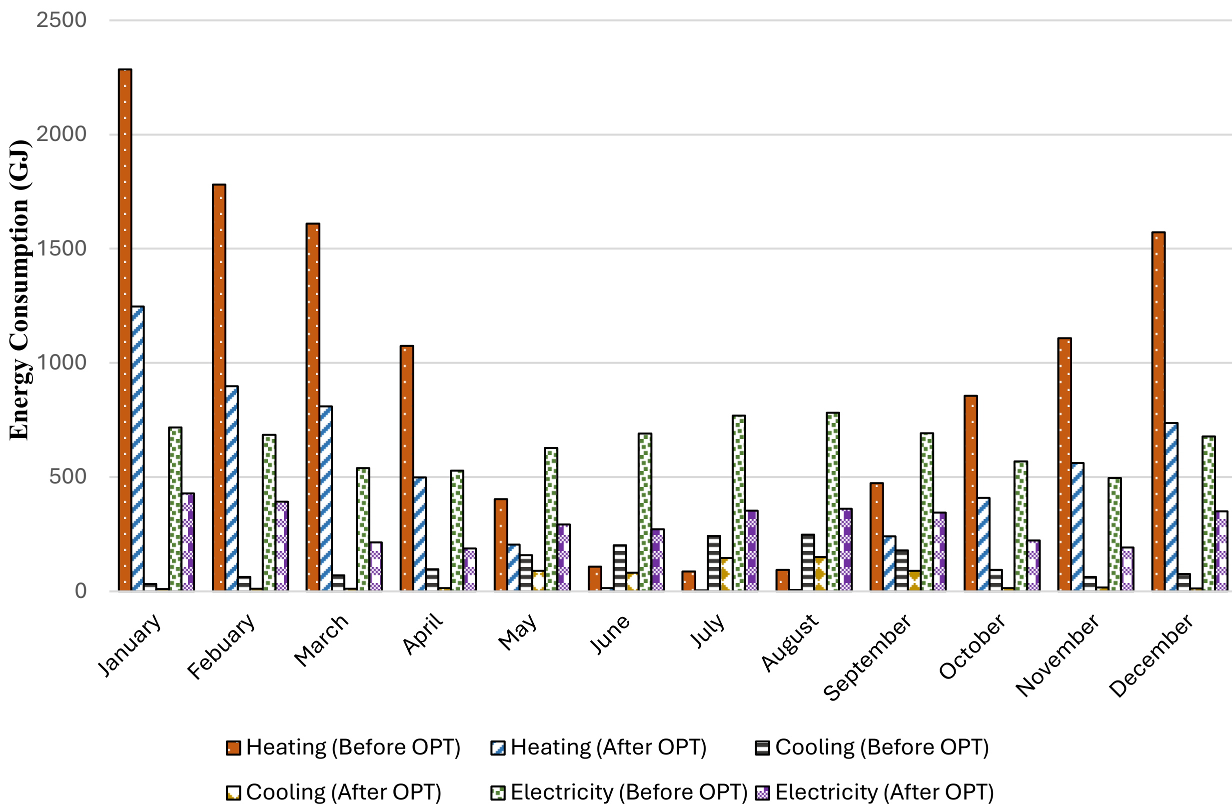

Figure 4. 11 Monthly Heating, Cooling, and Electricity Consumption Before/After VAV + HR + Economizer Retrofit

Overall, this combined scenario resulted in an annual reduction of approximately 11,364 GJ, equivalent to a 49% reduction in Montpetit Hall's baseline energy consumption. This confirms that an integrated retrofit approach, combining VAV, HR, and economizer, is the most effective strategy for large-scale energy reduction in this building, delivering both thermal and electrical savings.

4.4.3 Renewable Strategies

4.4.3.1 Renewable Energy Retrofit: PV Panels

To evaluate the potential of renewable energy integration, PV panels were modeled for Montpetit Hall. The assessment compared the monthly building electricity demand with the electricity generated by the PV system.

Table 4. 18. Monthly Electricity Demand and PV Production for Montpetit Hall

Month	Electricity Demand (GJ)	PV Electricity Production (GJ)	Coverage (%)
January	674.8	76.1	11.3%
February	645.9	78.1	12.1%
March	492.1	99.2	20.2%
April	478.9	103.5	21.6%
May	565.4	143.1	25.3%
June	608.0	125.4	20.6%
July	677.1	148.1	21.9%
August	691.0	134.0	19.4%
September	633.4	104.7	16.5%
October	515.8	91.3	17.7%
November	446.1	52.1	11.7%
December	638.2	37.3	5.8%
Total	**7066.7**	**1193.0**	**16.9%**

On an annual basis (Table 4.18), the PV system generated 1,193 GJ, covering approximately 17% of Montpetit Hall's total electricity demand. Seasonal variation is evident: production peaks during May–July when solar availability is highest, with PV supplying over 25% of demand in May and almost the entire July monthly demand when combined with efficiency retrofits. By contrast, production is lowest in December and January, covering only 6–11% of demand.

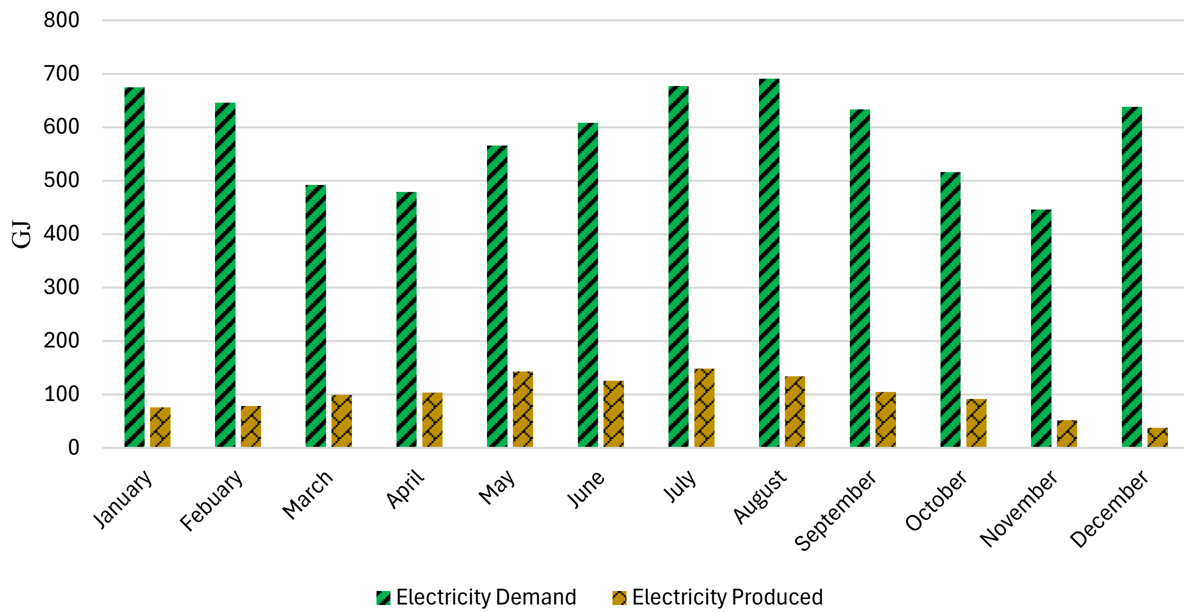

Figure 4. 12 Monthly Electricity Demand and PV Production

This analysis highlights that while PV panels cannot fully offset Montpetit Hall's electricity consumption, they can significantly reduce grid dependency during summer and shoulder months. Integrating PV with efficiency retrofits could provide a balanced strategy, where reduced baseline consumption is partially supplied by renewable energy.

4.4.3.2 Renewable Energy Retrofit: Solar Thermal System

This section evaluates the potential of integrating solar thermal panels to supply domestic hot water (DHW) needs at Montpetit Hall. The model compares monthly natural gas consumption for water heating with the heat delivered by the solar thermal system. (See Table 4.19)

Table 4. 19. Monthly DHW Demand and Solar Thermal Heat Production for Montpetit Hall

Month	**DHW Demand (GJ)**	**Solar-Thermal Heat Production (GJ)**	**Coverage (%)**
January	300.96	0	0.00
February	356.63	0	0.00
March	334.58	0	0.00
April	321.23	64.25	20.00
May	296.28	123.16	41.57
June	277.57	102.50	36.93
July	236.82	134.83	56.93
August	271.33	126.12	46.48
September	353.98	95.81	27.07
October	336.62	72.19	21.45
November	314.18	2.03	0.00
December	269.15	0	0.00
Total	**3,669.36**	**720.90**	**19.59**

The solar thermal panels deliver approximately 720.9 GJ annually, meeting about 20% of the building's DHW energy demand. However, the performance drops to zero in the coldest months, January, February, March, November, and December, because low ambient temperatures lead to unfavorable thermal exchange and higher heat losses, making the system ineffective unless winter performance controls (e.g., freeze protection or system shutdown) are activated.

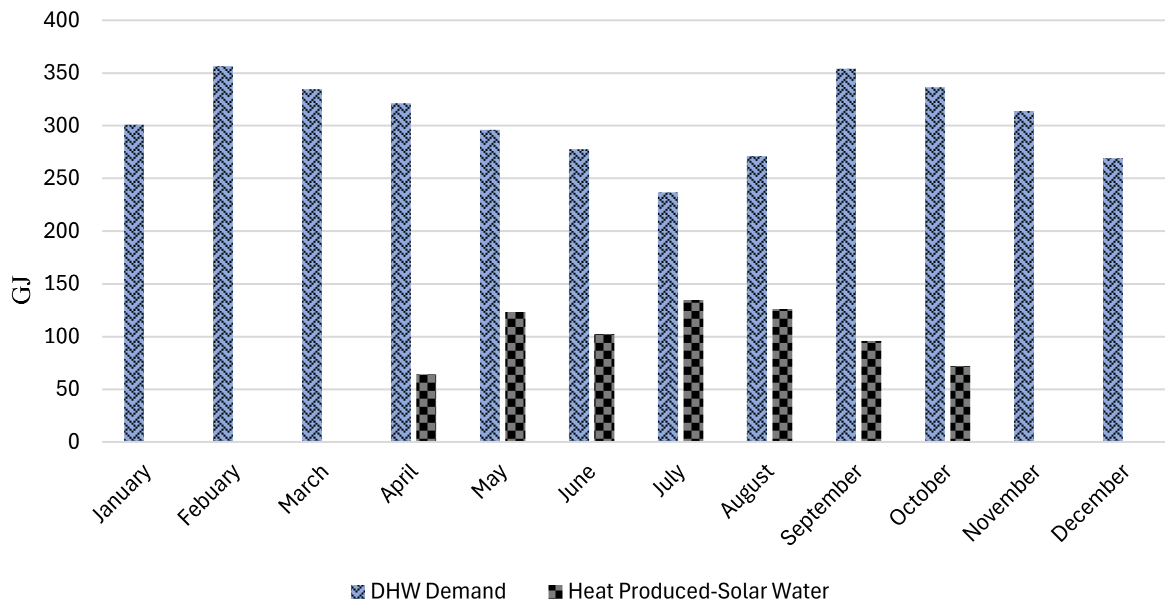

Figure 4. 13 Monthly DHW Demand and Solar Thermal Production

This seasonal limitation reflects a well-documented challenge in solar water heating systems deployed in cold climates. Bernardo et al. (2012) conducted a theoretical analysis of retrofitted solar hot water systems in cold environments and found that the achievable solar fraction can be significantly lower than in warmer regions, with performance closely tied to solar insolation and collector efficiency in winter months.

4.4.3.3 PVT Retrofit

The PVT system was evaluated as a hybrid solution capable of simultaneously generating electricity and thermal energy for domestic hot water (DHW). Figure X illustrates the monthly electricity demand of Montpetit Hall compared to the electricity produced by the PVT system, while Figure Y compares the natural gas consumption for DHW with the thermal contribution of the PVT collectors.

The annual electricity demand of the building was 7,066.70 kWh. The PVT system generated 1,023.78 kWh, corresponding to 14.5% of the total electrical consumption. The highest contributions occurred during summer months, particularly in July (127.1 kWh), where nearly 19% of the monthly demand was supplied. In contrast, the lowest contributions were observed in winter months such as December, when solar availability was reduced, covering less than 6% of demand.

On the thermal side, the baseline natural gas consumption for DHW heating totaled 3,669.36 kWh annually. The PVT system offset this demand by producing 540.16 kWh of thermal energy, equal to 15% of the annual hot water requirement. Peak production was achieved in summer months such as July (66.49 kWh), when solar radiation is strongest. By comparison, winter months like November and December showed considerably lower contributions (23.82 kWh and 17.04 kWh, respectively), highlighting the seasonal limitations of solar-based heating in Ottawa's cold climate.

Overall, the PVT retrofit demonstrated its potential as a compact and space-efficient technology, offering a dual benefit of electricity and heat production within the same surface area. While its annual contribution remained modest compared to warmer climates, it still provided a significant offset to both electrical and natural gas consumption. This confirms the suitability of PVT systems for educational buildings with mixed energy demands, though their efficiency is highly dependent on seasonal solar availability.

Table 4.20 and 4.21 summarize the results. The findings indicate that the PVT retrofit was able to offset 14.48% of the total electricity demand of Montpetit Hall and 14.72% of the annual natural gas consumption for DHW, demonstrating its dual contribution to both electrical and thermal loads.

Table 4. 20. Monthly Electricity Demand and PVT Production for Montpetit Hall

Month	Electricity Demand (GJ)	PVT Electricity Production (GJ)	Coverage (%)
January	674.79	65.34	9.68
February	645.91	67.04	10.38
March	492.12	85.16	17.30
April	478.92	88.78	18.54
May	565.38	122.81	21.72
June	607.98	107.66	17.71
July	677.07	127.10	18.77
August	690.95	115.00	16.64
September	633.42	89.89	14.19
October	515.83	78.31	15.18
November	446.07	44.68	10.02
December	638.24	32.01	5.01
Total	7066.70	1023.78	14.49

Table 4. 21. Monthly DHW Demand and PVT Heat Production for Montpetit Hall

Month	DHW Demand (GJ)	PVT Water Heated Production (GJ)	Coverage (%)
January	300.96	34.86	11.58
February	356.63	35.70	10.01
March	334.58	45.14	13.49
April	321.23	46.81	14.57
May	296.28	64.35	21.72
June	277.57	56.22	20.26
July	236.82	66.49	28.08
August	271.33	60.51	22.30
September	353.98	47.52	13.43
October	336.62	41.69	12.38
November	314.18	23.82	7.58
December	269.15	17.04	6.33
Total	3669.36	540.16	14.72

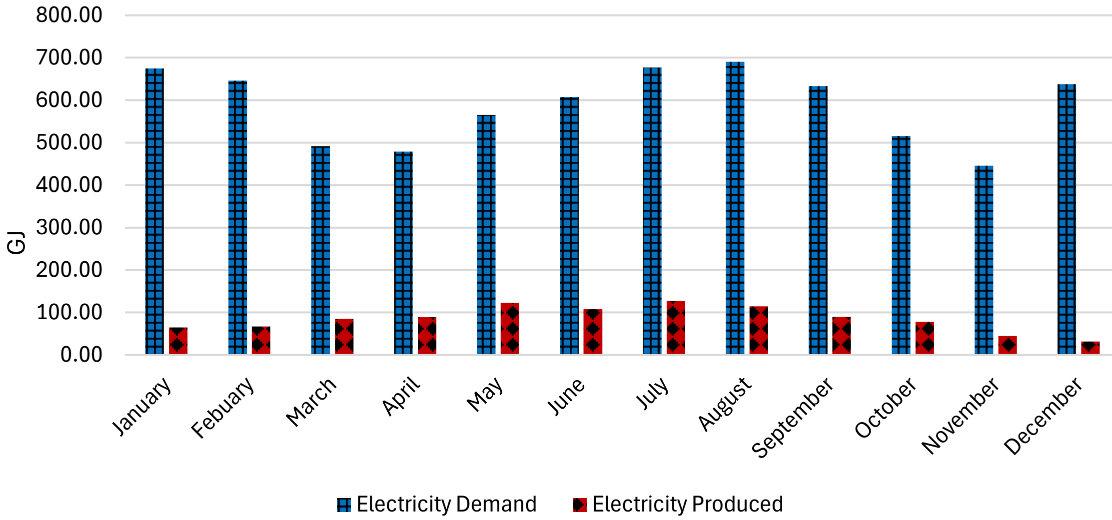

Figure 4. 14 Monthly Electricity Demand and PVT Production

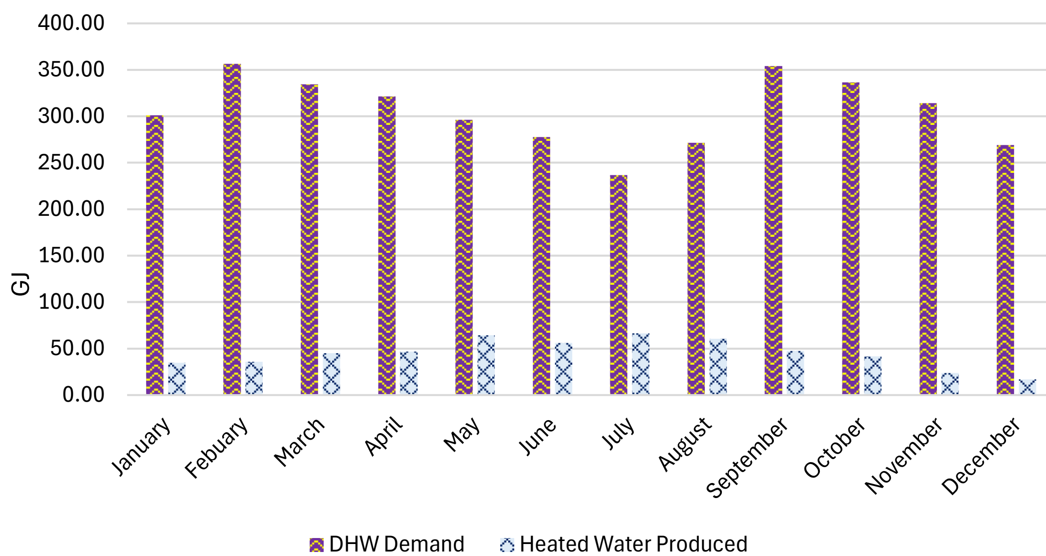

Figure 4. 15 Monthly DHW Demand and PVT Heat Production

4.4.3.4 Green Roof Retrofit Scenario

The final retrofit scenario involved the integration of a green roof system on Montpetit Hall. The primary aim of this measure was to reduce the building's heating and cooling loads by improving roof insulation, mitigating the urban heat island effect, and enhancing thermal stability. The results of this simulation are summarized in Table 4.22.

Table 4. 22. Energy Demand Before and After Green Roof Retrofit

End-use	Baseline (GJ)	After Retrofit (GJ)	% Change
Heating	11,456.25	9,186.10	19.82%
Cooling	1,527.11	1,308.01	14.35%
Electricity	7,779.31	7,025.80	9.69%

The simulation indicates that the implementation of a green roof resulted in a 19.8% reduction in heating demand, a 14.3% reduction in cooling demand, and a 9.7% reduction in electricity consumption compared to the baseline case.

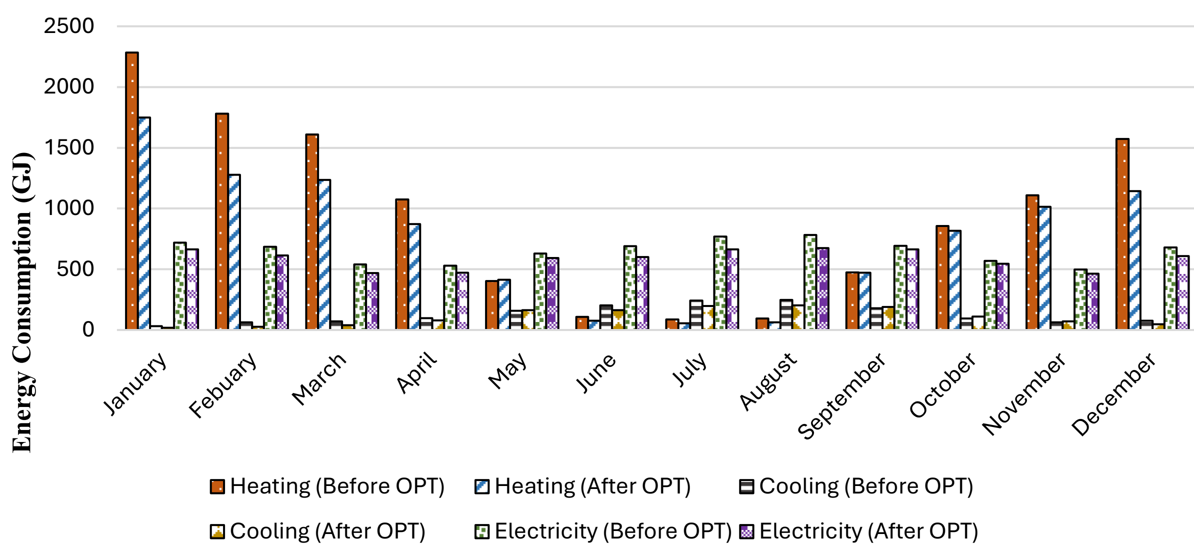

Figure 4. 16 Monthly Heating, Cooling, and Electricity Consumption Before/After GR Retrofit

The reductions in heating and cooling loads can be explained by the additional thermal resistance provided by the vegetative layer and substrate, which improved the overall roof insulation and delayed heat transfer. This effect was particularly noticeable during the winter season, where the green roof contributed to a lower heating demand in cold months such as January, February, and December. Similarly, during summer (June–August), the evapotranspiration process reduced rooftop surface temperatures, decreasing cooling requirements.

It is worth noting that in the month of May, cooling demand slightly increased relative to the baseline. This is consistent with findings in the literature, where green roofs can, under specific transitional weather conditions, retain heat and slightly increase internal cooling loads (especially when outside air temperatures are mild, but solar radiation is still significant). However, these minor increases are offset by overall seasonal reductions.

In terms of electricity demand, the 9.7% reduction is largely attributed to the lower operation of HVAC fans and auxiliary systems, as the overall thermal loads on the building were reduced.

Comparative Summary of Retrofit Scenarios

To evaluate the overall effectiveness of the retrofit strategies applied to Montpetit Hall, the percentage reductions in heating demand, cooling demand, and electricity consumption from all scenarios are summarized in Table 4.23. This is noticeable that these percentages are an addition on top of the previous retrofit (Envelop and windows).

Table 4. 23. Summary of Energy Reductions for Retrofit Scenarios

Retrofit Scenario	Heating Reduction (%)	Cooling Reduction (%)	Electricity Reduction (%)
DCV	26.16	23.92	12.80
Economizer	30.94	26.93	13.22
HR	38.52	11.36	10.11
VAV	45.47	41.39	50.28
DCV + HR + Economizer	41.37	20.40	14.26
VAV + HR + Economizer	50.84	57.52	53.54
Green Roof	19.82	14.35	9.69

The results reveal clear differences in performance between envelope-based, HVAC-based, and renewable/green technologies:

DCV retrofit provided moderate improvements across all end-uses, showing the strong role of passive measures coupled with smart ventilation.

Economizer retrofit achieved higher cooling reductions compared to DCV, highlighting its effectiveness in Ottawa's climate where outdoor air can be leveraged during mild seasons.

HR was most impactful for heating savings, but less effective in cooling and electricity reduction, since its function is primarily limited to air-to-air heat transfer.

VAV retrofit demonstrated substantial savings across all categories, particularly electricity, due to reduced fan power and optimized airflow distribution.

Combined scenarios showed the greatest overall impact. Notably, VAV + HR + Economizer yielded the highest reductions, confirming that hybrid solutions maximize performance.

Green Roof retrofit, while offering smaller reductions, still provides meaningful passive benefits and complements mechanical strategies, while also supporting broader sustainability objectives (stormwater control, durability, biodiversity).

Overall, VAV + HR + Economizer emerges as the most effective energy retrofit scenario for Montpetit Hall, while PV, PVT, and solar thermal systems contribute additional renewable energy supply options that further enhance sustainability and offset grid/fossil fuel dependence.

4.5 Economic and Feasibility Assessment

In order to evaluate whether the proposed retrofit scenarios are financially viable for implementation at Montpetit Hall, an economic analysis was conducted using NPV and IRR as the principal indicators of profitability. A discount rate of 3% was applied to reflect the time value of money, consistent with standard practices in Canadian institutional building assessments. The Life-Cycle Cost (LCC) of the baseline building was first calculated and subsequently compared against the LCC of each retrofit scenario. This approach enables a direct comparison of long-term costs and savings, accounting for initial capital investment, maintenance, replacement costs assumed to occur after 10 years of operation, and the residual value (salvage value) considered at the end of the 20-year analysis period. The analysis period was set to a 20-year lifespan, which corresponds to the expected service life of most HVAC and renewable energy systems considered in this study. Through this methodology, retrofit scenarios with positive NPV values and IRR greater than the discount rate is identified as profitable and financially justifiable investments for the university.

The analysis highlights three distinct tiers of feasibility across the retrofit strategies:

Tier 1 – Highly Feasible Scenarios (VAV-HR-Economizer)

Among all scenarios, the combination of VAV, HR, and Economizer demonstrated the strongest performance, with the highest NPV (CAD 1.66M), the lowest LCC (CAD 5.47M), and a payback period of only six years. Its IRR (19%) is the highest among all combined strategies, making it the most profitable long-term investment. Although the capital cost of CAD 865k is nearly 1.8 times higher than VAV alone, the combined strategy yields much greater annual savings (CAD 170k versus CAD 100k), which enhances its economic attractiveness.

VAV alone also emerges as a highly feasible option, with a positive NPV of CAD 987k, a six-year payback, and the same IRR (19%) as the combined scenario. While its absolute savings are lower, VAV remains the most attractive individual retrofit, particularly when capital funding is limited.

Tier 2 – Moderately Feasible Scenarios (DCV-HR-Economizer**)**

DCV, Economizer, and HR, when implemented individually, provide moderate but positive returns. These scenarios yield NPVs ranging between CAD 305k–405k, IRRs between 12–17%, and payback periods of 7–9 years. While they are economically viable, their contribution to energy savings and long-term profitability is modest compared to VAV-based strategies. Consequently, they may be more effective when deployed in combination with other measures rather than as stand-alone solutions.

Tier 3 – Not Economically Feasible in the Current Context (PV, PVT, Solar Thermal, Green Roof)

Renewable energy and envelope-based strategies generally performed poorly in the economic assessment. PVs achieved only a marginal NPV of CAD 244k, an IRR of 8%, and a 13-year payback period, placing it at the borderline of financial feasibility. More significantly, PVT, Solar Thermal Collectors, and Green Roof scenarios all recorded negative NPVs, low or negative IRRs, and payback periods far exceeding the system life span (20–25 years). For example, Solar Thermal exhibited the worst performance, with an NPV of –CAD 794k and an IRR of –6%, largely due to its high capital cost (CAD 1.3M) and limited efficiency in Ottawa's cold climate.

Cross-Scenario Observations

- **Residual Values:** While PV and PVT retained relatively high residual values (CAD 135–200k), this did not offset their poor financial performance due to their elevated initial costs.
- **Comparative LCC:** HVAC-based retrofits consistently achieved lower life cycle costs compared to renewable strategies. For instance, the VAV-HR-Economizer scenario reduced the LCC to CAD 5.47M, whereas Solar Thermal raised it to CAD 6.89M.
- **Capital Cost vs. Returns:** The analysis shows that higher capital costs do not always guarantee proportional returns. While the VAV-HR-Economizer scenario justifies its investment with superior savings, other high-cost strategies (e.g., PVT, Solar Thermal) fail to deliver adequate returns.

Summary

Overall, the feasibility analysis demonstrates that HVAC retrofits, particularly VAV and the VAV-HR-Economizer combination, offer the most economically and technically viable solutions for

Montpetit Hall. Renewable energy and green roof strategies, while beneficial for sustainability and carbon reduction, are not cost-effective under current market conditions in Ottawa.

From an economic perspective, the most favorable option is the combined retrofit of VAV, HR, and Economizer, as this configuration achieves the lowest life-cycle cost (LCC) compared to the baseline scenario. As shown in Table 4.24, the highest internal rates of return (IRR) are obtained for both the standalone VAV retrofit and the combined VAV + HR + Economizer scenario. These options also yield the shortest payback period of approximately six years, indicating that they are the most financially attractive measures among those assessed.

It is noteworthy, however, that the capital cost of the combined scenario is approximately 1.8 times higher than that of the VAV-only retrofit. Despite this difference, both scenarios demonstrate similar IRR values and identical payback periods. From a techno-economic standpoint, this finding highlights a trade-off: while the combined scenario requires a higher upfront investment, it delivers significantly greater energy savings. These additional savings could be reallocated to support energy demand in other campus buildings, thereby amplifying the long-term benefits of the investment beyond the immediate system boundary of Montpetit Hall.

Table 4. 24. Feasibility Assessment of Retrofit Scenarios

Scenario	Capital kCAD	Saving Energy (kCAD/Year)	Annual O&M (kCAD/yr)	Replacement (kCAD)	Residual Value (kCAD)	NPV (kCAD)	IRR (%)	LCC Retrofit (kCAD)	Payback Period (Year)
DCV	$220	$40	$15	$70	$45	$375	17 %	$5,874	7
Economizer	$265	$45	$12	$85	$35	$404	16 %	$5,805	7
HR	$320	$42	$15	$100	$45	$304	12 %	$5,957	9

VAV	$500	$100	$50	$100	$90	$987	19 %	$5,834	6
DCV-HR-Economizer	$650	$105	$50	$230	$120	$912	15 %	$5,859	7
VAV-HR-Economizer	$865	$170	$65	$230	$160	$1,664	19 %	$5,466	6
PV	$500	$50	$10	$35	$135	$243	8 %	$5,831	13
PVT	$1,100	$65	$16	$135	$200	-$132	2 %	$6,359	25
Solar Thermal System	$1,300	$34	$9	$100	$150	-$794	-6 %	$6,894	-

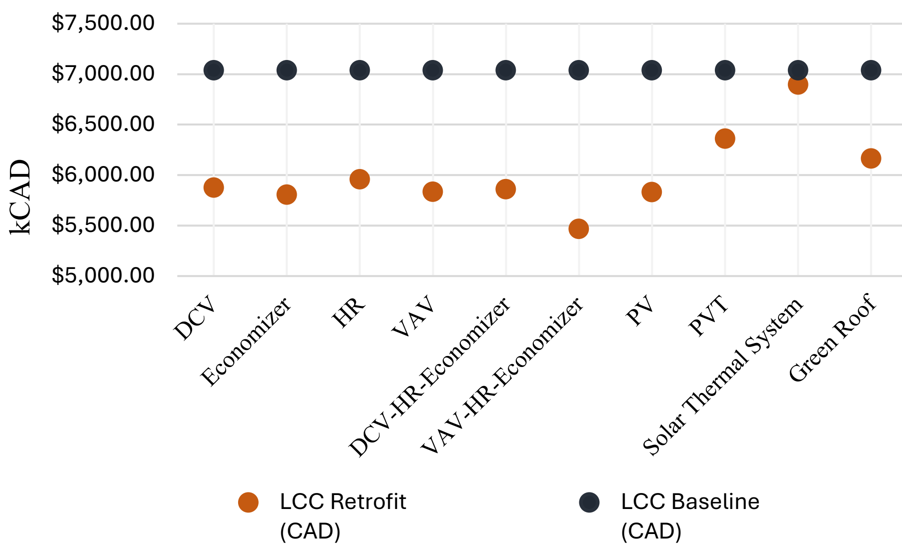

Figure 4. 17 Comparison of Base Model and Scenarios LCC

On the other hand, solar thermal panels represent the least favorable retrofit option. This scenario shows only a marginal improvement in life-cycle cost (LCC) compared to the baseline, making it economically unattractive. In general, the assessment indicates that renewable energy strategies, when implemented individually, do not provide substantial reductions in overall energy consumption.

The main reasons are twofold. From an economic standpoint, solar thermal retrofits are characterized by high capital costs, low internal rates of return (IRR) that fall below the discount rate, minimal differences in LCC relative to the existing condition, and extended payback periods that often exceed the expected system lifespan. From a technical standpoint, the low efficiency of solar thermal systems in the Canadian climate significantly limits their effectiveness, as cold conditions reduce the capacity for heat transfer and seasonal productivity. Together, these factors explain the relatively low feasibility and limited popularity of solar thermal retrofits in this context, particularly when compared with HVAC-based strategies that deliver both higher energy savings and superior financial performance.

5. Summary and Conclusions

5.1. Thesis Summary

This thesis presents a comprehensive simulation-based analysis of deep energy retrofit strategies for Montpetit Hall, a multifunctional institutional facility on the University of Ottawa campus. Constructed in 1972, the building is characterized by high energy use, outdated systems, and diverse operational requirements. In this result, the research aimed to enhance both energy performance and economic feasibility through an integrated framework that combines detailed energy modeling, simulation, calibration, and multi-objective optimization. A detailed 3D model was developed in Design Builder, capturing envelope properties, HVAC system configurations, and operational schedules, and simulated in Energy Plus. Baseline results were validated against 2022 utility data, achieving compliance with ASHRAE Guideline 14.

Optimization was carried out in two stages. Stage one evaluated envelope and window retrofits using the NSGA-II algorithm in MATLAB to generate Pareto-optimal solutions. Results highlighted the strong impact of semi-exposed floor, roof, and glazing upgrades, with significant reductions in heating demand under Ottawa's heating-dominated climate. Stage two assessed HVAC retrofits, including DCV, economizers, and HR. It delivered the greatest profit, reducing heating demand by nearly 38%. Combined envelope and HVAC measures achieved overall energy reductions exceeding 35%.

A comparative analysis of energy and cost outcomes identified retrofit packages that balance performance improvements with financial feasibility. The results confirm the potential for substantial energy and carbon reductions in cold-climate institutional buildings when guided by simulation-informed optimization.

5.2. Conclusion

The findings of this thesis demonstrate that deep energy retrofits in aging institutional buildings can deliver both significant energy savings and measurable financial benefits when guided by integrated modeling and optimization. The calibrated baseline confirmed Montpetit Hall's high heating and cooling demand, driven by its architectural design, cold-climate exposure, and year-round use.

Key conclusions include:

- The findings of this research demonstrate that both building envelope improvements and HVAC retrofits can significantly enhance the energy and economic performance of Montpetit Hall, albeit with varying levels of effectiveness. In terms of the envelope, upgrades to insulation and glazing yielded an overall annual reduction of approximately 2,637 GJ (13%), including decreases of 19.4% in heating, 6.7% in cooling, and 9.2% in electricity consumption. Among the window options considered, argon-filled low-E glazing achieved the greatest improvements by substantially reducing heat transfer compared to conventional air-filled systems. Furthermore, exterior walls, roofs, and semi-exposed floors were identified as the most influential components for retrofit interventions, as their exposure to Ottawa's severe climatic conditions makes them critical contributors to building heat loss.
- For HVAC systems, the most substantial benefits were observed when multiple measures were implemented in combination. The integrated retrofit scenario of VAV, heat recovery, and economizers produced the highest reductions, lowering heating demand by 50.8%, cooling by 57.5%, and electricity consumption by 53.5%, equivalent to annual cost savings of approximately CAD 171,600. Although this scenario required the largest capital investment

(CAD 865,000), it also achieved the most favorable financial outcome, with an NPV of CAD 1.66 million, an IRR of 19%, and a simple payback period of six years. These results confirm that, despite its relatively high initial cost, the integrated HVAC retrofit represents the most economically advantageous strategy.

- The VAV-only retrofit also demonstrated notable cost-effectiveness. With an investment of CAD 500,000, it generated annual savings of approximately CAD 100,000, resulting in an NPV of CAD 987,000, an IRR of 19%, and a payback period of six years. This indicates that even as a stand-alone measure, VAV conversion offers substantial reductions in energy consumption and operating costs. Other individual HVAC strategies, including DCV, HR, and economizers, produced positive outcomes, though with smaller economic returns, achieving NPVs in the range of CAD 300,000–400,000, IRRs between 12–17%, and payback periods of 7–9 years.
- In contrast, renewable energy technologies such as photovoltaic (PV), photovoltaic-thermal (PVT), solar thermal collectors, and green roofs demonstrated limited economic viability under current conditions. While these systems contribute to reducing heating and cooling loads and support long-term sustainability objectives, their extended payback periods and relatively modest financial savings compared to their high capital costs render them less attractive from a short- to medium-term investment perspective. These measures may, however, become more feasible in the future as technology costs decline or carbon pricing mechanisms are strengthened.
- In conclusion, the analysis confirms that envelope retrofits are particularly effective in reducing heating loads, argon-filled glazing provides the highest performance among window systems, and HVAC retrofits most notably VAV alone or in combination with HR and

economizers yield the most significant technical and economic benefits. Although renewable energy systems contribute to sustainability and decarbonization objectives, their current financial performance is not competitive with HVAC and envelope retrofits, which represent the most practical and economically sound strategies for Montpetit Hall within a 20-year planning horizon.

- In contrast, renewable energy options such as PV, PVT, solar thermal collectors, and green roofs were less convincing from a financial standpoint. While they can reduce heating and cooling loads and contribute to long-term decarbonization goals, their payback periods are far longer, and the savings are modest relative to the high capital cost. Under current conditions, these measures are not profitable within a 20-year planning horizon, though they could become more viable in the future as technology prices fall or stronger carbon policies are introduced.

Overall, the study concludes that envelope retrofits provide significant heating benefits, argon-filled windows deliver the best glazing performance, and VAV either on its own or integrated with HR and economizers offers the strongest combination of energy savings and financial return. Renewable energy systems remain valuable from a sustainability perspective, but for now, HVAC and envelope upgrades are the most practical and economically sound strategies for Montpetit Hall.

From a broader perspective, the results of this thesis also help to contextualize how far existing institutional buildings are from achieving net-zero energy performance. The deep retrofit scenarios investigated for Montpetit Hall, include advanced HVAC strategies (VAV, DCV, heat recovery, economizers), envelope measures, green roof implementation, and on-site renewable energy options demonstrated that substantial reductions in energy use and emissions are technically achievable. However, even with these measures, the building does not reach net-zero energy. This is mainly due to its inherently high ventilation and conditioning demands (gyms, pool, labs), the limitations of the existing structure and roof area for large-scale PV deployment, and the constraints imposed by its campus context and legacy infrastructure.

These findings suggest that, while the technologies and design principles required for net-zero buildings are already available, the full transformation of complex, mid-20th-century institutional buildings to net-zero remains a long-term challenge. Deep energy retrofits such as those evaluated in this study should therefore be viewed as critical intermediate steps: they significantly lower energy use intensity, improve operational efficiency, and prepare buildings for future integration of additional renewable systems. In this sense, Montpetit Hall does not yet reach net-zero energy, but the pathway outlined in this thesis illustrates how the performance gap can be meaningfully reduced and how existing campuses can progressively move toward net-zero targets over time.

5.3. Limitations and Future Work

Despite offering a detailed and comprehensive analysis, several limitations must be acknowledged. First, the model relied on assumptions for inputs such as plug loads, occupant behavior, and equipment schedules where measured data was unavailable. These generalizations may not fully capture real-world variability. Second, the framework did not explicitly address implementation constraints such as user disruption during construction, logistical challenges in occupied spaces, or budgetary cycles typical of large institutions. Some measures, particularly deep envelope retrofits, may face structural or heritage-related limitations.

Another limitation lies in the scope of evaluation, which was confined to energy and economic metrics. While these are critical for decision-making, broader aspects such as indoor environmental quality, occupant comfort, post-retrofit maintenance, and embodied carbon were not included. Addressing these dimensions would enable a more holistic sustainability assessment.

Future research should extend the framework by.

- Incorporating dynamic occupancy modeling, real-time operational data, and smart sensor integration to improve calibration accuracy.
- Expanding the evaluation criteria to include embodied carbon, life-cycle emissions, and indoor environmental quality.
- On the financial side, future studies should consider dynamic scenarios that account for fluctuations in energy prices, the introduction of carbon taxes, or the availability of government incentives, which could significantly alter the viability of renewable energy technologies.
- Exploring AI-driven predictive control and real-time optimization to maximize post-retrofit operational performance.

Together, these extensions would build on the present work and further strengthen the role of integrated modeling and optimization in advancing energy transition strategies for institutional buildings.

As part of future work, the integration of a solar panel tree system could be investigated as an alternative or complementary renewable energy strategy for Montpetit Hall. A solar tree typically consists of a vertical support structure with multiple photovoltaic (PV) modules arranged in a branching configuration, allowing electricity generation in locations were conventional large, flat PV arrays may be constrained by space, shading, or architectural limitations. For a dense campus context such as the University of Ottawa, solar trees could be considered for installation in adjacent outdoor plazas, pedestrian zones, or landscaped areas, thereby increasing the on-site renewable energy contribution without further loading the existing roof. A future study could quantify the potential annual electricity generation, evaluate the impact on the building's overall energy balance and greenhouse gas emissions, and compare the cost-effectiveness of solar trees with traditional rooftop PV installations. In addition, aspects such as visual integration with the campus environment, shading benefits for outdoor users, and maintenance requirements could be assessed to determine the practical feasibility of deploying solar trees as part of a broader campus sustainability strategy.

Reference

[1] "Global Energy Review 2025 – Analysis," IEA. Accessed: Sept. 21, 2025. [Online]. Available: https://www.iea.org/reports/global-energy-review-2025

[2] "Executive summary – Electricity 2025 – Analysis," IEA. Accessed: Sept. 29, 2025. [Online]. Available: http://www.iea.org/reports/electricity-2025/executive-summary

[3] H. Ahmad, M. Yaqub, and S. H. Lee, "Global trends in carbon neutrality: a scientometric review on energy transition challenges, practices, policies, and opportunities," *Environ. Dev. Sustain.*, Aug. 2025, doi: 10.1007/s10668-025-06507-7.

[4] "Sustainable Development Report 2024," Sustainable Development Solutions Network. Accessed: Sept. 21, 2025. [Online]. Available: https://www.unsdsn.org/resources/the-sustainable-development-report-2024/

[5] U. N. Environment, "Emissions Gap Report 2024 | UNEP - UN Environment Programme." Accessed: Sept. 29, 2025. [Online]. Available: https://www.unep.org/resources/emissions-gap-report-2024

[6] M. H. Rahman, A. U. Hoque, I. Nawar, M. R. Islam, and T. Jamal, "Electrifying Remote Communities in Malawi: Addressing Uncertainties in Design & Optimization of Hybrid Renewable Energy-Based System," in *2024 IEEE International Conference on Power System Technology (PowerCon)*, Kathmandu, Nepal: IEEE, Nov. 2024, pp. 1–5. doi: 10.1109/PowerCon60995.2024.10870531.

[7] A. Vilches, A. Garcia-Martinez, and B. Sanchez-Montañes, "Life cycle assessment (LCA) of building refurbishment: A literature review," *Energy Build.*, vol. 135, pp. 286–301, Jan. 2017, doi: 10.1016/j.enbuild.2016.11.042.

[8] M. T. Lakhiar, S. Sanmargaraja, A. Olanrewaju, C. H. Lim, V. Ponniah, and A. D. Mathalamuthu, "Energy retrofitting strategies for existing buildings in Malaysia: A systematic review and bibliometric analysis," *Environ. Sci. Pollut. Res.*, vol. 31, no. 9, pp. 12780–12814, Jan. 2024, doi: 10.1007/s11356-024-32020-x.

[9] A. Tejani, "Integrating energy-efficient HVAC systems into historical buildings: Challenges and solutions for balancing preservation and modernization," *ESP J. Eng. Technol. Adv.*, vol. 1, no. 1, pp. 83–97, 2021.

[10] S. R. Asaee, A. Sharafian, O. E. Herrera, P. Blomerus, and W. Mérida, "Housing stock in cold-climate countries: Conversion challenges for net zero emission buildings," *Appl. Energy*, vol. 217, pp. 88–100, May 2018, doi: 10.1016/j.apenergy.2018.02.135.

[11] Z. J. Zhai and J. M. Helman, "Implications of climate changes to building energy and design," *Sustain. Cities Soc.*, vol. 44, pp. 511–519, Jan. 2019, doi: 10.1016/j.scs.2018.10.043.

[12] M.-T. Huang and P.-M. Zhai, "Achieving Paris Agreement temperature goals requires carbon neutrality by middle century with far-reaching transitions in the whole society," *Adv. Clim. Change Res.*, vol. 12, no. 2, pp. 281–286, Apr. 2021, doi: 10.1016/j.accre.2021.03.004.

[13] L. Pérez-Lombard, J. Ortiz, and C. Pout, "A review on buildings energy consumption information," *Energy Build.*, vol. 40, no. 3, pp. 394–398, 2008, doi: 10.1016/j.enbuild.2007.03.007.

[14] Z. Ma, P. Cooper, D. Daly, and L. Ledo, "Existing building retrofits: Methodology and state-of-the-art," *Energy Build.*, vol. 55, pp. 889–902, Dec. 2012, doi: 10.1016/j.enbuild.2012.08.018.

[15] S. Ghorbany *et al.*, "Data driven assessment of built environment impacts on urban health across United States cities," *Sci. Rep.*, vol. 15, no. 1, p. 19998, June 2025, doi: 10.1038/s41598-025-04567-3.

[16] S. B. Sadineni, S. Madala, and R. F. Boehm, "Passive building energy savings: A review of building envelope components," *Renew. Sustain. Energy Rev.*, vol. 15, no. 8, pp. 3617–3631, Oct. 2011, doi: 10.1016/j.rser.2011.07.014.
[17] A. B. Huluka and S. Muthulingam, "Enhancing building roof thermal energy efficiency in hot climates: A novel dual-layer design with integrated phase change materials," *Energy Build.*, vol. 347, p. 116331, Nov. 2025, doi: 10.1016/j.enbuild.2025.116331.
[18] F. Ascione, N. Bianco, R. De Masi, G. Mauro, and G. Vanoli, "Design of the Building Envelope: A Novel Multi-Objective Approach for the Optimization of Energy Performance and Thermal Comfort," *Sustainability*, vol. 7, no. 8, pp. 10809–10836, Aug. 2015, doi: 10.3390/su70810809.
[19] M. Hamdy, A. Hasan, and K. Siren, "A multi-stage optimization method for cost-optimal and nearly-zero-energy building solutions in line with the EPBD-recast 2010," *Energy Build.*, vol. 56, pp. 189–203, 2013.
[20] S. Magli, C. Lodi, F. M. Contini, A. Muscio, and P. Tartarini, "Dynamic analysis of the heat released by tertiary buildings and the effects of urban heat island mitigation strategies," *Energy Build.*, vol. 114, pp. 164–172, Feb. 2016, doi: 10.1016/j.enbuild.2015.05.037.
[21] T. Dalla Mora, F. Peron, P. Romagnoni, M. Almeida, and M. Ferreira, "Tools and procedures to support decision making for cost-effective energy and carbon emissions optimization in building renovation," *Energy Build.*, vol. 167, pp. 200–215, May 2018, doi: 10.1016/j.enbuild.2018.02.030.
[22] "IEA EBC Annex 56 – Cost Effective Energy and Carbon Emission Optimization in Building Renovation." Accessed: Sept. 21, 2025. [Online]. Available: https://nachhaltigwirtschaften.at/en/iea/technologyprogrammes/ebc/iea-ebc-annex-56.php
[23] L. Pérez-Lombard, J. Ortiz, and C. Pout, "A review on buildings energy consumption information," *Energy Build.*, vol. 40, no. 3, pp. 394–398, 2008, doi: 10.1016/j.enbuild.2007.03.007.
[24] S. D'Oca, T. Hong, and J. Langevin, "The human dimensions of energy use in buildings: A review," *Renew. Sustain. Energy Rev.*, vol. 81, pp. 731–742, Jan. 2018, doi: 10.1016/j.rser.2017.08.019.
[25] M. Azima and S. Seyis, "Science mapping the knowledge domain of energy performance research in the AEC industry: A scientometric analysis," *Energy*, vol. 264, p. 125938, Feb. 2023, doi: 10.1016/j.energy.2022.125938.
[26] E. Mills, "A golden opportunity for reducing energy costs and greenhouse gas emissions," *Lawrence Berkeley Natl. Lab.*, 2009.
[27] M. Deng, X. Peng, and Y. Zhao, "A belief-desire-intention agent for modeling building managers' air-conditioning setpoint adjustment behavior under demand response," *Energy Build.*, vol. 346, p. 116248, Nov. 2025, doi: 10.1016/j.enbuild.2025.116248.
[28] T. Dietz, P. C. Stern, and E. U. Weber, "Reducing Carbon-Based Energy Consumption through Changes in Household Behavior," *Daedalus*, vol. 142, no. 1, pp. 78–89, Jan. 2013, doi: 10.1162/DAED_a_00186.
[29] T. T. Chow, J. W. Hand, and P. A. Strachan, "Building-integrated photovoltaic and thermal applications in a subtropical hotel building," *Appl. Therm. Eng.*, vol. 23, no. 16, pp. 2035–2049, Nov. 2003, doi: 10.1016/S1359-4311(03)00183-2.
[30] S. A. Kalogirou, "Solar thermal collectors and applications," *Prog. Energy Combust. Sci.*, vol. 30, no. 3, pp. 231–295, 2004, doi: 10.1016/j.pecs.2004.02.001.

[31] U. Berardi, "The outdoor microclimate benefits and energy saving resulting from green roofs retrofits," *Energy Build.*, vol. 121, pp. 217–229, June 2016, doi: 10.1016/j.enbuild.2016.03.021.
[32] Z. Ma, P. Cooper, D. Daly, and L. Ledo, "Existing building retrofits: Methodology and state-of-the-art," *Energy Build.*, vol. 55, pp. 889–902, 2012.
[33] J. Zuo and Z.-Y. Zhao, "Green building research–current status and future agenda: A review," *Renew. Sustain. Energy Rev.*, vol. 30, pp. 271–281, 2014.
[34] "Buildings – Breakthrough Agenda Report 2023 – Analysis," IEA. Accessed: Sept. 21, 2025. [Online]. Available: https://www.iea.org/reports/breakthrough-agenda-report-2023/buildings
[35] "Energy Fact Book, 2024-2025: Energy efficiency : Canadian Centre for Energy Information." Accessed: Sept. 21, 2025. [Online]. Available: https://energy-information.canada.ca/en/energy-facts/energy-efficiency
[36] C. Jayanuwan, "Thermal modeling, analysis of MUN CSF building, and feasibility study of space heating using electricity."
[37] W. Wei, L. Ni, W. Wang, and Y. Yao, "Experimental and theoretical investigation on defrosting characteristics of a multi-split air source heat pump with vapor injection," *Energy Build.*, vol. 217, p. 109938, June 2020, doi: 10.1016/j.enbuild.2020.109938.
[38] D. T. De Silva, "Predictive modelling of building degradation as influenced by contributing factors," PhD Thesis, RMIT University, 2024. Accessed: Sept. 29, 2025. [Online]. Available: https://research-repository.rmit.edu.au/articles/thesis/Predictive_modelling_of_building_degradation_as_influenced_by_contributing_factors/27599589
[39] L. Yang, R. Fu, W. He, Q. He, and Y. Liu, "Adaptive thermal comfort and climate responsive building design strategies in dry–hot and dry–cold areas: Case study in Turpan, China," *Energy Build.*, vol. 209, p. 109678, Feb. 2020, doi: 10.1016/j.enbuild.2019.109678.
[40] M. Z. Mistarihi, M. Kharseh, E. M. Abo-Zahhad, K. Alamara, M. Elasy, and K. Aldhuhoori, "Energy-efficient strategies for net-zero buildings in the UAE: a climate-resilient blueprint," *Energy Convers. Manag. X*, vol. 28, p. 101215, Oct. 2025, doi: 10.1016/j.ecmx.2025.101215.
[41] F. Amirifard, S. A. Sharif, and F. Nasiri, "Application of passive measures for energy conservation in buildings – a review," *Adv. Build. Energy Res.*, vol. 13, no. 2, pp. 282–315, July 2019, doi: 10.1080/17512549.2018.1488617.
[42] N. R. Canada, "Deep Retrofit Accelerator Initiative – Application Guide for the second call for applications." Accessed: Sept. 30, 2025. [Online]. Available: https://natural-resources.canada.ca/energy-efficiency/building-energy-efficiency/deep-retrofit-accelerator-initiative-application-guide-second-call-applications
[43] G. Costea, M. T. Pusch, D. Bănăduc, D. Cosmoiu, and A. Curtean-Bănăduc, "A review of hydropower plants in Romania: Distribution, current knowledge, and their effects on fish in headwater streams," *Renew. Sustain. Energy Rev.*, vol. 145, p. 111003, July 2021, doi: 10.1016/j.rser.2021.111003.
[44] C. E. Hoicka and R. Das, "Ambitious deep energy retrofits of buildings to accelerate the 1.5°C energy transition in Canada," *Can. Geogr. Géographies Can.*, vol. 65, no. 1, pp. 116–127, Mar. 2021, doi: 10.1111/cag.12637.
[45] R. Kilian, "The 4th International Conference on Energy Efficiency in Historic Buildings," May 2022.

[46] N. Yang, J. Chen, L. Ban, P. Li, and H. Wang, "Pre-planning and post-evaluation approaches to sustainable vernacular architectural practice: A research-by-design study to building renovation in Shangri-La's Shanpian House, China," *Sustainability*, vol. 16, no. 21, p. 9568, 2024.
[47] Y. Dadras and M. Kavgic, "The applicability of a simplified whole-building energy model for energy-efficiency retrofit analysis," in *12th eSim Building Simulation Conference. https://publications. ibpsa. org/proceedings/esim/2022/papers/esim2022_254. pdf*, 2022. Accessed: Sept. 29, 2025. [Online]. Available: https://publications.ibpsa.org/proceedings/esim/2022/papers/esim2022_254.pdf
[48] Y. Dadras, F. Mostafazadeh, M. Kavgic, and M. Ghobadi, "Enhancing building energy optimization efficiency: A performance analysis of simplification approaches," *J. Build. Eng.*, vol. 105, p. 112559, July 2025, doi: 10.1016/j.jobe.2025.112559.
[49] H. Li, Z. Wang, and T. Hong, "Occupant-Centric key performance indicators to inform building design and operations," *J. Build. Perform. Simul.*, vol. 14, no. 6, pp. 814–842, Nov. 2021, doi: 10.1080/19401493.2021.1876771.
[50] C. Czipf, "The impact of changing energy prices, interest rates, and investment costs on the net present value and internal rate of return for alternative energy projects," *Discov. Sustain.*, vol. 6, no. 1, p. 161, Mar. 2025, doi: 10.1007/s43621-025-00921-7.
[51] L. E. Excell and R. K. Jain, "Examining the impact of energy efficiency retrofits and vegetation on energy performance of institutional buildings: An equity-driven analysis," *Appl. Energy*, vol. 357, p. 121722, Mar. 2024, doi: 10.1016/j.apenergy.2023.121722.
[52] B. Wilbur, "Thermal system-specific and net-zero carbon least-cost design of new houses in Canadian cold climates," PhD Thesis, Toronto Metropolitan University, 2018. Accessed: Sept. 29, 2025. [Online]. Available: https://rshare.library.torontomu.ca/ndownloader/files/28139847
[53] J. M. Willis, "A Solar-Thermal Architecture for Grid-Independent Heating, Cooling, and Power Using Thermal Storage and Dual Stirling Engines".
[54] M. Manya, R. Sharma, and V. Richhariya, "Enhancing Software Maintainability Through Machine Learning Classification Technique for Security Requirements," in *Intelligent Vision and Computing*, A. K. Saha, H. Sharma, M. Prasad, L. Chouhan, and N. K. Chaudhary, Eds., in Studies in Smart Technologies. , Singapore: Springer Nature Singapore, 2025, pp. 323–342. doi: 10.1007/978-981-96-4722-4_25.
[55] S. B. Sadineni, S. Madala, and R. F. Boehm, "Passive building energy savings: A review of building envelope components," *Renew. Sustain. Energy Rev.*, vol. 15, no. 8, pp. 3617–3631, Oct. 2011, doi: 10.1016/j.rser.2011.07.014.
[56] C. A. Balaras, K. Droutsa, E. Dascalaki, and S. Kontoyiannidis, "Heating energy consumption and resulting environmental impact of European apartment buildings," *Energy Build.*, vol. 37, no. 5, pp. 429–442, May 2005, doi: 10.1016/j.enbuild.2004.08.003.
[57] L. Rodrigues, J. M. P. Q. Delgado, A. Mendes, A. G. B. Lima, and A. S. Guimarães, "Sustainability Assessment of Buildings Indicators," *Sustainability*, vol. 15, no. 4, p. 3403, Feb. 2023, doi: 10.3390/su15043403.
[58] G. Ali *et al.*, "Urban environment dynamics and low carbon society: Multi-criteria decision analysis modeling for policy makers," *Sustain. Cities Soc.*, vol. 51, p. 101763, Nov. 2019, doi: 10.1016/j.scs.2019.101763.
[59] F. Ascione, R. F. De Masi, F. De Rossi, S. Ruggiero, and G. P. Vanoli, "Optimization of building envelope design for nZEBs in Mediterranean climate: Performance analysis of

residential case study," *Appl. Energy*, vol. 183, pp. 938–957, Dec. 2016, doi: 10.1016/j.apenergy.2016.09.027.

[60] T. Li *et al.*, "Optimizing building energy consumption through synchronization and asynchronization of occupancy and air-conditioning behavior," *Energy Build.*, vol. 331, p. 115409, Mar. 2025, doi: 10.1016/j.enbuild.2025.115409.

[61] A. Arteconi *et al.*, "Thermal energy storage coupled with PV panels for demand side management of industrial building cooling loads," *Appl. Energy*, vol. 185, pp. 1984–1993, Jan. 2017, doi: 10.1016/j.apenergy.2016.01.025.

[62] V. Shekar, A. Caló, and E. Pongrácz, "Experiences from seasonal Arctic solar photovoltaics (PV) generation- An empirical data analysis from a research infrastructure in Northern Finland," *Renew. Energy*, vol. 217, p. 119162, Nov. 2023, doi: 10.1016/j.renene.2023.119162.

[63] J. Yang, A. Pantazaras, S. E. Lee, and M. Santamouris, "Retrofitting solutions for two different occupancy levels of educational buildings in tropics," *Int. J. Sustain. Energy*, vol. 37, no. 1, pp. 81–95, Jan. 2018, doi: 10.1080/14786451.2016.1177052.

[64] P. M. Cuce and E. Cuce, "Ventilated Facades for Low-Carbon Buildings: A Review," *Processes*, vol. 13, no. 7, p. 2275, 2025.

[65] M. Posani, R. Veiga, and V. P. De Freitas, "Retrofitting Historic Walls: Feasibility of Thermal Insulation and Suitability of Thermal Mortars," *Heritage*, vol. 4, no. 3, pp. 2009–2022, Aug. 2021, doi: 10.3390/heritage4030114.

[66] M. Sun and E. J. Cha, "Probabilistic Building Functionality Estimation Framework for Buildings Subjected to Hurricane Winds," *J. Struct. Eng.*, vol. 148, no. 10, p. 04022147, Oct. 2022, doi: 10.1061/(ASCE)ST.1943-541X.0003411.

[67] B. Li *et al.*, "A review of research on intelligent technology in building air conditioning system optimisation," *Int. J. Refrig.*, vol. 176, pp. 205–225, Aug. 2025, doi: 10.1016/j.ijrefrig.2025.04.027.

[68] R. Roshan Kharrat, "Dynamic and Adaptive Photovoltaic Shading Systems: Design and Architectural Integration for Energy Production and Indoor Comfort.," PhD Thesis, Politecnico di Torino, 2024. Accessed: Sept. 30, 2025. [Online]. Available: https://webthesis.biblio.polito.it/33696/

[69] Y. Akhmetov, E. Fedotova, and M. M. Frysztacki, "Flattening the peak demand curve through energy efficient buildings: A holistic approach towards net-zero carbon," *Appl. Energy*, vol. 384, p. 125421, Apr. 2025, doi: 10.1016/j.apenergy.2025.125421.

[70] N. R. Canada, "Natural Resources Canada." Accessed: Sept. 20, 2025. [Online]. Available: https://natural-resources.canada.ca/

[71] H. Zhang, "Life cycle costing analysis of deep energy retrofits of a mid-rise building to understand the impact of energy conservation measures," Apr. 02, 2023, *arXiv*: arXiv:2304.00456. doi: 10.48550/arXiv.2304.00456.

[72] P. Pease, J. Chhabra, and Z. Zolfaghari, "Planning for net zero by 2050, what HVAC system interventions will today's code minimum commercial buildings require?," Nov. 06, 2021, *arXiv*: arXiv:2111.03899. doi: 10.48550/arXiv.2111.03899.

[73] B. Chenari, S. Saadatian, and M. Gameiro da Silva, "Experimental Assessment of Demand-Controlled Ventilation Strategies for Energy Efficiency and Indoor Air Quality in Office Spaces," *Air*, vol. 3, no. 2, p. 17, 2025.

[74] R. Talib, N. Nabil, and W. Choi, "Optimization-based data-enabled modeling technique for HVAC systems components," *Buildings*, vol. 10, no. 9, p. 163, 2020.

[75] B. Rismanchi, J. M. Zambrano, B. Saxby, R. Tuck, and M. Stenning, “Control Strategies in Multi-Zone Air Conditioning Systems,” *Energies*, vol. 12, no. 3, p. 347, Jan. 2019, doi: 10.3390/en12030347.
[76] E. Saloux, J. A. Candanedo, C. Vallianos, N. Morovat, and K. Zhang, “From theory to practice: A critical review of model predictive control field implementations in the built environment,” *Appl. Energy*, vol. 393, p. 126091, Sept. 2025, doi: 10.1016/j.apenergy.2025.126091.
[77] F. Iqbal and S. Mirzabeigi, “Digital Twin-Enabled Building Information Modeling–Internet of Things (BIM-IoT) Framework for Optimizing Indoor Thermal Comfort Using Machine Learning,” *Buildings*, vol. 15, no. 10, p. 1584, May 2025, doi: 10.3390/buildings15101584.
[78] F. Ghawash, “Energy Optimal Control of Cooling and Ventilation Systems,” 2024, Accessed: Sept. 30, 2025. [Online]. Available: https://ntnuopen.ntnu.no/ntnu-xmlui/handle/11250/3164045
[79] M. R. Sanzana, M. O. M. Abdulrazic, J. Y. Wong, T. Maul, and C.-C. Yip, “Effects of external weather on the water consumption of Thermal-Energy-Storage Air-Conditioning system,” *Energy Nexus*, vol. 10, p. 100187, June 2023, doi: 10.1016/j.nexus.2023.100187.
[80] S. Soudian and U. Berardi, “Development of a performance-based design framework for multifunctional climate-responsive façades,” *Energy Build.*, vol. 231, p. 110589, 2021.
[81] J. Ma, A. Khoury, and M. Rodgers, “Evaluation of PV Snow Loss Models in the East Coast of Canada Using AI Computer Vision,” in *2023 IEEE 50th Photovoltaic Specialists Conference (PVSC)*, San Juan, PR, USA: IEEE, June 2023, pp. 1–5. doi: 10.1109/PVSC48320.2023.10360003.
[82] K. S. Hayibo, A. Petsiuk, P. Mayville, L. Brown, and J. M. Pearce, “Monofacial vs bifacial solar photovoltaic systems in snowy environments,” *Renew. Energy*, vol. 193, pp. 657–668, June 2022, doi: 10.1016/j.renene.2022.05.050.
[83] B. Ghaleb, S. A. Abbasi, and M. Asif, “Application of solar PV in the building sector: Prospects and barriers in the GCC region,” *Energy Rep.*, vol. 9, pp. 3932–3942, 2023.
[84] H.-J. Joo, Y.-S. An, M.-H. Kim, and M. Kong, “Long-term performance evaluation of liquid-based photovoltaic thermal (PVT) modules with overheating-prevention technique,” *Energy Convers. Manag.*, vol. 296, p. 117682, 2023.
[85] F. Masood *et al.*, “A review of recent developments and applications of compound parabolic concentrator-based hybrid solar photovoltaic/thermal collectors,” *Sustainability*, vol. 14, no. 9, p. 5529, 2022.
[86] G. D. Shekata, G. S. Tibba, and A. T. Baheta, “Recent advancements in indirect solar dryer performance and the associated thermal energy storage,” *Results Eng.*, vol. 24, p. 102877, Dec. 2024, doi: 10.1016/j.rineng.2024.102877.
[87] S. Vilčeková, J. Budajová, K. Harčárová, P. Mésároš, E. Krídlová Burdová, and R. Zimermann, “The impact of green roofs’ composition on its overall life cycle,” *J. Environ. Manage.*, vol. 369, p. 122363, Oct. 2024, doi: 10.1016/j.jenvman.2024.122363.
[88] L. M. Anderson and K. M. Wan, “Effects of Mixed-Use Green Roof on Student Community & Subjective Well-Being: A Case Study of the University of British Columbia’s Exchange Residence Green Roof,” 2021, Accessed: Sept. 30, 2025. [Online]. Available: https://open.library.ubc.ca/soa/cIRcle/collections/graduateresearch/66428/items/1.0421538
[89] S.-H. Chiu, C.-Y. Chiang, S.-K. Lee, and C.-Y. Chen, “Development of a Location-based Rapid Building Performance Simulation Tool Combined with Design of Experiment Method

for Energy Efficiency Enhancement in Existing Healthcare Building Retrofitting," *Sens. Mater.*, vol. 37, no. 4, p. 1615, Apr. 2025, doi: 10.18494/SAM5364.

[90] A. P. Vargas and L. Hamui, "Thermal energy performance simulation of a residential building retrofitted with passive design strategies: a case study in Mexico," *Sustainability*, vol. 13, no. 14, p. 8064, 2021.

[91] F. Del Ama Gonzalo, B. Moreno Santamaría, and M. J. Montero Burgos, "Assessment of building energy simulation tools to predict heating and cooling energy consumption at early design stages," *Sustainability*, vol. 15, no. 3, p. 1920, 2023.

[92] M. Alhammad, M. Eames, and R. Vinai, "Enhancing building energy efficiency through building information modeling (BIM) and building energy modeling (BEM) integration: A systematic review," *Buildings*, vol. 14, no. 3, p. 581, 2024.

[93] R. RASHID, "BIM AUTOMATION: DESIGN OPTIONEERING TOWARDS ENERGY PERFORMANCE OPTIMIZATION."

[94] M. Khan and J. A. Berthelsen, "A Data-Driven Digital Twin Framework for Simulation-Based Energy and Comfort Optimization in Existing Buildings."

[95] N. Rafati, M. Hazbei, and U. Eicker, "Louver configuration comparison in three Canadian cities utilizing NSGA-II," *Build. Environ.*, vol. 229, p. 109939, Feb. 2023, doi: 10.1016/j.buildenv.2022.109939.

[96] F. Islam, I. Ahmed, and L. Mihet-Popa, "Development and testing of an IoT platform with smart algorithms for building energy management systems," *Energy Build.*, vol. 344, p. 115970, Oct. 2025, doi: 10.1016/j.enbuild.2025.115970.

[97] R. Verma and D. Rakshit, "Comparison of reflective coating with other passive strategies: A climate based design and optimization study of building envelope," *Energy Build.*, vol. 287, p. 112973, May 2023, doi: 10.1016/j.enbuild.2023.112973.

[98] F. Mostafazadeh, S. J. Eirdmousa, and M. Tavakolan, "Energy, economic and comfort optimization of building retrofits considering climate change: A simulation-based NSGA-III approach," *Energy Build.*, vol. 280, p. 112721, Feb. 2023, doi: 10.1016/j.enbuild.2022.112721.

[99] Y. Dadras, F. Mostafazadeh, M. Kavgic, and M. Ghobadi, "Enhancing building energy optimization efficiency: A performance analysis of simplification approaches," *J. Build. Eng.*, vol. 105, p. 112559, 2025.

[100] "Internal Rate of Return Method - an overview | ScienceDirect Topics." Accessed: Sept. 30, 2025. [Online]. Available: https://www.sciencedirect.com/topics/engineering/internal-rate-of-return-method

[101] M. Gilbert, K. Barati, and X. Shen, "Lifecycle cost analysis of residential buildings considering thermal performance and financial uncertainties," *Energy Build.*, vol. 348, p. 116442, Dec. 2025, doi: 10.1016/j.enbuild.2025.116442.

[102] I. Youssefi, T. Celik, and A. Azimli, "Financial feasibility analysis for different retrofit strategies on an institutional building," *Sustain. Energy Technol. Assess.*, vol. 52, p. 102342, 2022.

[103] H. Tian, Z. He, and Z. Li, "A combined cooling solution for high heat density data centers using multi-stage heat pipe loops," *Energy Build.*, vol. 94, pp. 177–188, May 2015, doi: 10.1016/j.enbuild.2015.03.002.

[104] B. P. Kemery, "Analysis and design of a solar-combisystem for high solar fraction Canadian housing with diurnal and seasonal water-based thermal stores," PhD Thesis,

Carleton University, 2017. Accessed: Sept. 20, 2025. [Online]. Available: https://carleton.scholaris.ca/bitstreams/91a2a02f-a931-4e3c-8f1d-3da8a12569c7/download
[105] D. Forgione, "MAPPING AND MODELLING URBAN SOLAR ENERGY POTENTIALS USING GEOSPACIAL DATA."
[106] E. and C. C. Canada, "Canada's Changing Climate Report." Accessed: Sept. 20, 2025. [Online]. Available: https://www.canada.ca/en/environment-climate-change/services/science-technology/canadas-changing-climate-report.html
[107] "U.S. Department of Energy. EnergyPlus Engineering Reference: The Reference to EnergyPlus Calculations. Zone Heat Balance section. - Google Search." Accessed: Jan. 05, 2026. [Online]. Available: https://www.google.com/search?q=U.S.+Department+of+Energy.+EnergyPlus+Engineering+Reference%3A+The+Reference+to+EnergyPlus+Calculations.+Zone+Heat+Balance+section.&oq=U.S.+Department+of+Energy.+EnergyPlus+Engineering+Reference%3A+The+Reference+to+EnergyPlus+Calculations.+Zone+Heat+Balance+section.&gs_lcrp=EgZjaHJvbWUyBggAEEUYOTIHCAEQIRiPAjIHCAIQIRiPAjIHCAMQIRiPAtIBCDEwNjJqMGo3qAIAsAIA&sourceid=chrome&ie=UTF-8
[108] S. Soudian and U. Berardi, "Impact of future climate scenarios on thermal performance and resilience of building façades: Canadian climate case study," *Build. Environ.*, vol. 267, p. 112245, Jan. 2025, doi: 10.1016/j.buildenv.2024.112245.
[109] U. Berardi, Ed., *Multiphysics and Multiscale Building Physics: Proceedings of the 9th International Building Physics Conference (IBPC 2024) Volume 2: Urban Physics and Energy Efficiency*, vol. 553. in Lecture Notes in Civil Engineering, vol. 553. Singapore: Springer Nature Singapore, 2025. doi: 10.1007/978-981-97-8309-0.
[110] N. R. C. Canada, "National Energy Code of Canada for Buildings 2020." Accessed: Sept. 20, 2025. [Online]. Available: https://nrc.canada.ca/en/certifications-evaluations-standards/codes-canada/codes-canada-publications/national-energy-code-canada-buildings-2020
[111] S. Abedini, "Optimization of the thermal performance of the Montpetit Hall envelope: A case study," PhD Thesis, Université d'Ottawa| University of Ottawa, 2024. Accessed: Sept. 20, 2025. [Online]. Available: https://ruor.uottawa.ca/items/2bd7e9d0-66ec-47e0-8d9f-4e970b2974ac
[112] D. Tanguay, "International Performance Measurement and Verification Protocol (IPMVP)," Efficiency Valuation Organization (EVO). Accessed: Sept. 20, 2025. [Online]. Available: https://evo-world.org/en/products-services-mainmenu-en/protocols/ipmvp
[113] S. A. Sharif and A. Hammad, "Simulation-Based Multi-Objective Optimization of institutional building renovation considering energy consumption, Life-Cycle Cost and Life-Cycle Assessment," *J. Build. Eng.*, vol. 21, pp. 429–445, Jan. 2019, doi: 10.1016/j.jobe.2018.11.006.
[114] M. Tavakolan, F. Mostafazadeh, S. Jalilzadeh Eirdmousa, A. Safari, and K. Mirzaei, "A parallel computing simulation-based multi-objective optimization framework for economic analysis of building energy retrofit: A case study in Iran," *J. Build. Eng.*, vol. 45, p. 103485, Jan. 2022, doi: 10.1016/j.jobe.2021.103485.
[115] P. Naghipour and A. Naghipour, "Energy performance analysis of residential buildings in Bandar Anzali: Influence of orientation and aspect ratio," *Sustain.*, vol. 5, p. 100140, 2025, doi: 10.1016/j.nxsust.2025.100140.

[116] S. K. Khare, A. Gupta, and D. Vashist, “Hybrid NSGA-III and multi-objective TLBO for post-Pareto optimization of energy, cost, and carbon in modular steel buildings toward net-zero compliance,” *Asian J. Civ. Eng.*, Sept. 2025, doi: 10.1007/s42107-025-01524-3.
[117] K. Alexakis, V. Benekis, P. Kokkinakos, and D. Askounis, “Genetic algorithm-based multi-objective optimisation for energy-efficient building retrofitting: A systematic review,” *Energy Build.*, vol. 328, p. 115216, Feb. 2025, doi: 10.1016/j.enbuild.2024.115216.
[118] W. Short, D. J. Packey, and T. Holt, “A manual for the economic evaluation of energy efficiency and renewable energy technologies,” National Renewable Energy Lab.(NREL), Golden, CO (United States), 1995. Accessed: Jan. 05, 2026. [Online]. Available: https://www.osti.gov/biblio/35391
[119] M. Vaughn, “ASHRAE Research Report: 2020-2021.,” *ASHRAE J.*, vol. 63, no. 10, pp. 73–87, 2021.
[120] *Canada’s cost-benefit analysis guide for regulatory proposals*. Ottawa, Ontario, Canada: Treasury Board of Canada Secretariat = Secrétariat du Conseil du trésor du Canada, 2022.
[121] “The process of NSGA-II evolution.,” ResearchGate. Accessed: Jan. 05, 2026. [Online]. Available: https://www.researchgate.net/figure/The-process-of-NSGA-II-evolution_fig4_362891652
[122] K. Deb, A. Pratap, S. Agarwal, and T. Meyarivan, “A fast and elitist multiobjective genetic algorithm: NSGA-II,” *IEEE Trans. Evol. Comput.*, vol. 6, no. 2, pp. 182–197, Apr. 2002, doi: 10.1109/4235.996017.
[123] J. Kneifel, “Building Life Cycle Cost (BLCC) User Guide,” National Institute of Standards and Technology, Gaithersburg, MD, NIST TN 2346, 2025. doi: 10.6028/NIST.TN.2346.
[124] “Department of Energy.” Accessed: Sept. 20, 2025. [Online]. Available: https://www.energy.gov/eere/femp/downloads/annual-energy-savings-performance-contract-espc-espc-enabling-contracts-guidance
[125] J. D. Kneifel, “LIFE CYCLE COSTING MANUAL for the Federal Energy Management Program,” National Institute of Standards and Technology, Gaithersburg, MD, NIST HB 135e2022, 2025. doi: 10.6028/NIST.HB.135e2022.
[126] “ISO 15686-5:2017,” ISO. Accessed: Sept. 20, 2025. [Online]. Available: https://www.iso.org/standard/61148.html
[127] M. Vaughn, “ASHRAE Research Report: 2019-2020.,” *ASHRAE J.*, vol. 62, no. 10, pp. 73–89, 2020.
[128] S. Edwards, E. Bartlett, and I. Dickie, *Whole life costing and life-cycle assessment for sustainable building design*. CRC, 2000.
[129] “Standard 90.1.” Accessed: Sept. 20, 2025. [Online]. Available: https://www.ashrae.org/technical-resources/bookstore/standard-90-1
[130] A. Rana, “Financial incentives for green buildings in Canada: a spatio-temporal analysis,” PhD Thesis, University of British Columbia, 2021. Accessed: Sept. 20, 2025. [Online]. Available: https://open.library.ubc.ca/soa/cIRcle/collections/ubctheses/24/items/1.0401419

Appendix

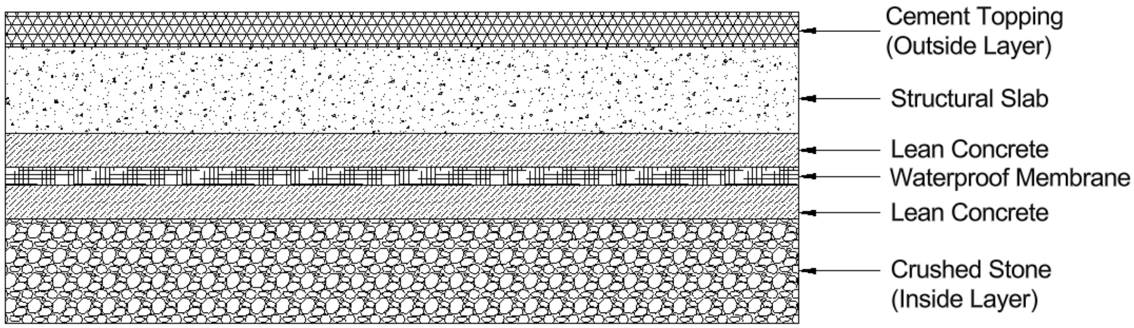

Figure A. 1 The Construction Design for the Montpetit Hall Underground Floor

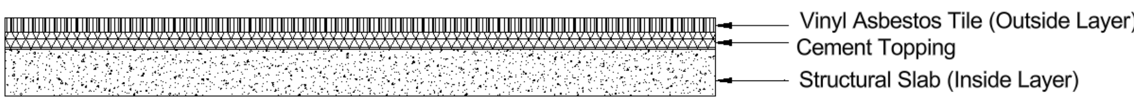

Figure A. 2 The Construction Design for the Montpetit Hall Interior Floor

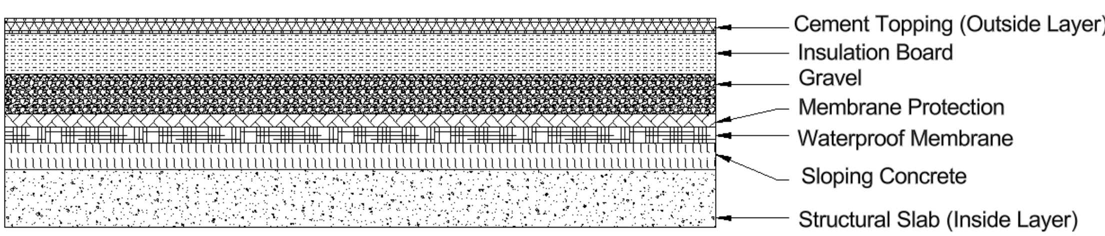

Figure A. 3 The Construction Design for the Montpetit Hall Exterior Floor

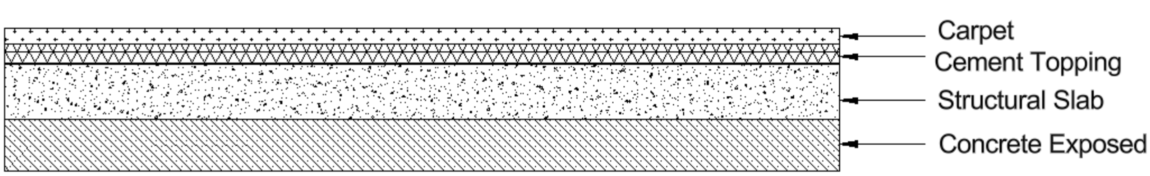

Figure A. 4 The Construction Design for the Montpetit Hall Semi-exposed Floor

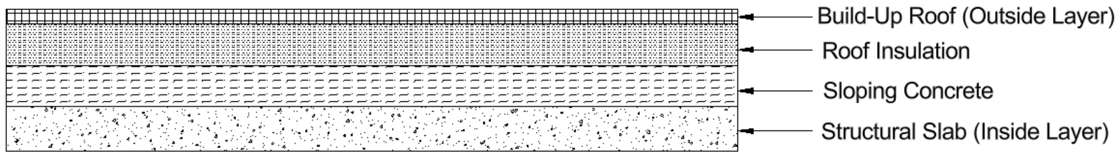

Figure A. 5 The Construction Design for the Montpetit Hall Roof

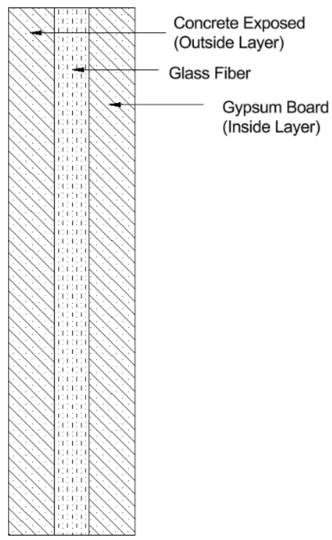

Figure A. 6 The Construction Design for the Montpetit Hall Exterior Wall

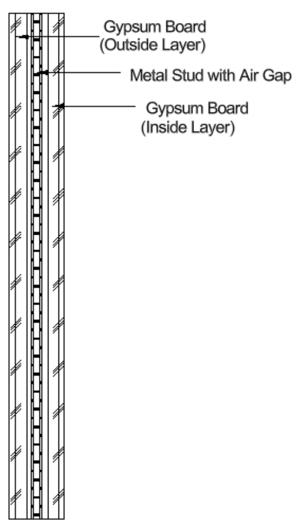

Figure A. 7 The Construction Design for the Montpetit Hall Interior Wall

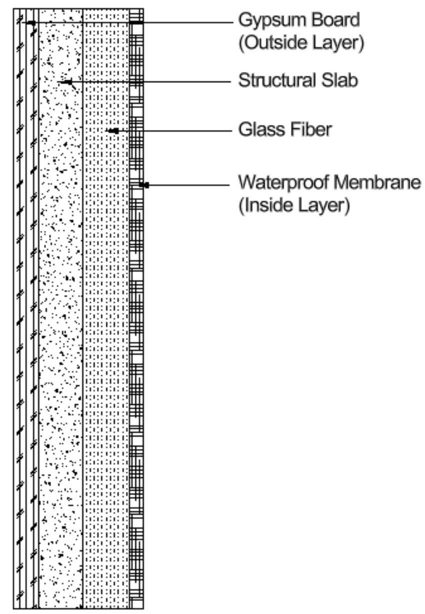

Figure A. 8 The Construction Design for the Montpetit Hall Underground Wall

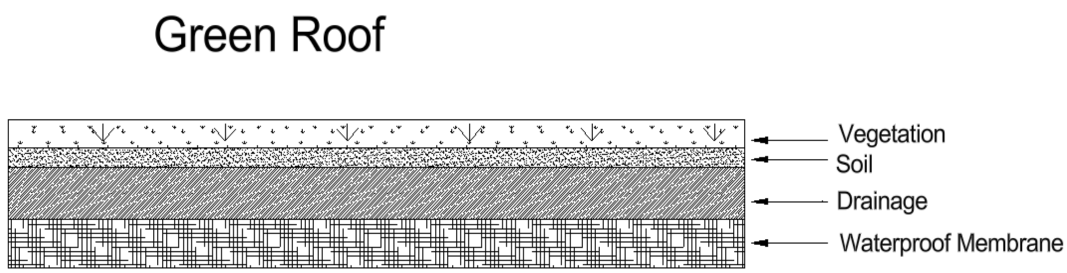

Figure A. 9 The Construction Design for the Montpetit Hall Green Roof

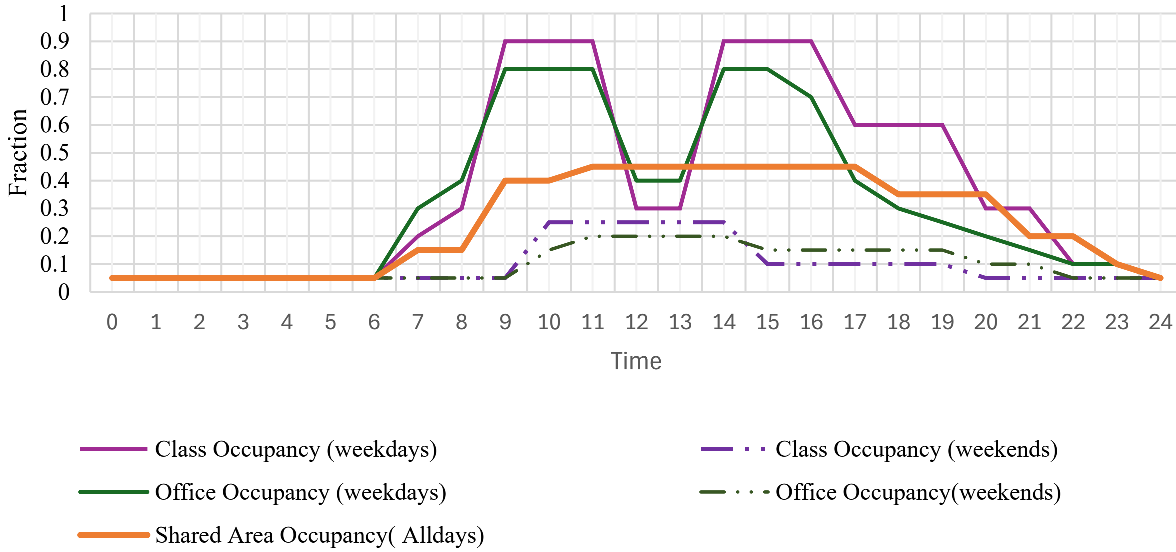

Figure A. 10 Class and Office People's Fractions for Fall and Winter Semester

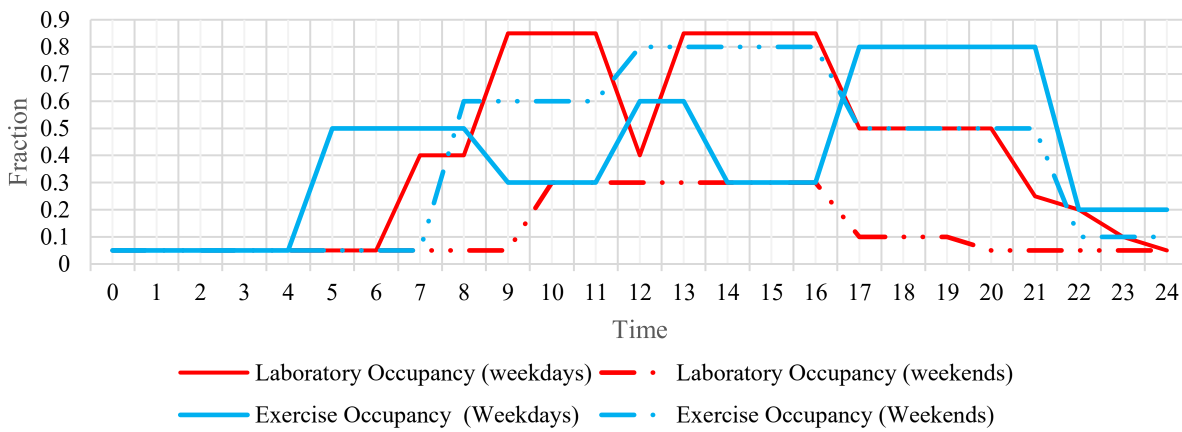

Figure A. 11 Laboratory and Exercise People's Fractions for Fall and Winter Semester

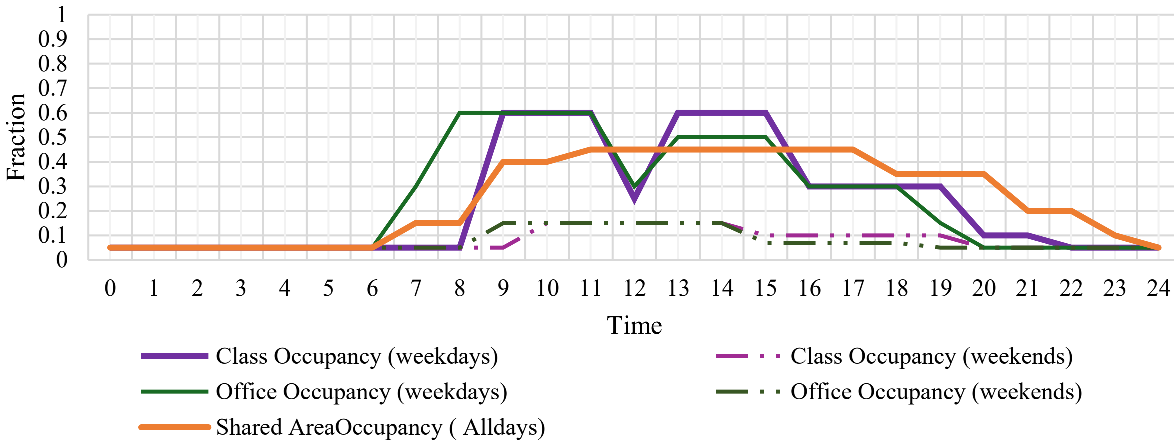

Figure A. 12 Class and Office People's Fractions for Spring and Summer Semester

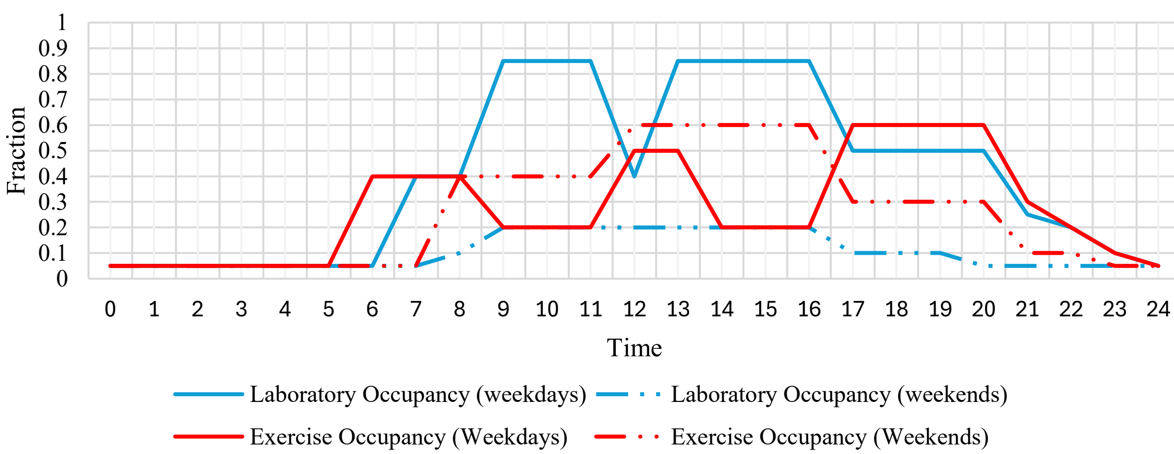

Figure A. 13 Laboratory and Exercise People's Fractions for Spring and Summer Semester

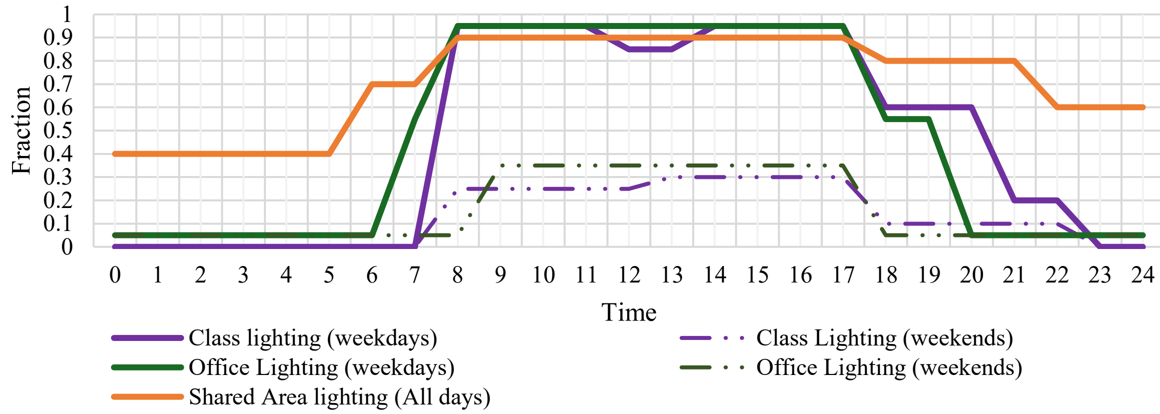

Figure A. 14 Class and Office Lightning's Fractions for Fall and Winter Semester

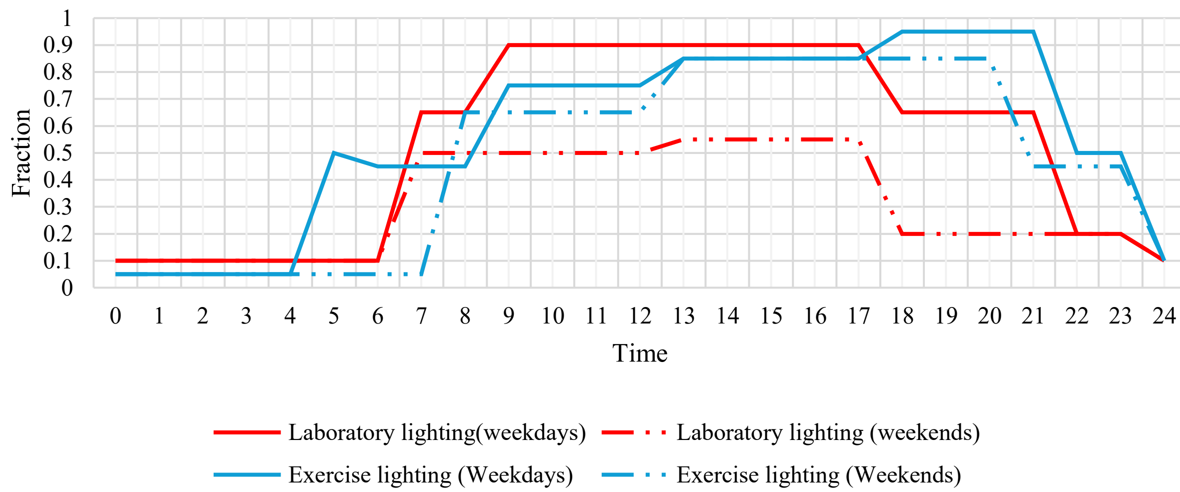

Figure A. 15 Laboratory and Exercise Lightning's Fractions for Fall and Winter Semester

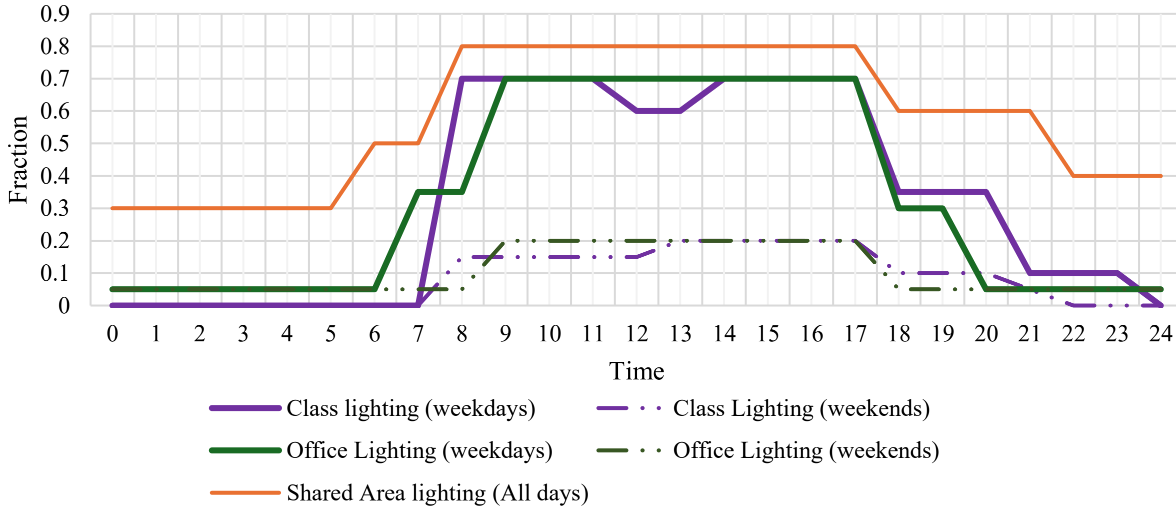

Figure A. 16 Class and Office Lightning's Fractions for Spring and Summer Semester

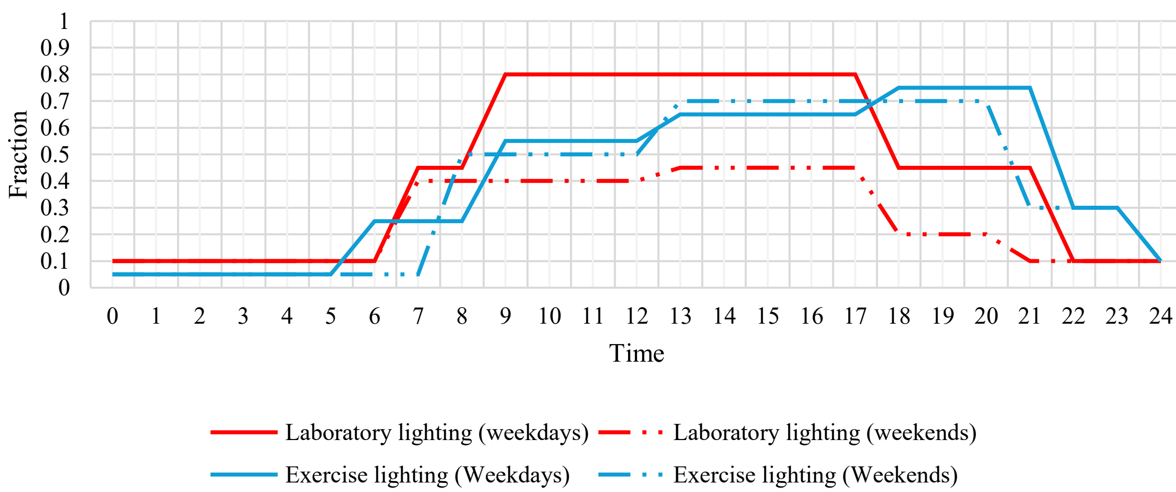

Figure A. 17 Laboratory and Exercise Lightning's Fractions for Spring and Summer Semester

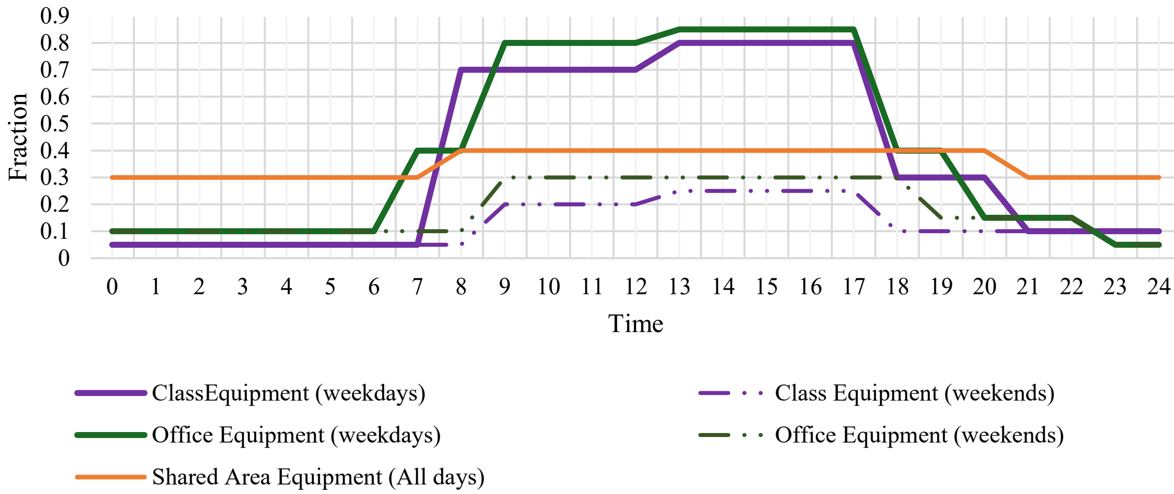

Figure A. 18 Class and Office Equipment's Fractions for Fall and Winter Semester

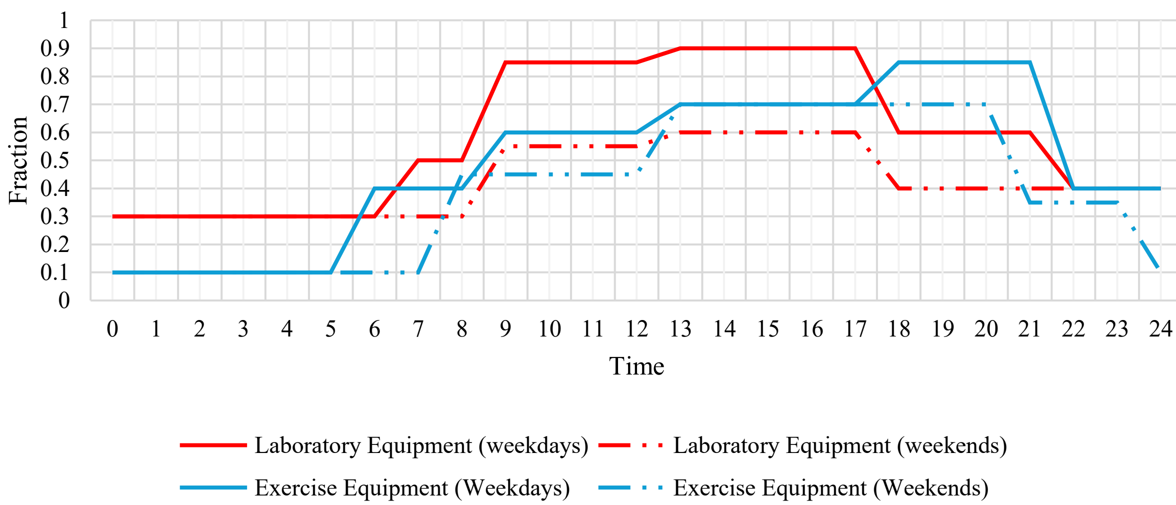

Figure A. 19 Laboratory and Exercise Equipment's Fractions for Spring and Summer Semester

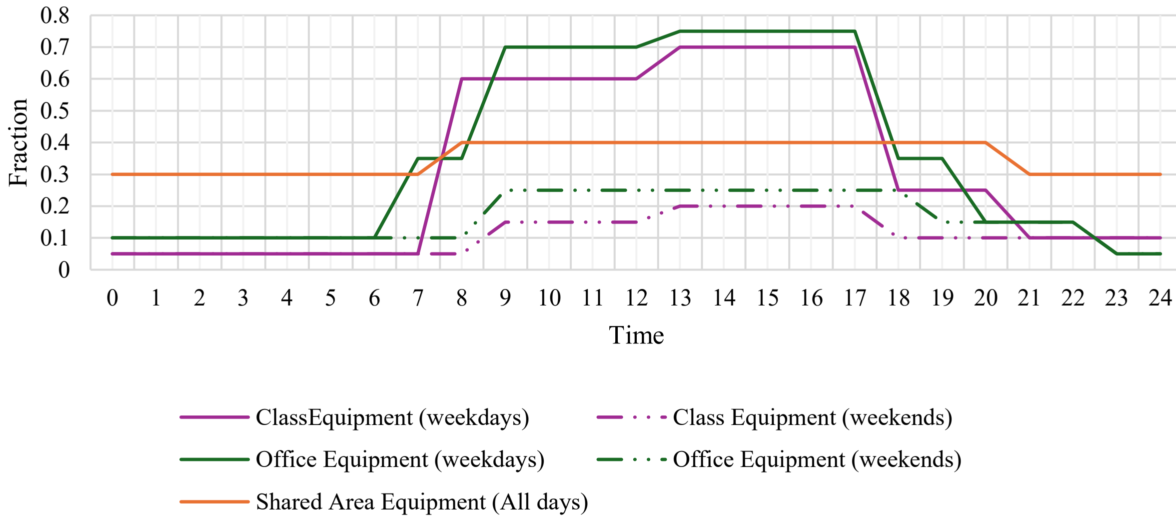

Figure A. 20 Class and Office Equipment's Fractions for Spring and Summer Semester

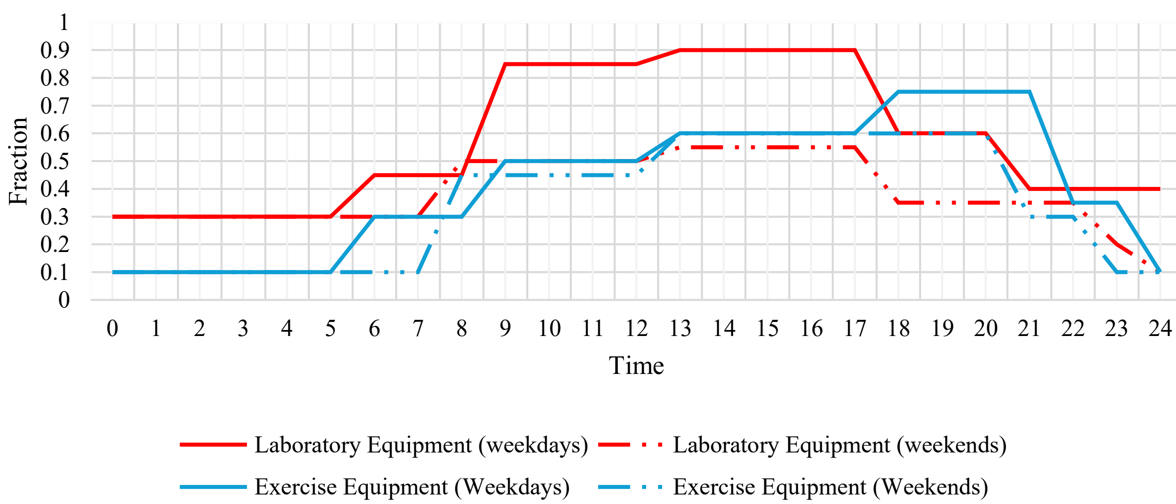

Figure A. 21 Laboratory and Exercise Equipment's Fractions for Spring and Summer Semester

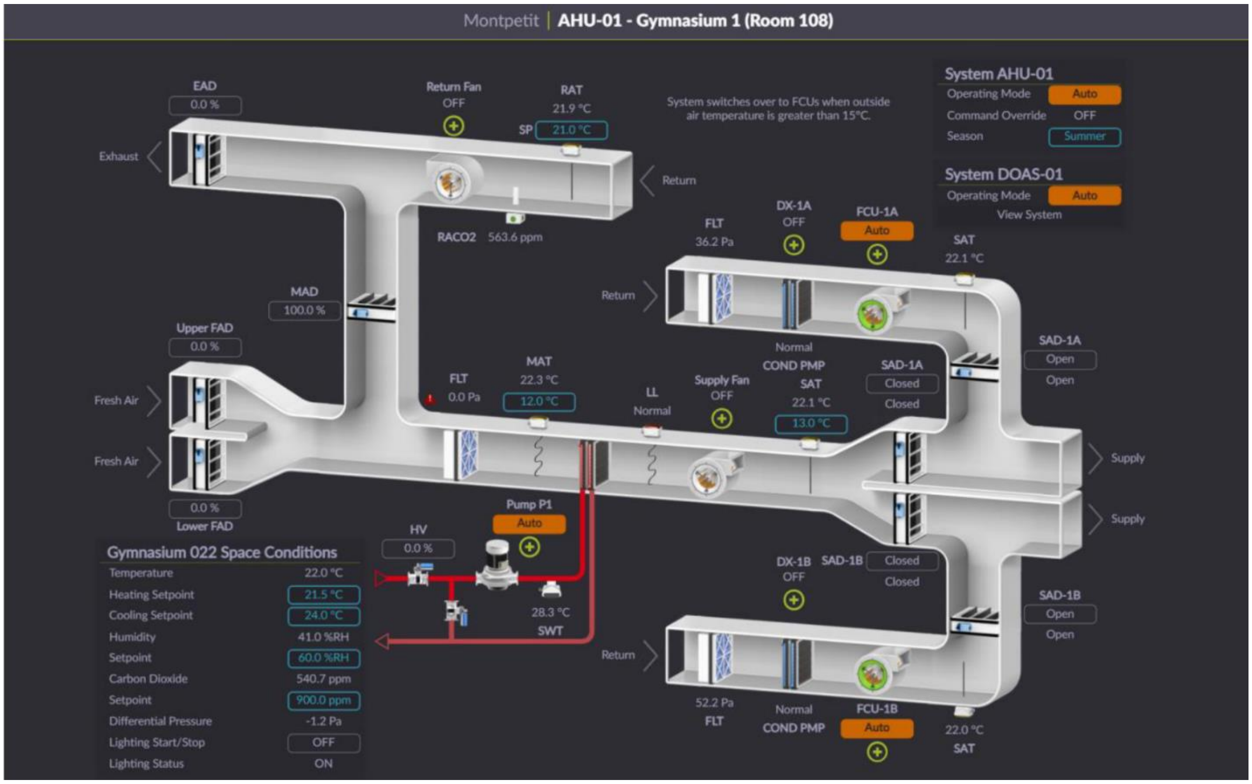

Figure A. 22 MNT Gymnasium HVAC Schematic (AHU1, 2, and 3)

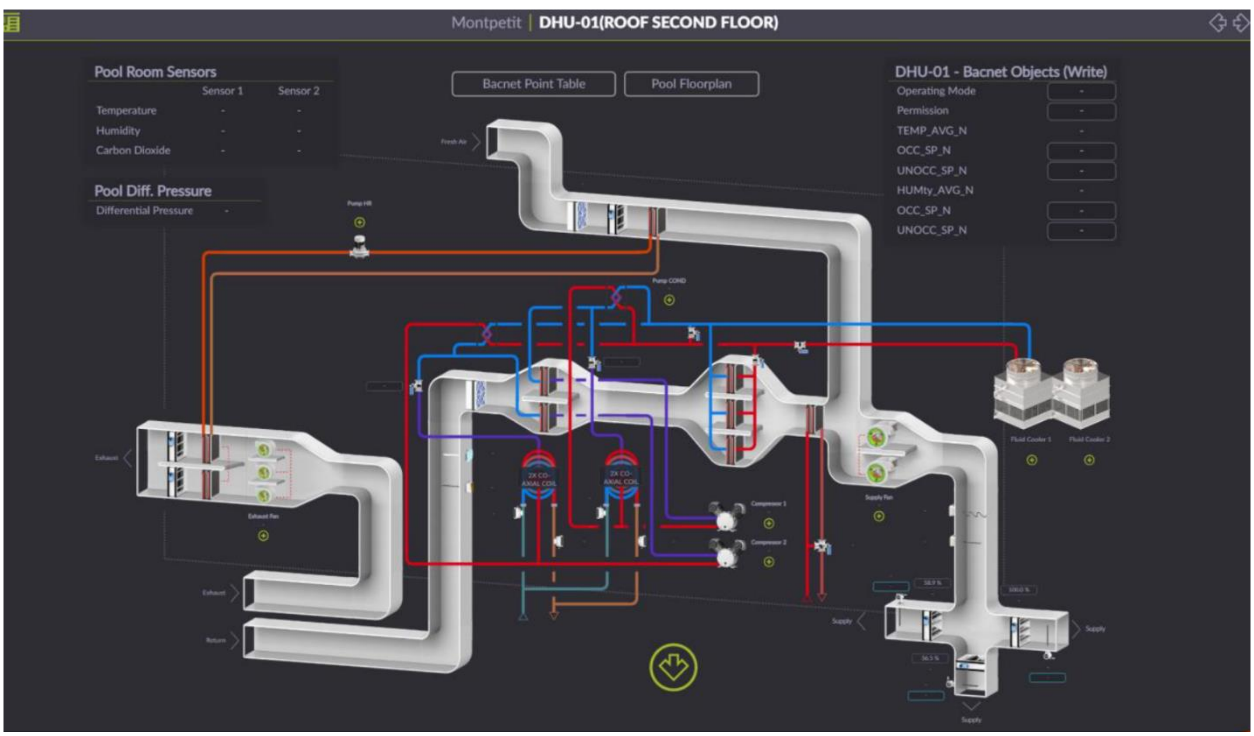

Figure A. 23 MNT Pool HVAC Schematic (AHU 4)

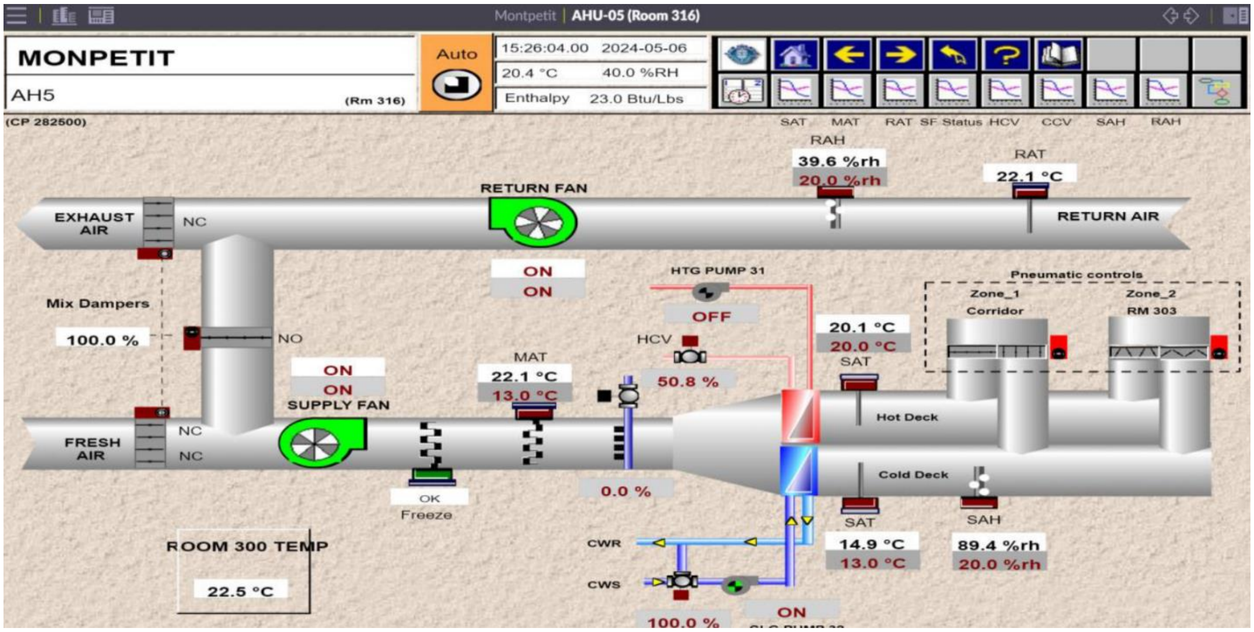

Figure A. 24 MNT Centre Core HVAC Schematic (AHU-5)

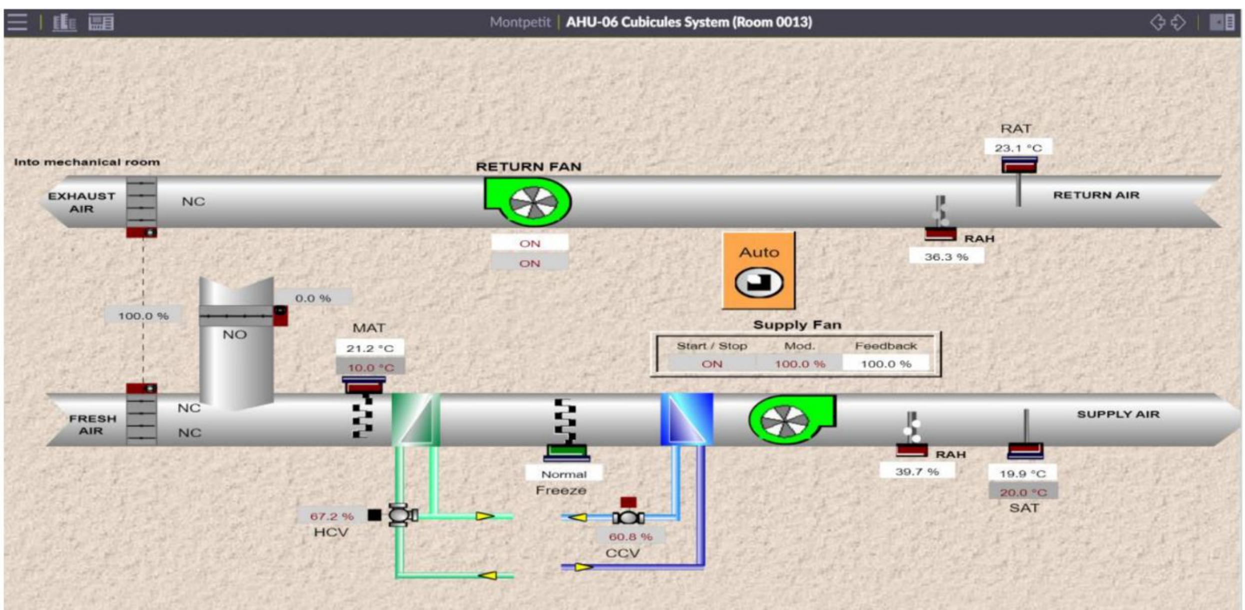

Figure A. 25 MNT Cubicles Area HVAC Schematic (AHU-6)

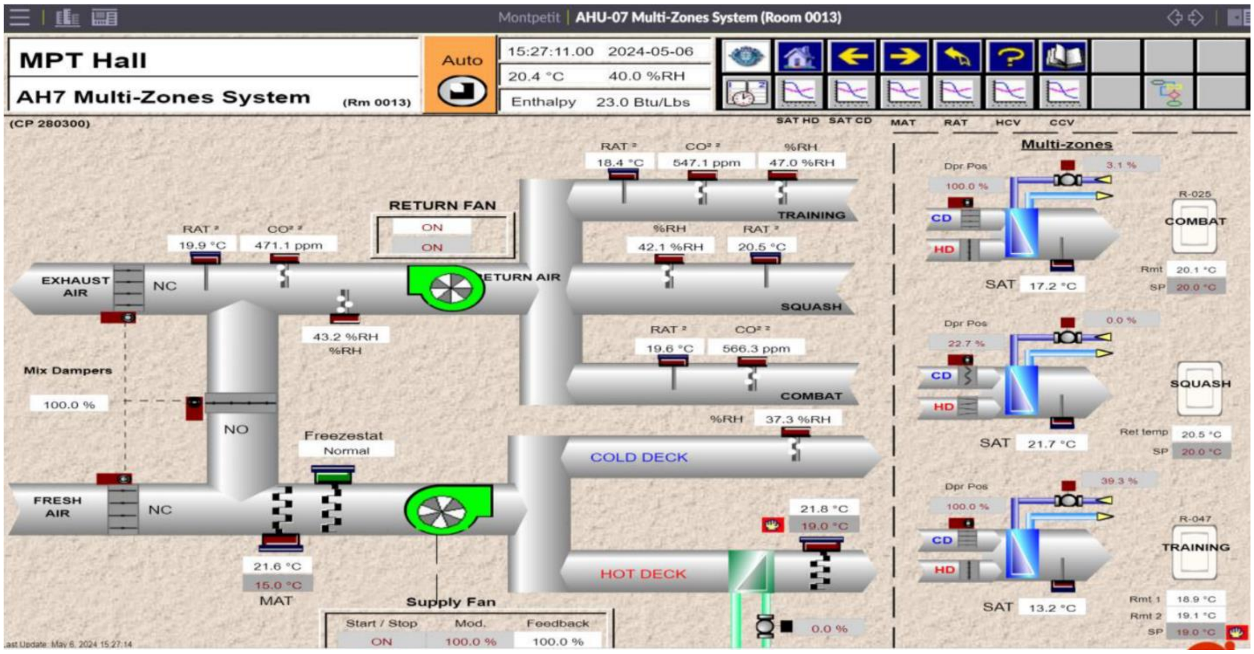

Figure A. 26 Fitness Space HVAC Schematic (AHU-7)

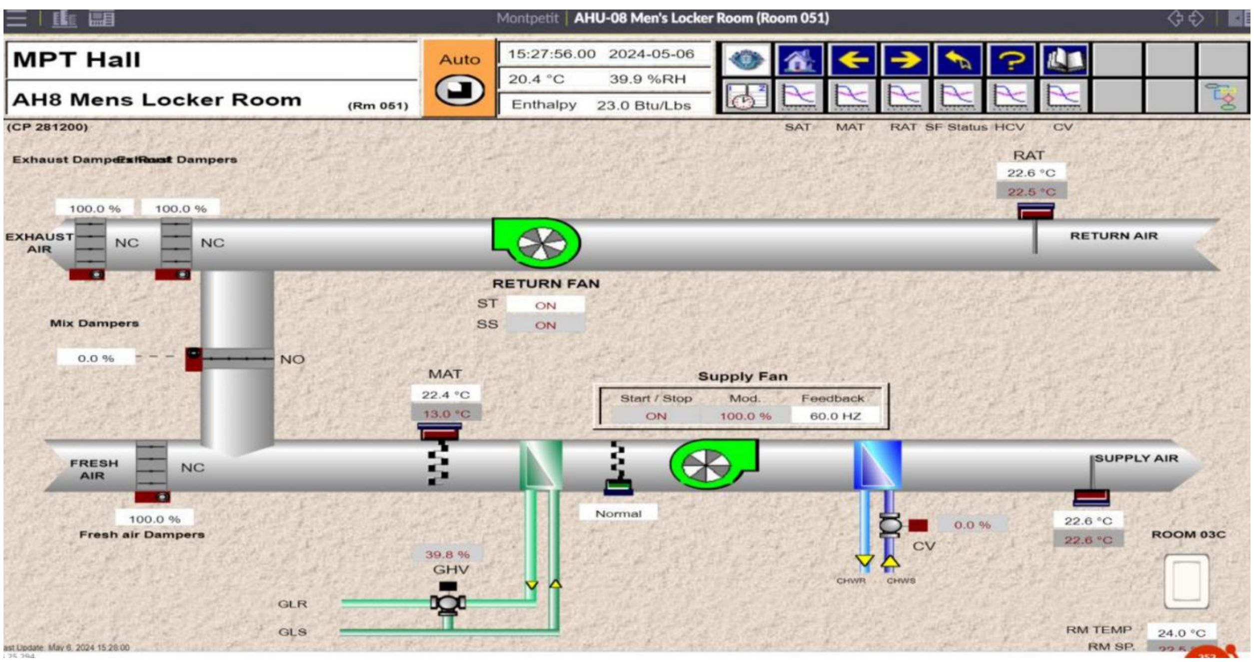

Figure A. 27 Locker Room HVAC Schematic (AHU-8)

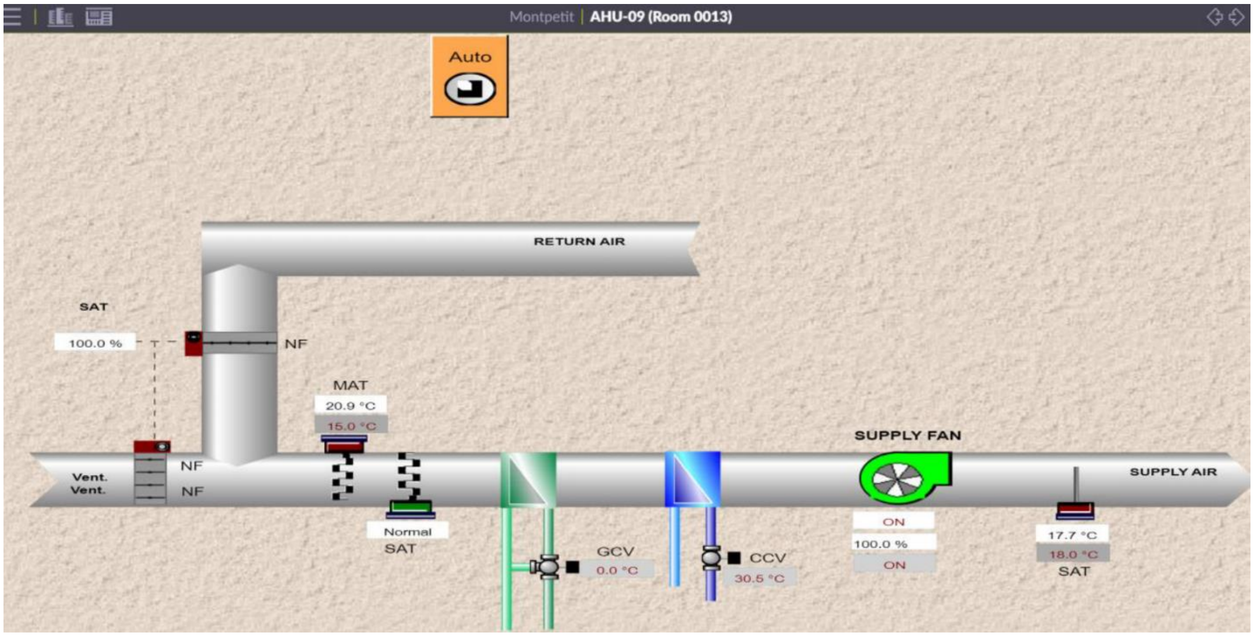

Figure A. 28 Basement and Mechanical Room HVAC Schematic (AHU-9)

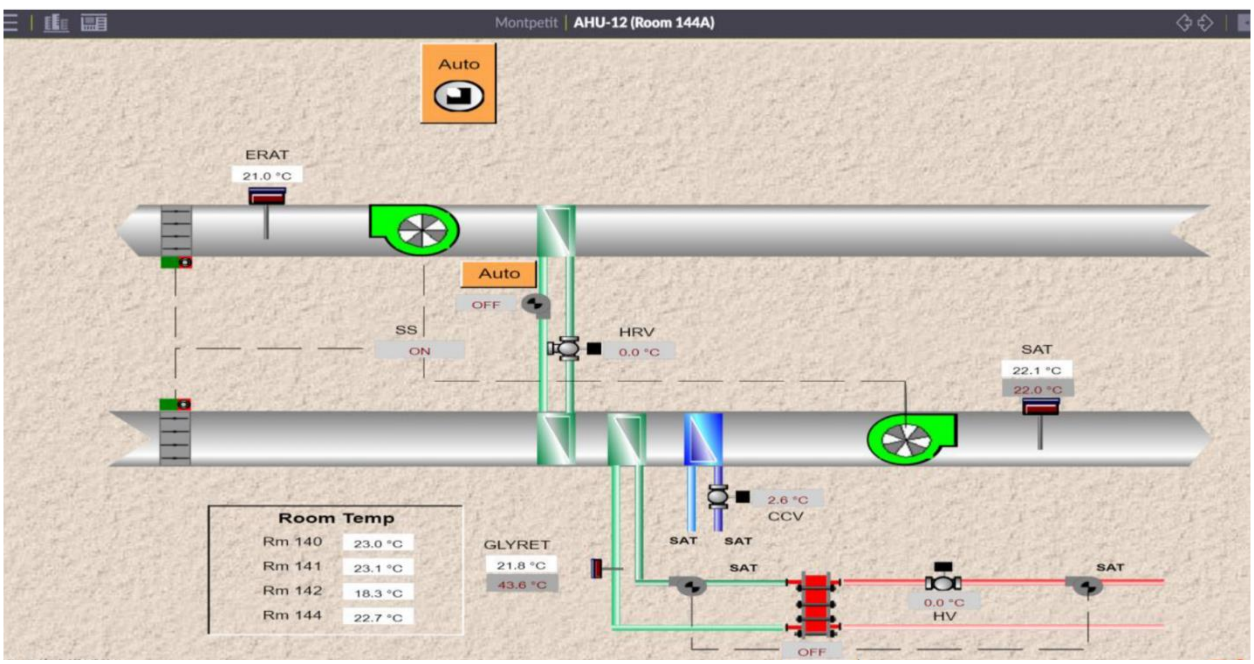

Figure A. 29 Computer Laboratory HVAC Schematics (AHU-12)

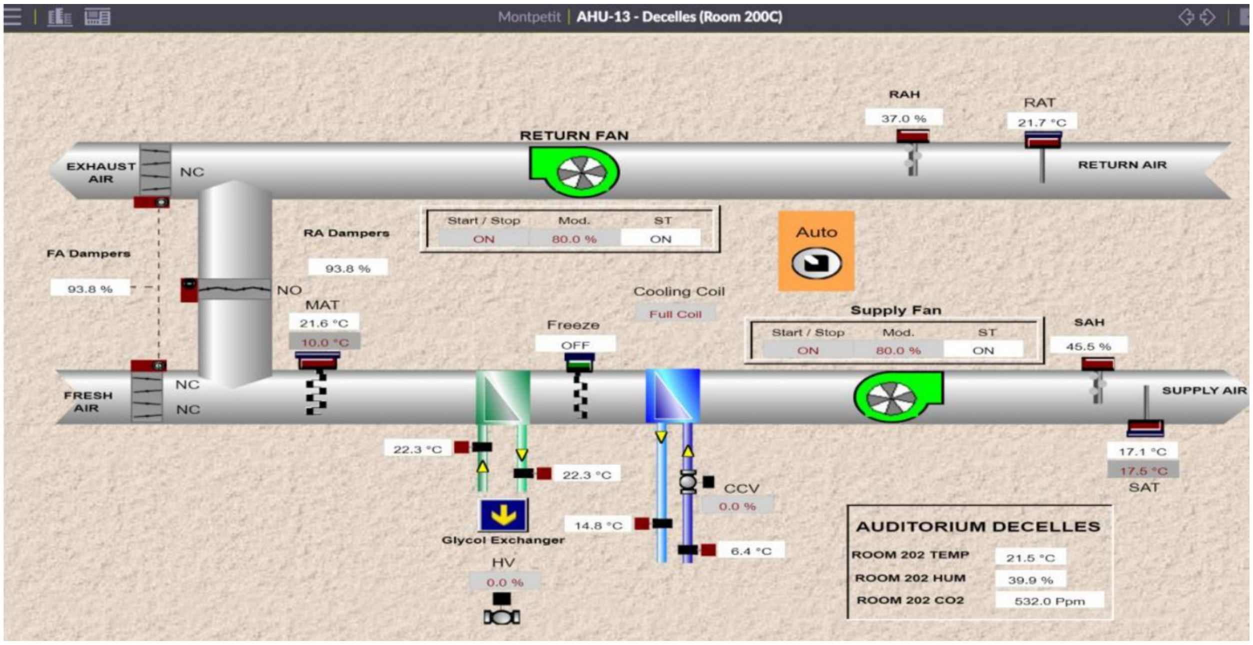

Figure A. 30 Descales Auditorium HVAC Schematics (AHU-13)

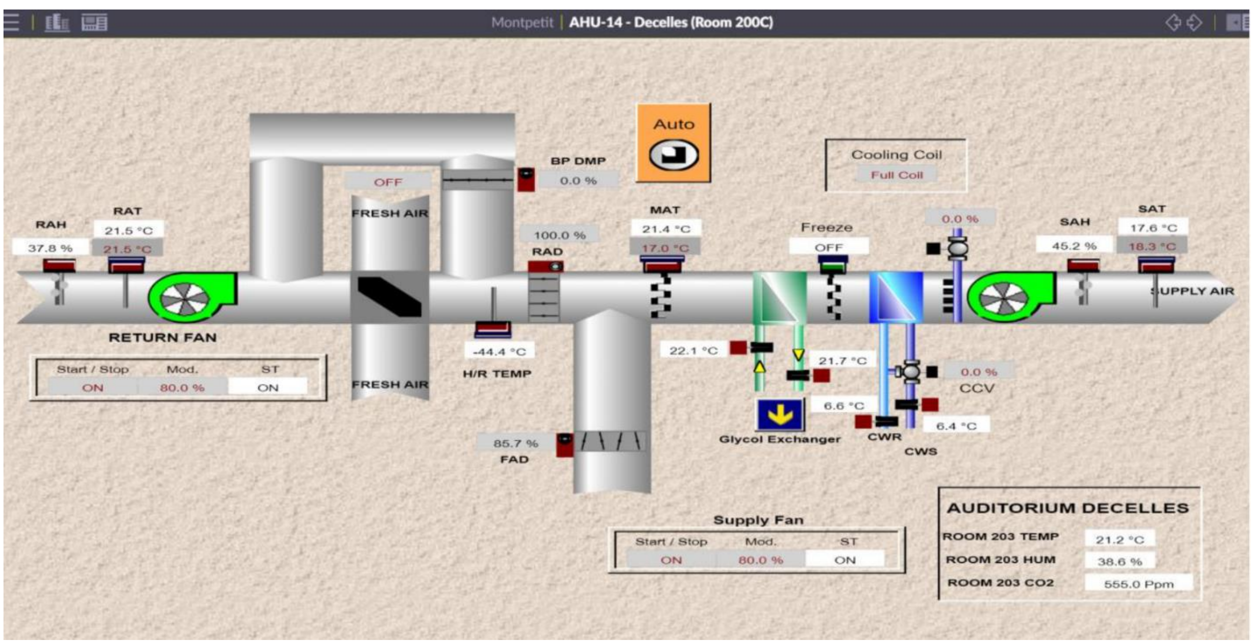

Figure A. 31 Descales Auditorium HVAC Schematic (AHU-14)

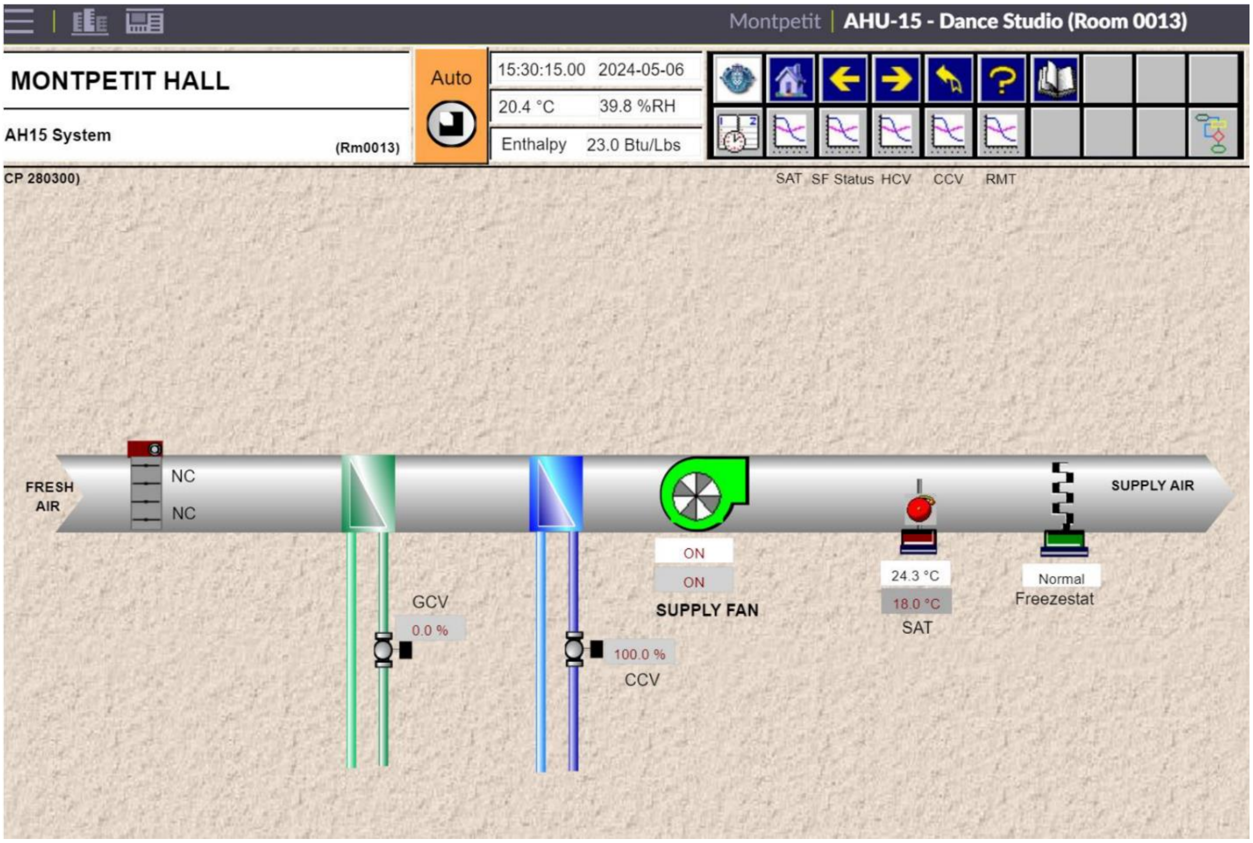

Figure A. 32 Dance Studio HVAC Schematic (AHU-15)